DESIGN OPTIMIZATION OF A GRID SCALE HYBRID ENERGY STORAGE SYSTEM TO MAXIMIZE SOLAR PV INTEGRATION

Hasini Chamudika Ganege

218108N

Master of Philosophy

Department of Electrical Engineering
Faculty of Engineering

University of Moratuwa
Sri Lanka

May 2025

DESIGN OPTIMIZATION OF A GRID SCALE HYBRID ENERGY STORAGE SYSTEM TO MAXIMIZE SOLAR PV INTEGRATION

Hasini Chamudika Ganege

218108N

Thesis submitted in partial fulfillment of the requirements for the degree
Master of Philosophy

Department of Electrical Engineering
Faculty of Engineering

University of Moratuwa
Sri Lanka

May 2025

DECLARATION

I declare that this is my own work and this Thesis does not incorporate without acknowledgement any material previously submitted for a Degree or Diploma in any other University or Institute of higher learning and to the best of my knowledge and belief it does not contain any material previously published or written by another person except where the acknowledgement is made in the text. I retain the right to use this content in whole or part in future works (such as articles or books).

Signature: Date: 16/05/2025

The supervisor should certify the Thesis with the following declaration.

The above candidate has carried out research for the Master of Philosophy Thesis under my supervision. I confirm that the declaration made above by the student is true and correct.

Name of Supervisor: Prof. D.P. Chandima

Signature of the Supervisor: Date: 16/05/2025

DEDICATION

This thesis is dedicated to my beloved parents and family, whose unconditional love, encouragement, and sacrifices have been the foundation of my achievements.

To my supervisor, who has guided and inspired me throughout this journey with his wisdom and patience.

And to my friends, who have stood by me through the challenges, providing support and motivation when I needed it most.

ACKNOWLEDGEMENT

I would like to express my sincere gratitude to all those who contributed to the successful completion of this Master of Philosophy.

First and foremost, I extend my heartfelt thanks to my supervisor, Prof. D. P. Chandima, of the Department of Electrical Engineering, Faculty of Engineering, University of Moratuwa. His valuable guidance, insightful feedback, and unwavering support were essential throughout this journey.

I am deeply grateful to the lecturers and other supporters at the Faculty of Engineering, University of Moratuwa, for their assistance and encouragement during my studies. I would like to particularly acknowledge Prof. J. P. Karunadasa for his guidance and support during my academic endeavors.

I am also thankful to my colleagues and the staff at the Faculty of Technology, University of Ruhuna, for their cooperation and understanding, which allowed me to balance my work and academic commitments effectively.

Lastly, I owe my deepest gratitude to my beloved parents and family, whose unconditional love, encouragement, and sacrifices have been the foundation of all my achievements. Their constant support has been my greatest source of strength.

ABSTRACT

The global utilization of renewable energy is increasing as an environmentally sustainable approach to reduce greenhouse gas emissions, which are major contributors to air pollution and climate change, by decreasing reliance on oil-fired thermal power generation. This research aims to minimize oil-fired thermal generation and maximize solar photovoltaic (PV) generation through a grid-connected Hybrid Energy Storage System (HESS) that integrates lithium-ion Battery Storage (BS) and Pumped Hydro Storage (PHS). Solar energy is prioritized due to its technological maturity and cost-effectiveness compared to other sustainable energy sources. The HESS is employed to optimize storage performance, utilizing high efficiency and energy management capabilities of lithium-ion BS and the large-scale energy storage potential of PHS. Both technologies are well-established, offering reliability and low investment risks.

A novel optimization algorithm, based on the Non-dominated Sorting Genetic Algorithm (NSGA-II), is developed to minimize total expenditures. This includes capital, operational, and replacement costs associated with solar PV, lithium-ion BS, and PHS systems, as well as expenses related to solar power curtailment and supplementary oil-fired thermal energy. The multi-objective optimization problem is solved using the open-source Python framework Pymoo (multi-objective optimization in Python), and Python code developed and executed on Google Colaboratory (Colab). The algorithm determines optimal capacities for lithium-ion BS and solar PV systems at short-term intervals throughout the project planning horizon. The capacity of PHS is identified through a feasibility study conducted for a specific region, considering geological constraints. An innovative energy management strategy is proposed to optimize solar energy utilization within the HESS. This strategy ensures the efficient utilization of solar energy, maintains grid stability, optimizes HESS operations within system limitations, and minimizes dependence on thermal power generation.

The research includes a case study of the Sri Lankan power system, supported by economic and environmental assessments to identify the most sustainable scenarios. Sensitivity analysis is conducted to evaluate capacity variations under fluctuating interest rates. A roadmap for solar PV and BS capacity expansions is developed for two-year intervals throughout the planning horizon, along with the optimal timeline for integrating PHS. The final results indicate minimal variations in total cost, ranging from -14.05 % to 56.69 %, and an increase in solar PV generation by 2.19 % at the lowest interest rate and 5.13 % at highest interest rate. The solar PV capacities determined from the optimization algorithm are compared with the projected capacities of solar power plants outlined in Sri Lankan generation expansion plan to evaluate their alignment with the renewable energy targets in the country. The results demostrats strong agreement with the national energy plan.

Keywords: Hybrid Energy Storage, Solar PV Generation, Genetic Algorithm, Techno-economic optimization

TABLE OF CONTENTS

LIST OF FIGURES

LIST OF TABLES

LIST OF ABBREVIATIONS

Abbreviation	**Description**
BS	Battery Storage
CAES	Compressed Air Energy Storage
CAPEX	Capital Expenditures
CEB	Ceylon Electricity Board
CSP	Concentrated Solar Power
DOD	Depth of Discharge
DRL	Deep Reinforcement Learning
EMO	Evolutionary Multi-Objective Optimization
FES	Flywheel Energy Storage
GA	Genetic Algorithm
GHG	Greenhouse Gas Emission
HESS	Hybrid Energy Storage System
IEA	International Renewable Energy Agency
IRR	Internal Rate of Return
JICA	Japan International cooperation Agency
LAES	Liquid air energy storage
LCOE	levelized cost of electricity
Li-ion	Lithium Ion
LNG	Liquefied Natural Gas
LR	Lower Reservoir
NaS	Sodium sulfur
NOCT	Nominal Operating Cell Temperature
NPV	Net Present Value
NSGA	Non-dominated Sorting Genetic Algorithm
OPEX	Operational Expenditures
Pb-acid	Lead-acid
PHS	Pumped Hydro Storage
PSO	Particle Swarm Optimization
PUCSL	Public Utilities Commission of Sri Lanka
PV	Photovoltaic
Pymoo	Multi-Objective Optimization in Python
RE	Renewable Energy
REPEX	Replacement Expenditures

Abbreviation	Description
RFB	Redox flow battery
SOC	State of Charge
SOFC	Solid Oxide Fuel Cell
STC	Standard Test Conditions
UR	Upper Reservoir

LIST OF APPENDICES

CHAPTER 1

INTRODUCTION

1.1 Background and problem identification

The world is facing significant challenges, including rising temperatures, increasing sea levels, more severe weather events, species loss, and food insecurity, all driven by global warming. Global temperatures are currently rising at an estimated rate of 0.2 °C per decade, primarily due to human activities since the industrial revolution. The decade from 2011 to 2020 has been identified as the warmest decade, with an average temperature increase of 1.1 °C [1]. Greenhouse gas emissions (GHGs) are main contributors to global warming, as these gases absorb heat radiation in the atmosphere, leading to higher atmospheric temperatures. Since the industrial revolution, GHG emissions have significantly increased due to human activities such as fossil fuel combination, deforestation, agriculture expansion, and waste disposal. Consequently, finding alternative solutions to reduce GHG emissions and mitigate climate change has become a global priority.

In response to climate change, individual countries and groups of nations have committed to goals and agreements aimed at reducing environmentally harmful human activities. The United Nations Sustainable Development Goals and the terms of the Paris Agreement have significantly influenced the global focus on eco-friendly alternatives. Furthermore, the long-term temperature goal of the Paris Agreement is to limit the global temperature rise to 1.5 °C, or at minimum, keep it below 2 °C [2, 3]. To achieve these targets, the adoption of sustainable practices is widely recognized as essential for ensuring a sustainable future and minimizing the environmental impact of human activities.

Globally, the primary drivers of GHG emissions include the power industry, industrial combustion and process, transport, building and agriculture. The global GHG emissions experienced a significant reduction in 2020 due to the COVID-19 pandemic, with a decrease of 3.7 % compared to the levels observed in 2019. However, emissions increased in 2022, exceeding 2019 levels by 2.3 % and 2021 levels by 1.4 % [4]. In 2022, 89 % of CO_2 emissions were attributed to energy combustion and industrial processes [5, 6]. Based on these figures, the energy sector is identified as the largest contributor to GHG emissions compared to other sectors. To meet energy demands, alternative energy generation methods must be adopted, reducing reliance on fuel combustion for electricity production.

Moreover, future energy consumption is expected to increase due to growth of population, economic development and technological advancements, further driving energy demand. To address this growing energy demand, alternative solutions should be implemented that focus not only on reducing fuel-based energy generation but also on meeting future energy needs. Additionally, to reduce dependency on the fossil fuels, energy generation is move to renewable energy (RE) sources from fossil fuel power plants, providing a sustainable alternative to the ongoing energy crisis.

In the 1970s, the global attention was especially focused on oil imports due to world completely dependence on oil [7]. Nowadays, the global energy crisis is significantly broader and more complex than its historical requirements. However, current energy challenges span multiple dimensions, all of which must be addressed to ensure affordable and secure energy services [8]. Considering the current situation, the primary global objective is to reduce thermal energy generation in the face of growing electricity demand, aiming to minimize GHG emissions that contribute to climate change and decrease reliance on fossil fuels.

To address global challenges, RE sources are increasingly prioritized for energy generation, with future energy plans incorporating RE solutions. By the end of 2019, the installed capacity of RE was distributed as follows: 44.6 % from hydro, 23.3 % from wind, 23 % from solar, and 9.1 % from other RE sources such as biogas, and geothermal energy, according to published data from the International Renewable Energy Agency (IEA) [9]. As per the global energy plan, RE sources are expected to grow significantly, rising from 28 % in 2021 to approximately 50 % by 2030 and reaching 80 % or 85 % by 2050 [8, 10]. Furthermore, according to the *"General Policy Guidelines in Respect of the Electricity Industry"*, the national energy policy in Sri Lanka aims to achieve 70 % of generated power from RE sources by 2030 and to reach net-zero CO_2 emissions in electricity generation by 2050 [11]. Both globally and within Sri Lanka, the goal is to increase the share of RE to meet future requirements.

Among RE sources, solar and wind power plants are globally popular due to their cost effectiveness with the technological advancements, abundant availability and scalability. When comparing the two sources, solar energy is often preferred due to practical reasons, such as more accessibility with adequate sunlight, lower initial installation costs for solar panels, scalability from small residential systems to large solar farms with greater flexibility and lower maintenance costs due to fewer moving parts compared to wind power plants. However, when maximizing solar energy, several common issues arise, including rapid fluctuations in supply due to intermittency, limited predictability, and a demand gap during nighttime. To address these challenges, an energy storage system can beutilized as a controllable device, storing excess energy during periods of high solar generation and releasing it when solar production is low, thereby enhancing controllability. Moreover, large-scale energy storage systems enhance the flexibility, reliability and stability of the energy system, while improving overall system performance. They help smooth out demand, prevent price spikes during period of high electricity demand, and improve economic performance, enabling greater penetration of RE. Additionally, they act as a buffer for fluctuations in energy supply, facilitate load levelling and peak shaving, regulate frequency, dampen energy oscillations, and improve power quality. The ability to achieve all the requirements for a specific application is limited with a single energy storage. Therefore, Hybrid Energy Storage Systems (HESS), which combine multiple technologies, can provide a more versatile solution.

Various technologies can be utilized to implement HESS, significantly improving the overall performance of the entire system. high-energy and high-power storage can be identified as a two primary categories of storage technologies [12]. For high-energy storage, battery technologies, hydrogen, or fuel cell technologies are often the focus. In contrast, high-power storage typically involves flywheels, super-capacitors or ultra-capacitors or superconducting magnetic energy storage. In large-scale energy storage applications, Pumped Hydro Storage (PHS) and Compressed Air Energy Storage (CAES) are two of the typically deployed technologies. However, these technologies face development challenges due to geological and environmental conditions [13, 14]. PHS is chosen for the implemented HESS because of its proven and established technology, low investment risk, low power generation costs, and ability to supply peak demand without requiring ramp-up time [15]. In addition, battery technology is selected for its ability to balance with fast response times and economic benefits. Among battery technologies, Lithium ion (Li-ion) battery systems are chosen for this study due to their high energy and power density, as well as their efficiency. Li-ion battery technology is considered a potential solution for grid-scale HESS, especially when combined with PHS [16, 17].

Most research has concentrated on determining the appropriate technologies for HESS through comparisons of different energy storage options, while some studies have examined solutions that integrate multiple RE resources, such as wind and solar. The focus of most of these studies is on utilizing batteries and super-capacitors for HESS [18]. While much of the research focuses on determining system capacities for the planning horizon after selecting energy storage technologies and renewable energy sources, this study takes a further step by identifying the optimal capacities for solar photovoltaic (PV) and HESS. The study also explores the most appropriate periods for integrating these capacities to ensure maximum system benefits The Non-dominated Sorting Genetic Algorithm II (NSGA-II) is employed to identify a diverse set of solutions using non-dominated sorting and crowding distance, providing efficient sorting without the need for assigning additional weights to objectives in solving the multi-objective optimization problem. A new multi-objective optimization algorithm, together with an energy management control strategy, is also introduced to efficiently coordinate energy generation and storage while adhering to system constraints.

Considering global and national requirements, this research focuses on maximizing solar energy generation as an alternative solution for electricity production, aiming to reduce thermal (oil) generation, which contributes significantly to GHG emission due to oil combustion. To address the limitations of solar energy, HESS is employed by integrating PHS and Battery Storage (BS). The study aims to determine the optimal capacities of solar PV power plants and HESS within a short time frame over the planning horizon.

1.2 Objectives

This research primary objective is to implement a roadmap for incorporating capacities of solar PV, PHS, and Li-ion BS, based on the results of a novel developed sizing and costing optimization algorithm for gird-scale HESS. A multi-objective optimization model, which integrates both PHS and BS systems, has been proposed, aiming to maximize solar PV generation while reducing thermal energy production. The model focuses to minimize installation, operational, and replacement costs over the lifespan of the project, while also reducing expenses related to solar power curtailment and the additional reliance on oil-fired thermal energy generation.

Additionally, the sub-objectives involve developing an innovative multi-objective sizing and costing optimization algorithm, as well as a new multi-objective energy management control strategy to address the solar PV and HESS component limitations. These developed models are intended to determine the optimal capacities for solar PV, PHS, and BS systems, as well as identify the best time period for integrate to the system for maximize overall benefits. Furthermore, this research aims to create a roadmap for incorporating solar PV, PHS, and BS, taking into account both economical and environmental considerations. The effectiveness of the proposed optimization algorithm and energy management strategies is demonstrated through a case study based on real-world data. Additionally, a sensitivity analysis is carried out to identify the optimal scenario that exhibits the least cost variability under fluctuating interest rates.

1.3 Significance of the study

This study primaraly aims to increse the use of RE for electricity generation as a solution to reduce the GHG emissions caused by fossil fuel combustion. Among the available RE sources, solar PV is selected due to its cost-effectiveness, the potential for leveraging advanced technologies, and the ease of installation within a shorter time period. The introduced HESS is designed to address the limitations of solar PV, such as unpredictability and intermittency, and functions as a controllable device within the proposed system. Furthermore, the energy storage system is proposed as a hybrid solution, utilizing multiple technologies to enhance the overall performance of the HESS. Among the selected technologies, PHS can handle bulk energy, facilitating peak shaving and time shifting, while BS ensures effective energy management, enhancing power quality and reliability. Ultimately, the HESS provides a solution to the challenge of energy surplus and unmet demand, promoting a more efficient and resilient energy system.

Advanced optimization technologies are utilized to calculate the capacities of solar PV and BS, aiming to identify the most effective solutions with multi-objectives. These optimal solutions are determined for short time periods within the planning horizon, providing the optimal capacities for each duration to maximize the overall benefits of the system. Furthermore, PHS capacities are identified based on feasibity studies conducted for specific countries or regions, ensuring that the results are practical and applicable for implementation in the targeted areas.

1.4 Thesis overview

This chapter outlines the research background, problem identification, motivation, objectives, and significance of the study. It provides background for the importance of the proposed system in addressing the identified problem by enhancing renewable energy generation.

The second chapter provides a comprehensive review of established studies on solar PV systems, energy storage technologies, and optimization algorithms. Furthermore, it discusses relevant studies in this field and identifies knowledge gaps that form the foundation of this research. The third chapter presents the research methodology, including the design and implementation of the optimization algorithm using NSGA-II, energy management control strategies, input parameters, assumptions, and evaluation criteria relevant to this study.

The fourth chapter describes all the parameters considered to validate the proposed algorithms using the Sri Lankan power system. The fifth chapter discusses the results and analysis of the study, highlighting key findings such as the roadmap for optimal solar PV and HESS capacities and evaluating their alignment with the energy requirements of the country. Finally, the concluding chapter summarizes the key findings of the research and provides recommendations of the future studies.

CHAPTER 2

LITERATURE REVIEW

The literature in this field has grown substantially in recent years, driven by the global focus on expanding renewable energy generation to mitigate the environmental impacts of fossil fuel combustion. This chapter provides an overview of renewable energy sources, highlights the rationale for prioritizing solar energy generation, and examines various energy storage methods. It also explains the selection of PHS and BS for this study, discusses the choice of optimization algorithms, and reviews recent research on RE and energy storage systems. Additionally, It also identifies existing research gaps, emphasizing the need for future advancements in optimizing RE systems and storage technologies.

The primary global aim is to adopt alternative approaches that reduce thermal energy generation, thereby reducing GHG emissions that contribute to air pollution and climate change. The global focus is shifting toward significantly increasing renewable energy generation in the coming decades. Fig. 2.1 illustrates the projected energy generation by source, highlighting a significant increase in wind and solar energy generation, while coal and oil-fired thermal energy production is expected to decline significantly [19].

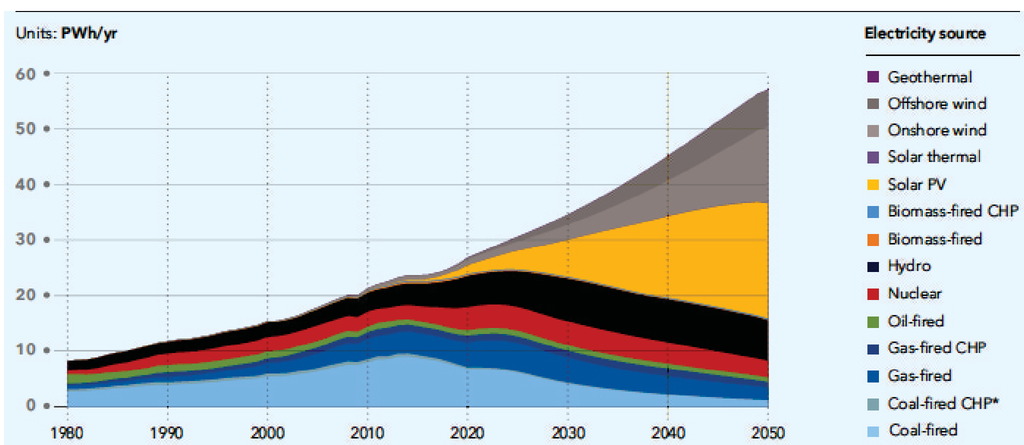

Fig. 2.1: Electricity generation by source through to 2050 •• • ••••

Wind and solar energy are the most widely utilized renewable energy sources, mainly due to their technological maturity and widespread accessibility. This study focuses on solar energy because of its substantial potential, cost-effectiveness, continuous technological advancements, scalability, and widespread availability throughout the year. Consequently, the levelized cost of energy (LCOE) for solar PV systems has consistently decreased over time, as shown in Fig. 2.2 [9]. Solar energy has been prioritized for maximization as a renewable energy source due to its numerous advantages. However, the growth of solar PV capacity is limited by challenges such as unpredictability and intermittency. To overcome these limitations, energy storage systems are identified as the most effective solution to ensure stable and reliable energy supply.

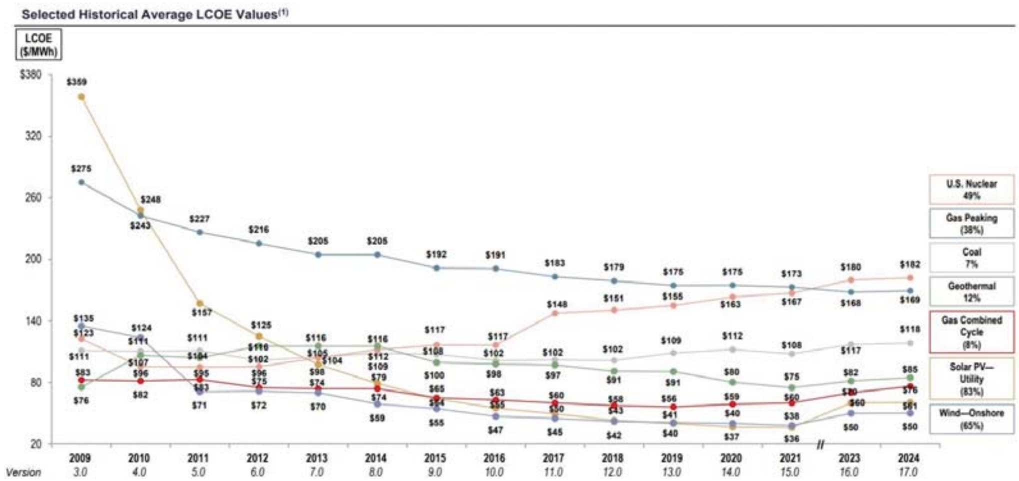

Fig. 2.2: LCOE comparison with RE methods in utility-scale generation based on histrorical data

Various energy storage technologies are available, and their suitability depends on the specific application and requirements. A generic overview of different storage units including their applications, limitations, benefits, and their oles in integrating higher shares of renewable energy has been discussed in several research papers [20–22].

2.1 Selection of energy storage technology for the proposed system

Energy storage systems utilize a variety of technologies, each suited to different applications. These systems can be classified according to their energy storage methods, such as direct electrical, chemical, thermal, electrochemical, and mechanical storage. Table 2.1 provides a summary of these energy storage technologies, categorized by their respective energy conversion techniques.

Direct electrical storage systems store energy in the form of electrical energy for immediate use, eliminating the need for intermediate conversion processes. However, these systems are limited by their storage capacity and are generally not suitable for large-scale grid storage applications. Chemical energy storage involves storing energy in the form of chemical compounds, such as hydrogen, ammonia, synthetic natural gas, and methanol [23]. In this method, electricity is converted into gases or liquids, which can later be used for energy generation or direct applications. For safety reasons, chemical energy storage systems are typically located away from generation plants.

TABLE 2.1: TYPES OF ENERGY STORAGE TECHNOLOGIES CLASSIFIED BY ENERGY CONVERSION METHODS ....

Electrical Storge Systems	Direct electrical	Capacitors
		Super-capacitors
		Superconducting Magnetic Energy Storage
	Chemical	Hydrogen
		Ammonia
		Synthetic Natual Gas
		Methanol
	Thermal	Sensible Heat
		Latent heat
		Thermochemical
	Electrochemical	Sodium- Sulfur Battery
		Lithium-Ion Battery
		Lead Acid Battery
		Redox Flow Battery
		Zinc-bromine Flow Battery
	Mechanical	Pumped-Hydro Energy Storage
		Compressed Air Energy Storage
		Flywheel Energy Storage
		Liquid Air Energy Storage

The interaction between storage and generation in these systems can be advantageous for long-term storage. However, the need for separate facilities for both storage and generation increases the complexity of the system and it is not sutaible for short-term storage applications.

Thermal energy storage can be categorized into three types: sensible heat, latent heat, and thermochemical storage. These systems store energy through processes such as temperature changes, phase transitions, or changes in the chemical structure of materials. Like chemical energy storage, thermal storage systems require separate facilities for the charging and discharging processes. This storage method is often used in conjunction with concentrated solar power (CSP) plants to enable dispatchable generation, but its application is generally confined to CSP systems. Given these considerations, direct electrical, chemical, and thermal storage methods are not considered for the proposed HESS design.

Lead-acid batteries (Pb-acid) and Lithium-ion (Li-ion) batteries are most common example for electrochemical energy storage technologies. Sodium sulfur batteries(NaS) and Redox flow batteries (RFB) are also used with commercial applications [24, 25]. Battery technologies are widely used as energy storage solutions due to their effective energy management characteristics. They are particularly suitable for microgrid and grid-level applications and are highly compatible with renewable energy systems. These systems operate based on electrochemical reactions to store and release energy [23].

Pb-acid batteries are cost-effective, highly reliable, and technologically mature. However, they have limitations such as low efficiency, low energy density, a shorter lifespan under high depths of discharge, and requirement of periodic water maintenance. In contrast, NaS batteries are widely utilized for commercial electrical power storage because of their high energy efficiency, high energy density, and long cycle life. Nevertheless, their usage is limited with high capital costs, the requirement for high operating temperatures, and associated safety hazards [26, 27].

Li-ion batteries are considered as an advanced energy storage technology and have been successfully utilized in various applications, including portable electronics and electric/hybrid electric vehicles (EVs/HEVs). Further, Li-ion batteries are a promising solution for grid-level storage due to their high power, energy density, and efficiency. However, in the coming years, their widespread use may face challenges due to the limited availability of lithium resources and the resulting cost increases, particularly for large-scale electrical energy storage applications. Further, RFB technology offers a well-balanced solution for integrating renewable energy with the current electricity grid. It features low maintenance costs, high charge tolerance, and high-depth discharge performance. However, RFB technology is still in the development phase, which limits its current wide utilization [28].

Considering the discussed electrochemical energy storage methods, Li-ion batteries are selected as the most suitable option for renewable energy application. Although Pb-acid batteries are commonly used in renewable energy applications due to their low cost and reliability, but they are gradually being replaced by Li-ion batteries. This transition is primaraly due to the limitations of Pb-acid batteries, such as low efficiency and the need for periodic maintenance. Consequently, Li-ion batteries are selected as the preferred battery technology for this study to effectively manage energy in renewable energy applications.

PHS, CAES, Flywheel energy storage (FES), and Liquid air energy storage (LAES) are examples of mechanical energy storage systems. These systems store and release energy by utilizing potential energy or kinetic energy [23]. These mechanical storage methods produce minimal pollutants throughout their lifecycle. However, the systems are subject to geological considerations and high installation costs [29]. In addition to BS, mechanical power storage is an effective solution for grid-level energy storage due to its ability to handle large volumes of energy.

PHS requires two reservoirs to store water. Excess energy generated from solar PV is used to pump water upstream for storage. During peak demand periods, the stored water is released to flow downstream, generating electricity in a manner similar to a conventional hydroelectric plant [29, 30]. In CAES, an electrically powered compressor is used to compress air to high pressure for store the energy. During the discharge cycle, the compressed air is expanded, and turbines are driven by mixing the expanded air with fuel. The compression cycle requires cooling, and the expansion cycle necessitates preheating. LAES stores energy by liquefying air and storing it in insulated tanks. During the discharge cycle, the liquefied air is evaporated, and the resulting gas is used to drive turbines. However, it is not considered an ideal technology for large-scale energy storage due to its relatively low efficiency. In FES, electrical energy is stored as rotational energy. It is implemented to manage short-term voltage disturbances and improve power quality.

Among mechanical energy storage technologies, PHS identifies as the most suitable for renewable energy applications. It is capable of handling bulk energy storage, and due to its maturity and well-established technology, gives low implementation risk. Moreover, PHS is highly effect during peak demand periods due to its low ramping time. It can also serve as a black start solution in the event of a total blackout [15, 31]. However, PHS has limitations due to geological factors, and its construction and installation are complex and expensive. Despite these challenges, PHS benefits from very low maintenance costs compared to other energy storage technologies.

When considering various energy storage technologies, Li-ion BS and PHS can be identified as the most applicable energy storage methods for managing and controlling the energy generated from solar PV.

2.2 HESS applications with different technologies

A HESS combines two or more energy storage technologies to optimize system performance. HESSs have recently gained significant growth in various applications, including power systems, renewable energy integration, smart grids, microgrids, and electric vehicles. Integrating multiple energy storage technologies enhances the overall performance of the system compared to relying on a single storage technology. This integration improves reliability, flexibility, efficiency, and economic benefits, including increased financial profitability and extended system lifespan.

The performance of the HESS was assessed by comparing the use of a single storage technology to the integration of multiple technologies. This includes identifying the most suitable technologies to integrate into the HESS for optimal performance, considering the specific application. In [32], the proposed photovoltaic/fuel cell/battery hybrid system is identified as a lower-cost, high-efficiency solution with fewer PV modules when compared to a single storage system. HESS integrating BS and supercapacitors are highly considered in research, as they address challenges such as durability, charging and discharging cycles, temperature rise, manufacturing cost and lifespan of the HESS. To improve the efficiency and lifespan of the HESSs, supercapacitors are integrated with BS, offering significant power density and a long life period although with lower energy density [33]. In [34], a similar HESS approach is introduced for solar PV systems to reduce stress on the battery and extend its lifespan. Further, supercapacitors are used to maintain the stability of the power system by considering frequecy regulation and reducing mismatch between the demand and generation [35].

Similarly, Solid Oxide Fuel Cells (SOFCs) can also be integrated with the BS system to maintain system frequency stability during severe disturbances [36]. This integrated system enables consistent power supply from renewable energy, thereby enhancing the overall performance of the power system. Moreover, in addition to BS and supercapacitors, a third energy storage technology, CAES, is also integrated with HESS. A genetic algorithm (GA) is employed to solve the optimization problem with the objective of minimizing the annual total cost. The results indicate that the combination of wind, solar PV, and HESS can effectively meet power demand while ensuring good economic performance [37].

To address the high costs associated with electromechanical energy storage systems, an optimization framework is developed with a cost minimization objective function for solar PV systems, wind systems, and virtual energy storage system. Integrating PV with virtual energy storage systems can significantly enhance economic feasibility [38]. Furthermore, studies have been conducted to evaluate the performance of HESS with PHS. A case study carried out for Ometepe Island in Nicaragua demonstrated that the cost of energy derived from the model results can serve as an international reference values [39]. Renewable energy systems integrated with PHS demonstrate significant practical potential for providing continuous power supply in remote areas [40]. The operational performance of a hybrid pumped and BS system was evaluated by analyzing the energy balance of the proposed system. After one year of simulation, the system achieved a 66.4 % overall storage performance, a 7.3 % storage usage factor, and a 16.5 % energy utilization ratio [41].

Combining two storage technologies is often more effective than using a single technology to maximize the overall benefits of energy storage. Research has been conducted to identify the most suitable technologies for integration. Additionally, HESS is utilized to address challenges associated with renewable energy integration into the power system. With its high energy and power density, as well as its capability to effectively manage renewable energy sources, BS is a key technology for HESS. Similarly, PHS is suitable for handling bulk energy storage, peak shaving, and providing low ramping times. However, fewer studies have been conducted on integrating these two technologies into a HESS, primarily due to the complexity associated with PHS implementation.

2.3 Optimization techniques relevant to renewable energy applications

Optimization techniques are used to determine the most suitable solution for a given problem, considering its objectives and constraints. In this study, it is essential to apply optimization techniques to determine the optimal solar PV and HESS capacities for the proposed system due to the complexity of the algorithm. The choice of optimization techniques to solve an identified problem depends on the number of objectives involved. Techniques such as linear programming, non-linear programming, and dynamic programming are suitable for solving single-objective functions. For multi-objective problems, particularly those with large-scale problems, techniques like GA and Particle Swarm Optimization (PSO) are commonly used.

The generic formulation of a single-objective optimization problem can be mathematically expressed as shown in Eq. (2.1), Eq. (2.2), and Eq. (2.3). These equations represent the objective function, inequality constraints, and equality constraints, respectively, that define the optimization problem.

$$\begin{pmatrix} min \\ x \in X \end{pmatrix} f(x) \tag{2.1}$$

Subjected to,

$$g_i(x) \leq 0, i = 1, 2, ..., m \tag{2.2}$$

$$h_i(x) = 0, j = 1, 2, ..., p \tag{2.3}$$

Where,

X - The feasible set of decision vectors

$f : R^n \rightarrow R$ - Minimization or maximization of the objective function (Over the n-variable vector x)

$g_i(x) \leq 0$ - Inequality constraints

$h_i(x) = 0$ - Equality constraints

The objective function is determined according to the specific goal to be optimized, while the associated constraints uniquely define the problem. Typically, the objective function represents costs with monetary significance, such as investment and operational costs over the planned horizon, as economic optimization is the traditional and most common approach. Economic justification has long been recognized as a primary challenge in deploying HESS, which is why optimization efforts primarily focus on economic objectives. However, beyond economic optimization, other technical objectives, such as emissions reduction and improved power system reliability, can also be addressed using a multi-objective optimization approach.

Eq. (2.4), Eq. (2.5), and Eq. (2.6) represent the generic formulation of a multi-objective optimization problem.

$$\begin{pmatrix} min \\ x \in X \end{pmatrix} f(x) = [f_1(x), f_2(x), ..., f_k(x)]^T \tag{2.4}$$

Subjected to,

$$g_i(x) \leq 0, i = 1, 2, ..., m \tag{2.5}$$

$$h_i(x) = 0, j = 1, 2, ..., p \tag{2.6}$$

Where,

X - The feasible set of decision vectors

$f : R^n \rightarrow R$ - The objective functions to be minimized or maximized (Over the n-variable vector x) and $k \geq 2$

$g_i(x) \leq 0$ - Inequality constraints

$h_i(x) = 0$ - Equality constraints

Multi-objective optimization is utilized to identify optimal solutions for complex problems involving multiple objectives. A novel optimal sizing strategy was introduced for HESS integrating BS and supercapacitors in a micro-grid. This approach, employing a multi-objective genetic algorithm, achieved an 18 % reduction in BS capacity compared to traditional sizing methods [42]. For real-time scheduling, a deep reinforcement learning (DRL) method is proposed to minimize the total cost of generation and smooth power fluctuations based on the deep deterministic policy gradient algorithm, while maintaining the effectiveness of the system [43]. Further, deep reinforcement learning agent is taken to maxmize net profit and maintain the stablilty of the system and it demonstrates more than 90 % profit accuracy [44]. The same approach is employed to minimize operating and energy exchange costs within the networked microgrids. In terms of computational load, the proposed system achieves cost reductions of 12.9 % and 17 % compared to the dueling deep and deep Q-network methods, respectively. Additionally, with respect to computational time, it provides reductions of 17.13 % and 25.6 % compared to the dueling deep and deep Q-network methods, respectively [45].

An optimized fuzzy logic controller is developed using the Particle Swarm Optimization (PSO) algorithm, considering operation and maintenance costs and the loss of power supply probability. The results shows a 57 % lower operation and maintenance costs and 33 % lower the loss of power supply probability [46]. Moreover, the Non-dominated Sorting Multi-Objective Grey Wolf Optimizer and the NSGA-II are compared, demonstrating their validated performance in [47].

NSGA-II is used to optimize the hybrid BS system combining Lithium Iron Phosphate (LIP) and Lithium Titanate Oxide (LTO) to minimize cost, maximize efficiency, and extend the system's lifetime. This approach results in a 29.6 % reduction in total cost compared to the baseline [47]. HESS integrating batteries and supercapacitors is identified as the optimal solution for applications like electric vehicles or smart home energy systems. This integration extends battery lifetime, reduces size, and effectively minimizes the magnitude and fluctuation of the battery current. The Multiplicative-Increase-Additive-Decrease (MIAD) principle is applied to optimize energy storage by minimizing both the magnitude and fluctuation of the battery current as well as the SOC energy loss [48].

Li-ion and Vanadium Redox Flow Battery (VRFB) technologies are used to design HESS aimed at minimizing costs and carbon dioxide emissions. The Mixed Integer Linear Programming (MILP) optimization technique is used to optimize the energy storage system for achieving these multi objectives. The economic and environmental performance of battery technologies is highly sensitive to the weighting factors assigned to costs and CO_2 emissions [49]. A case study conducted in China examines a multi-objective optimization model for a HESS integrated with wind power plants operating independently from the grid. A NSGA-II is used to optimize the combination of batteries and supercapacitors, aiming at maximizing annual profit and minimizing the wind curtailment rate [50].

In the context of RE integration, optimizing the energy management control strategy to effectively address uncertainties and fluctuations of the power is essential. As presented in [51], a deep reinforcement learning algorithm is integrated with an intelligent probabilistic wavelet fuzzy neural network to improve the efficiency of the energy management system. This method achieves a computational accuracy greater than 98 %. Additionally, the voltage/frequency (V/F) index is regulated using an intelligent probabilistic wavelet Petri neuro-fuzzy inference algorithm, successfully reducing V/F fluctuations [52]. The study in [53] employs the Multi-Objective Bees Algorithm (MOBA) for load frequency control within an interconnected multi-area power system, achieving strong dynamic performance through effective suppression of frequency and tie-line power deviations.

2.4 Technical and economic models for energy storage

The increasing global shift toward sustainable energy generation has made optimization in renewable energy and energy storage a critical area of research and development. Several studies have investigated solutions for grid-connected renewable energy system, with a strong emphasis on integrating various energy storage technologies to overcome the limitations of renewable energy. For example, energy storage needs for Europe by 2050 are estimated to range between 126 and 272 GW, with a focus on optimizing spatial distribution for storage expansion, assuming a renewable share of 89 %of the total annual gross power generation by 2050 [54]. Another research group estimates 432 GW of storage will be required by 2050, proposing an optimization model that divides Europe into 18 country groups. Their analysis estimates a required investment of 403 billion EUR for Europe power grid with LCOE expected to increase from 6.7 to 9.0 ctEUR/kWh [55].

A techno-economic analysis conducted in Scotland utilized actual wind and market data sets to investigate the relationship between the capacity of the on-site energy storage and their level of curtailment. From this research, Li-ion technology was recognized as the most sutaible energy storage option for on-site storage. Following the case study, it was determined that the storage capacities for the two wind farms were 100 MWh and 125 MWh, which would have which would have reduced total energy curtailment by 19 % and 20.2 %, respectively [56]. Another study analyzed the techno-economic potential of utilizing wind energy curtailment in the UK as a case study. It focus to the replacement of gas turbine power plants with large-scale battery storage systems. A techno-economic model was developed to size and optimize a Li-ion BS system to commercial feasibility of the grid-scale energy applications.

The optimized BS capacity of 1.25 GWh was identified, 15 % daily wind energy curtailment and a BS cost of £200/kWh to meet an annual peak demand of 285 GWh. The model also summarized the its related net present value (NPV) of £22.4m, an internal rate of return (IRR) of 1.7 % and a 14 years payback period [57]. In the southernmost region of Japan, high solar energy curtailments occur due to the continuous increase in capacity of solar energy. a cost-optimal assessment is conducted to evaluate the problem caused by these curtailments. The proposed financial assessment utilizes Monte Carlo random sampling with hourly simulations to analyze and identify the most effective solutions to minimize the impact of energy curtailment. This study introduces a cost penalty due to energy curtailment and the investment cost associated with energy storage. To balance these costs, a growth trajectory for the cost-optimal storage capacity is proposed. This optimal trajectory helps reduce CO_2 emissions, maximize solar PV generation, and maintain costs at a manageable level while minimizing curtailment.

A technical and economic assessment was conducted using real-time data from Kyushu, Japan, focusing on the integration of large-scale solar PV and a PHS system. The study primarily discusses the impact of solar PV integration on the demand curve and storage dispatch. It considers both technical constraints of solar PV integration and economic requirements to simulate the system's economic performance. The results of the study show that around 50.0 % of PV production is curtailed, with the capacity of maximum solar PV generation and peak load ratio reaching 1.02 due to technical limitations. In this simulation, only PHS was used as the energy storage technology. The study highlighted that PHS can maintain a low LCOE by saving additional solar energy production. When considering the geology of the studied area, PHS is identified as an ideal solution for managing solar energy curtailment compared to other energy storage options. However, the study shows that the income generated from surplus solar PV energy is not sufficient to cover the total required investment for PHS. Despite this, PHS is seen as a valuable initial investment that can significantly improve the overall performance of the power system [50].

2.5 Optimal storage growth trajectory approach for renewable energy intergration

The integration of RE with sith either a single energy storage system or HESSs has gained significant global attention as an effective solution to address the inherent variability and unpredictability of RE sources. This approach is becoming more economical and cost effective with the use of mature technologies. Further, it improves overall system efficiency and power quality. By minimizing the dynamic stress on the secondary energy storage system, it supports to enhance the energy storage capacity and plant lifetime, and it provides optimal operation. Renewable energy generation is increased in the world with the interest of RE to reduce GHG emission. Because of that, each year energy storages need to add to the power system to avoid the problems occurred with the increasing RE. This optimal growth trajectory has been introduced to identify the technical and economically optimal energy storage capacities on the planned horizon every year.

A method is proposed for determining the optimal capacity of an energy storage system integrated with RE, considering the complex degradation behavior of Li-ion batteries. The suggested sizing algorithm calculates the revenue of the power plant considering the impact of energy storage operation on degradation of BS. In this system, the energy storage is exclusively designed using Li-ion batteries. Consequently, the batteries must be replaced before significant capacity fade occurs within the planning horizon. According to the algorithm, additional battery capacity is limited by the original energy storage capacity due to the additional cost for battery storage containers. On the other hand, when energy storage is integrated with solar power, wind power generation provides higher profitability with optimal storage capacity, as demonstrated by data from South Korea [58]. This research primarily aims to identify the optimal year for additional battery storage installation to ensure uninterrupted operation of the renewable power plant, despite battery degradation over the planning horizon. The proposed optimal method is the sub-optimal method and researchers are recommended to implement an optimization algorithm for decision-making under uncertainty.

A techno-economic analysis was conducted to determine the optimal growth trajectory of the system in Japan, Kyushu region [8]. The study emphasizes minimizing soalr energy curtailment by using HESS that integrating PHS and Li-ion batteries. Monte Carlo random sampling was used to substantially decrese the computational requirements of the analysis and to test a wide range of intervals. SLinear programming optimization was employed to generate sample growth trajectories, optimizing energy flow based on technical performance. This involved calculating the energy balance using solar PV capacity under various energy storage scenarios. An equation for LCOG was introdused to provide a financial assessment of the optimal growth trajectory.

In contrast, only a few previous works have focused on HESS integrating pumped-hydro and batteries to maximize solar energy generation and minimize thermal energy generation in power systems. Further, most of the studies are based on sizing energy storage systems considering limited to renewable energy power plant projects. This proposed study focuses to identify the optimal growth trajectory with supporting rapid PV capacity growth by developing multi-objective optimization sizing and costing algorithm for HESS combining PHS and BS.

CHAPTER 3

METHODOLOGY

This chapter outlines the methodology followed in this study to determine the optimal capacities for solar PV and HESS, including the identification of the optimal time periods for integrating system capacities into the system. The determination of the techno-economic and environmental optimal roadmap for the proposed system is illustrated in Fig. 3.1, including the sequential flow leading to the final results.

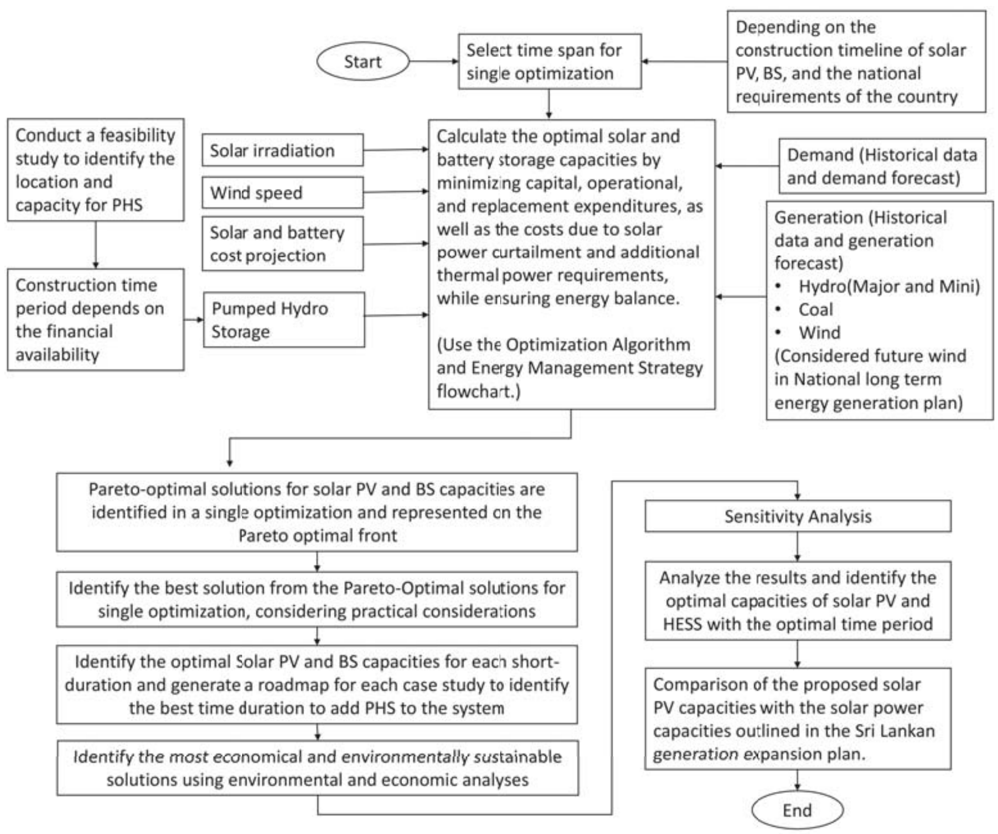

Fig. 3.1: Determination of techno- economic and environmental optimal roadmap for the proposed system

The proposed solar PV and HESS systems are designed for a long-term duration. However, to achieve the most effective solution, an optimization algorithm is developed for short-term durations, allowing for the identification of optimal capacities for each specific period. The methodology begins by selecting the time span for single optimization, based on the construction period of solar PV and BS. Next, the optimal capacities for solar PV and BS are calculated using an optimization algorithm and energy management strategies. The input parameters for the optimization algorithm and energy management system include solar irradiation, wind speed, energy demand and generation, solar PV and battery cost projections, PHS capacities, and other relevant parameters. After several iterations, the optimization algorithm generates multiple solutions for the short-term, which are represented on a Pareto optimal front. All solutions on the Pareto front are considered as optimal solutions. To identify the most suitable solution, practical considerations and constraints are incorporated.

As a result of the optimization algorithm, the capacities of the BS system are determined. Due to the complexity of the PHS system, its capacity is determined following a feasibility study. To determine the optimal time period for integrating PHS into the system, various cases are analyzed by adjusting the years of PHS addition to the system at predefined stages.

After identifying optimal results for each short-term period across different cases, roadmaps are developed for each case. The roadmap with the lowest economic and environmental impact is then identified by conducting environmental and economic analyses for all cases with the optimal capacities. A sensitivity analysis is conducted to define the optimal roadmap from the identified lower economic and environmental solutions considering interest rate of the country. As a final result, the best time periods for adding solar PV, BS and PHS capacities are determined ensuring minimal cost variations for the proposed system. For justify the results, the proposed solar PV capacities are compared with the long-term generation plan in the country to ensure alignment with the national solar energy requirements.

This chapter provides a detailed discussion of all the steps, including the models for each system, the theoretical development of the optimization algorithm, and the energy management control strategies.

3.1 System configuration and modelling

The proposed power system primarily consists of power generation plants, energy storage systems, and connected loads. The power generation plants considered in this study include thermal power plants (coal and oil), major and minor hydro power plants, utility-scale and rooftop solar power plants, and wind power plants, based on the studied power system. This selection can be adjusted to align with the specific features of the power system under study and may include other types of power plants, such as nuclear or liquefied natural gas (LNG) power plants. The energy storage systems considered include Li-ion BS and PHS systems. If any additional energy storage systems are integrated into the power system, they should also be included. The energy management system can be adjusted based on the selected energy storages technologies and is responsible for managing the newly added solar PV and HESS energy.

AC/AC converters are used to connect AC-generated loads, such as thermal power plants and hydro power plants, to the AC bus. Pumped hydro power plants, which operate on AC, are also connected to the AC bus via AC/AC converters. DC/DC converters link solar PV power plants and BS systems with DC output to the DC bus. A DC/AC inverter is used to interconnect the DC and AC buses, ensuring energy balance between the buses within the system. The system configuration for the proposed system, considering these connections is illustrated in Fig. 3.2.

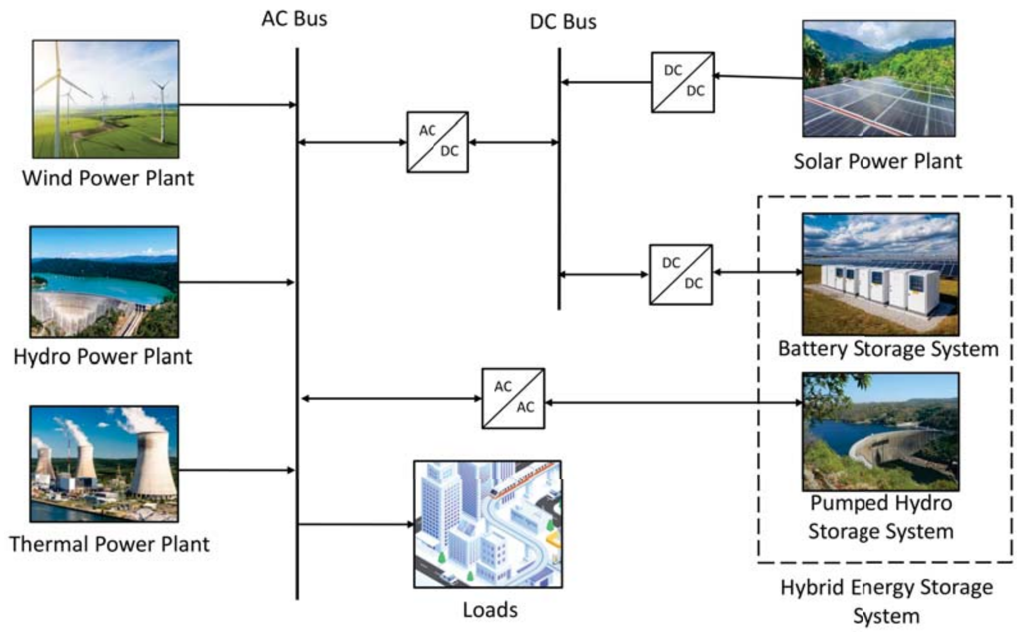

Fig. 3.2: System configuration for HESS

After connecting all the equipment to the system, the status of each power plant and load is continuously monitored to balance energy demand and generation. This includes parameters such as energy generation from existing power plants, newly added solar PV power, the SOC of the BS, the water level of the PHS, and electricity demand. Using an energy management system, surplus solar energy is stored in the HESS, and energy is released back into the system when needed. The energy management system ensures the optimal utilization of integrated resources and efficiently manages energy storage.

Sizing strategies for the solar PV, BS, and PHS systems are defined to facilitate the implementation of the optimization algorithm and the energy management system.

3.1.1 Solar PV System

To calculate the energy generated by the proposed solar PV system, an accurate solar PV model is developed that incorporates solar irradiation and temperature as variable input parameters. Solar irradiation and temperature directly affect the voltage and current characteristics of a solar PV module. In addition, these parameters vary over time due to changing weather conditions, they are considered time-varying inputs in the developed model. The power generated by the solar PV panels at time t can be calculated by using Eq. (3.1) [59].

$$p_{pv(t)} = P_{R,pv} \times \left[\frac{R_{(t)}}{R_{ref}}\right] \times \left[1 + N_T(T_{c(t)} - T_{ref})\right] \tag{3.1}$$

Where,

$p_{pv(t)}$ - The power generated by the PV panels at time t in W

$P_{R,pv}$ - The selected PV panel rated power in W

$R_{(t)}$ - The solar irradiation in W/m^2

R_{ref} - The solar irradiation at reference conditions in W/m^2

T_{ref} - The cell temperature at reference conditions in $°C$

N_T - The temperature coefficient of the selected PV panel in $°C^{-1}$

$T_{c(t)}$ - The cell temperature in $°C$

R_{ref} and T_{ref} are usually set as $1000W/m^2$ and $25\,°C$, respectively, under Standard Test Conditions (STC). The value of $P_{R,pv}$ and N_T depend on the selected solar PV panel and $R_{(t)}$ varies based on the chosen location for implementing the solar PV power plant. $T_{c(t)}$ can be calculated by using Eq. (3.2).

$$T_{c(t)} = T_{air} + \left[\left[\frac{NOCT - 20}{800}\right] \times R_{(t)}\right] \tag{3.2}$$

Where,

T_{air} - The ambient air temperature in $°C$

$NOCT$ - The nominal operating cell temperature (NOCT) in $°C$, is a characteristic parameter of the PV module, typically provided by the module manufacturer.

The overall solar PV power generated by the designed solar PV plant at time t can be calculated using Eq.(3.3), and it depends the number of solar panels connected in the solar PV system. Additionally, Eq.(3.4) provides the output energy of solar PV system at time t [60].

$$P_{pv(t)} = N_{pv} \times p_{pv(t)} \tag{3.3}$$

Where,

N_{pv} - The number of solar PV panel for a proposed solar PV systems

$p_{pv(t)}$ - The output solar PV panel relevant to the solar irradiation at time t in W

$P_{pv(t)}$ - The overall generated solar PV power in W

$$E_{pv(t)} = P_{pv(t)} \times \Delta t \tag{3.4}$$

Where,

$E_{pv(t)}$ - The output energy of solar PV system at time t in *Wh*

$P_{pv(t)}$ - The overall generated solar PV power in W

Δt - The time difference between the samples in sec

Using the designed model, the solar PV energy generated by the power plant at time t is calculated based on the solar irradiation and temperature at that specific time.

3.1.2 Battery storage (BS) System

BS is selected as a one of the technologies for implementing the HESS. Among various battery technologies, Li-ion BS is chosen for this study due to its fast response times, high power and energy density, higher round-trip efficiency, independence from natural conditions, and better performance compared to other battery technologies. Additionally, it has favorable energy-to-power ratio, and technological maturity.

When generation exceeds energy demand at a specific time, the BS is used to store the excess solar PV energy. Alternatively, when available sources cannot meet the required energy demand from power generation sources, the BS is used to release the necessary energy. The transition between the charging and discharging states of the BS is determined by energy management control strategies. The BS enters a charging state when the total solar PV generation output exceeds the energy demand. The energy quantity of the BS system at time t after the charging process, can be calculated using Eq. (3.5). Conversely, the BS enters a discharging state when the total solar PV generation output is lower than the energy demand. The energy quantity of the BS at time t after the discharging process is given in Eq. (3.6) [60, 61].

$$E_{BS\ (t)} = \left[E_{BS\ (t-1)} - (1 - \sigma)\right] + \left[E_{PV\ (t)} - \frac{E_{load\ (t)}}{\eta_{inv}}\right] \times \eta_{BS} \tag{3.5}$$

$$E_{BS\ (t)} = \left[E_{BS\ (t-1)} - (1 - \sigma)\right] - \left[\left[\frac{E_{load\ (t)}}{\eta_{inv}} - E_{PV\ (t)}\right] / \eta_{BS}\right] \tag{3.6}$$

Where,

$E_{BS\ (t)}$ - The energy quantities of the BS system at time t in *Wh*

$E_{BS\ (t-1)}$ - The energy quantities of the BS system at time $(t-1)$ in *Wh*

σ - The hourly self-discharge rate

η_{inv} - The inverter efficiency of the BS system

η_{BS} - The charge efficiency of the BS system

$E_{PV\ (t)}$ - The generated solar PV energy at time t in *Wh*

$E_{Load\ (t)}$ - The required load energy at time t in *Wh*

When considering the limitations of the designed BS system, two key constraints are identified: the limitations of energy quantity and the limitations of the SOC. The stored energy in the BS at any given time should be maintained within the selected Li-ion BS maximum and minimum energy quantity limits, as defined in Eq. (3.7). In this equation, $E_{BS\ ,min}$ and $E_{BS,max}$ represent the minimum and maximum values of the BS system. The maximum energy storage capacity of the BS is calculated by its nominal capacity (C_{BS}) and the minimum energy quantity of BS is determined by the maximum Depth of Discharge (DOD), as outlined in Eq. (3.8) [59].

$$E_{BS\ ,min} \leq E_{BS\ (t)}\ \leq E_{BS,max} \tag{3.7}$$

$$E_{BS\ ,min} = \ (1\ -\ DOD)\ \times C_{BS} \tag{3.8}$$

The SOC at a specific time t is computed using Eq. (3.9). Here, $E_{ES,nom}$ gives the nominal energy of the BS. Eq. (3.10) shows the limitations of the SOC, considering the minimum and maximum SOC values for the BS. $SOC_{BS,\ min}$ and $SOC_{BS,\ max}$ represent the minimum and maximum SOC values, respectively.

$$SOC_{BS}(t) = \ \frac{E_{BS}(t)}{E_{ES,nom}} \tag{3.9}$$

$$SOC_{BS,\ min} \leq SOC_{BS}(t) \leq SOC_{BS,\ max} \tag{3.10}$$

3.1.3 Pumpued hydro storage (PHS) system

To implemet the HESS, PHS is also selected as the storage technology due to its key features, such as low investment risk, low power generation cost, mature and established technology, and the ability to provide readily available electricity during peak power demand without requiring ramp-up time. Pumped hydropower plants can start within a few minutes and serve as a ‘black start’ source in case of a power blackout in the power system [39]. PHS energy generation and storage depend on the water availability in the lower reservoirs (LR) and upper reservoirs (UR) of the PHS system. Furthermore, the catchment area of the reservoir and weather conditions affect the water availability in the reservoir. The general expression for the water stored in the UR ($Q_{UR(t)}$) and LR ($Q_{LR(t)}$) is given in Eq. (3.11) and Eq. (3.12), respectively.

$$Q_{UR(t)} = Q_{UR(t-1)}(1-\tau) + \int_{t-1}^{t} q_p(t)dt - \int_{t-1}^{t} q_t(t)dt + G_{qUR}(t-1) \tag{3.11}$$

$$Q_{LR(t)} = Q_{LR(t-1)}(1-\tau) - \int_{t-1}^{t} q_p(t)dt + \int_{t-1}^{t} q_t(t)dt + G_{qLR}(t-1) \tag{3.12}$$

Where,

$Q_{UR(t)}$ - The water stored in the UR at time t in m^3

$Q_{LR(t)}$ - The water stored in the LR at time t in m^3

τ - The self-discharge/loss incurred in PHS due to leakage and evaporation in t in m^3

$G_{qUR(t)}$ - The quantity of water in UR gained from direct rainfall over the lake and contributions from the catchment area at time t in m^3

$G_{qLR(t)}$ - The quantity of water in LR gained from direct rainfall over the lake and contributions from the catchment area at time t in m^3

$q_{p(t)}$ - The quantity of water used during the pumping mode (transferred to the UR from the LR) at time in t in m^3

$q_{t(t)}$ - The quantity of water used during the generating mode (released to the LR from the UR) at time t in m^3

The PHS operates in two modes: pump mode, where water is pumped to store energy, and hydro mode, where water is released to generate energy. In pump mode, the quantity of water transferred to the UR ($q_{p(t)}$) is calculated using Eq. (3.13). Conversely, during hydro mode, the quantity of water used for energy generation ($q_{t(t)}$) is determined by Eq. (3.14) [62].

$$q_{p(t)} = \frac{\eta_{pump} \times P_{c\to p(t)}}{\rho g h} \tag{3.13}$$

$$q_{t(t)} = \frac{P_{g\rightarrow c(t)}}{\eta_{gen} \times \rho g h} \tag{3.14}$$

Where,

η_{pump} - The efficiency of the pumping system

η_{gen} - The efficiency of the turbine system

$P_{c\rightarrow p(t)}$ - The power is stored when PHS operates in pumping mode (W)

$P_{g\rightarrow c(t)}$ - The power is generated when PHS operates in generating mode (W)

ρ - The density of water in kgm^{-3}

g - The acceleration of gravity in ms^{-2}

h - The net head in m

When considering the PHS system, due to complexity of the construction, installation and identifying suitable locations, a feasibility study must be conducted to determine the optimal location. The limitations of the PHS system is identifed as its parameters depend on the chosen location. The limits of water stored in the UR and LR are defined by Eq. (3.15) and Eq. (3.16), respectively. $Q_{UR,min}$ and $Q_{UR,max}$ denote the mimimum and maximum values of the UR, while $Q_{LR,min}$ and $Q_{LR,max}$ give the mimimum and maximum values of the LR, respectively. All these values need to be identified as a part of feasibility study. Finally, Eq. (3.17) gives the limitations for the capacity of the PHS system considering selected geological locations. $C_{PHS,min}$ and $C_{PHS,max}$ represent the boundaries of the PHS capacities.

$$Q_{UR,min} \leq Q_{UR(t)} \leq Q_{UR,max} \tag{3.15}$$

$$Q_{LR,min} \leq Q_{LR(t)} \leq Q_{LR,max} \tag{3.16}$$

$$C_{PHS,min} \leq C_{PHS,nom} \leq C_{PHS,max} \tag{3.17}$$

3.2 Theoretical Developments for Optimization

Optimal capacities for solar PV and HESS are determined by considering the objectives to be achieved after implementing the proposed system. To accomplish this, objective functions, constraints, and decision variables must be clearly defined. An optimization algorithm is implemented to achive the objectives within the defined limitations, and an energy management strategies is used to balance the energy generation and demand in power system. In this section, the theoretical developments relevant to the optimization algorithm and energy managment strategies are described.

3.2.1 Objective functions and constrains

This study focuses on identifying the optimal capacities for solar PV and HESS using a newly developed optimization algorithm, while maximizing solar PV energy generation and minimizing oil-fired thermal generation throughout the planning horizon. To implement the optimization algorithm, two objectives functions are identified. The primary objective is to minimize the total system cost, as represented in Eq. (3.18) and Eq. (3.19). This objective focuses on reducing capital expenditures (CAPEX), operational expenditures (OPEX), and replacement expenditures (REPEX) throughout the prroject lifetime. Total implementation and operation cost of the proposed system throughout the planning horizon is calculated using Eq. (3.18). The goal of this objective is to minimize the cost for each system without over-sizing,

$$f_{TOTEX} = f_{CAPEX} + f_{OPEX} + f_{REPEX} \tag{3.18}$$

Where,

f_{TOTEX} - The total cost of the proposed system (USD)

f_{CAPEX} - The capital expenditures for all systems, including solar PV, BS and PHS systems (USD)

f_{OPEX} - The operational expenditures for all systems, including solar PV, BS and PHS systems (USD)

f_{REPEX} - The replacement expenditures, respectively, for all systems, including solar PV, BS and PHS systems (USD)

Eq. (3.19) represents the summation of all system expenditures, including detail notations. Where sys_0, sys_1 and sys_2 give the solar PV, BS and PHS systems, respectively. Replacement expenditures are applied only to the BS system during the lifetime of the project, considering the lifespan of the BS. The lifetime of the other two systems, solar PV and PHS, are sufficient for long period. They can function for at least 25 years after installation,with the assumption that no replacements are needed during the planning horizon. Therefore, replacement expenditures are not included with the solar PV and PHS systems. The number of BS replacements required over the lifetime of the system is calculated using Eq. (3.20).

$$f_{TOTEX} = \sum_{sys_i = sys_0}^{sys_n} \left\{ C_{sys_i} \left[\gamma_{sys_i} + \beta_{sys_i} \sum_{n=1}^{T_{life}-T_{sopt}} (1+r)^{(T_{sopt}+n)} \right] \right\}$$
$$+ C_{BS,rep} \left[\gamma_{sys_1} \sum_{j=1}^{N_{BS,rep}} (1+r)^{(T_{sopt}+(T_{BS,rep,yr} \times j))} \right] \tag{3.19}$$
$$Where, i = 0, 1, 2$$

$$N_{BS,rep} = \frac{T_{life} - Y_{opt}}{T_{BS,rep,yr}} \tag{3.20}$$

Where,

C_{sys_i} - The system capacity for each system, where sys_0, sys_1 and sys_2

$C_{BS,rep}$ - The replacement capacity for BS system for planning horizon

γ_{sys_i} - The unitary capital cost for each system in USD/kW

β_{sys_i} - The unitary operational cost for each system in USD/kW-yr

r - The annual interest rate in $\%$

$T_{BS,rep,yr}$ - The battery lifetime for a selected li-ion BS system (years)

n - The index n starts from 1 and increments until it reaches T_{life}

T_{sopt} - The time span for single optimization during the proposed system's lifetime $(years)$

$N_{BS,rep}$ - The number of times the BS needs to be replaced within the planning horizon

T_{life} - The lifetime of the proposed system $(years)$

Y_{opt} - The number of years considered for a single short-term optimization $(years)$

The second objective is to reduce expenditures related to curtailment of solar power and the additional demand for oil-fired thermal power generation. This secondary objective aims to minimize the costs arising from curtailed solar energy due to excess generation of solar PV energy and the additional oil-fired thermal energy generation required to fulfill the system energy demand due to the unavailability or insufficiency of storage capacities. In Eq.(3.21), $f_{Surcharges}$ represents the combined expenditures from solar power curtailment and thermal energy generation. Eq.(3.22) provides the detailed equation for calculating the costs related to solar curtalment and oil-fired thermal energy generation.

$$f_{Surcharges} = f_{CSC} + f_{CTB} \tag{3.21}$$

Where,

f_{CSC} - The costs associated with solar energy curtailment

f_{CTB} - The costs associated with the additional oil-fired thermal energy required to meet the energy demand

$$f_{Surcharges} = \sum_{n=Y_{opt}}^{Y_{opt}+T_{sopt}} (\alpha_{pv} E_{SC} + \alpha_{thermal} E_{TB}) (1 + r)^n \tag{3.22}$$

Where,

α_{pv} - The unitary cost of the solar PV generation in USD/kWh

$\alpha_{thermal}$ - The unitary cost of the oil-fired thermal generation in USD/kWh

E_{SC} - The total solar PV energy that cannot be absorbed by the energy storage system in kWh

E_{TB} - The total energy supplied by oil-fired thermal power plants, when the energy storage system is unable to meet the demand in kWh

Y_{opt}, T_{opt}, T_{sopt}, r and n have similar meanings in Eq.(3.19).

3.2.2 System active power balance

To maintain power system stability, energy generation and demand need to be balanced. Therefore, the power generated from each power plant (hydro, wind, coal, and solar PV) and the released energy from the HESS must be balanced in each interval. To keep the power system stable, it is necessary to identify the power plants responsible for handling the base load. These identified power plants, responsible for handling the base load, can be kept fixed throughout the planning horizon, considering the national requirements of the country. For this study, coal and hydro power generation are assumed to be fixed power plants for the entire duration of the lifetime of the system, as indicated in Eq. (3.23).

$$P_{FPP(t)} = P_{coal(t)} + P_{Hydro(t)} \tag{3.23}$$

Where,

$P_{Hydro(t)}$ - The hydro power generation at time t in W

$P_{coal(t)}$ - The coal power generation at time t in W

$P_{FPP(t)}$ - The power generation from fixed power plants in W, it is depended on the considered power system as fixed power plants

The capacity of PHS cannot be directly determined by using the optimization algorithm due to the complexities and constraints associated with the design and installation of PHS, especially in relation to geological factors. Additionally, PHS cannot be implemented within a short-time duration, as it involves a lengthy implementation process. The PHS capacities can be identified after conducting a feasibility study specific to the region or country where the power system is to be deployed. After determining the capacities from the feasibility studies, the optimal time period for integrating PHS into the system can be identifed through case studies. The BS capacities can be determined as the result of the optimization algorithm. The power stored in the HESS is given in Eq. (3.24), which consists of the power stored in both the BS and PHS. When HESS is in charging mode, $P_{HESS(t)}$ in Eq. (3.24) is negative, and when HESS is in discharging mode, $P_{HESS(t)}$ is positive.

$$P_{HESS(t)} = P_{BS(t)} + P_{PHS(t)} \tag{3.24}$$

Where,

$P_{HESS(t)}$ - Available power quantity in HESS at time t in W

$P_{PHS(t)}$ - Available power quantity in BS at time t in W

$P_{BS(t)}$ - Available power quantity in PHS at time t in W

Power generated from fixed power plants, wind power plants, and solar power plants are considered as power generation sources. Scheduled wind power plants, as outlined in the energy generation expansion plan of the country, are considered for planning horizon, as wind power is a renewable energy source. Existing solar PV power plants and the capacities determined by the optimization algorithm are taken as the solar energy sources.

Further, the total generated power from each source should be greater than or equal to the connected load in each interval, as shown in Eq. (3.25), to ensure system balance. If the generated power is insufficient to provide the system requirement, it will be supplied by oil-fired thermal power plants.

$$P_{L(t)} \geq P_{PV(t)} + P_{wind(t)} + P_{HESS(t)} + P_{FPP(t)} \tag{3.25}$$

Where,

$P_{PV(t)}$ - The power generated by the installed solar PV system at time t in W

$P_{wind(t)}$ - The power generated by the installed wind plant at time t in W

$P_{L(t)}$ - The connected load at time t in W

$P_{HESS(t)}$ and $P_{FPP(t)}$ have similar meanings as previously described.

3.2.3 Decision variables

The decision variables include the capacities of the HESS, which collectively influence system performance and energy capture from solar resources. Implementing HESS requires determining the appropriate capacities for both BS and PHS. In this study,the solar PV capacity (C_{PV}), and BS capacity (C_{BS}), are selected as the primary decision variables within the optimization framework.

This algorithm determines the best combination of decision variables to achieve the specified objectives. Eq. (3.26) and (3.27) establish the optimization space for these identified variables, focus on exclude non-feasible regions from the feasible region and thereby enhance computational efficiency during the optimization process.

$$C_{PV,min} \leq C_{PV} \leq C_{PV,max} \tag{3.26}$$

Where,

$C_{PV,min}$ - The minimum solar PV capacities

$C_{PV,max}$ - The maximum solar PV capacities

$$C_{BS,min} \leq C_{BS} \leq C_{BS,max} \tag{3.27}$$

Where,

$C_{BS,min}$ - The minimum battery storage capacities

$C_{BS,max}$ - The maximum battery storage capacities

3.2.4 The optimization algorithm incorporating energy management control strategy

Multi-objective optimization is used to address problems involving multiple objective functions that need to be optimized simultaneously. The NSGA-II, a variant of the Genetic Algorithm (GA), is employed to solve the optimization problem. Single optimization is conducted over a short time period to identify the solar PV capacity and BS capacity for each short-time duration. The time duration for single optimization is determined based on the construction and installation periods of solar PV and battery storage systems, together with the national energy demands of the selected region or country. An energy management strategy is integraded with the optimization algorithm, calculating the energy quantities during the charging and discharging of each energy storage system. Furthermore, the project lifetime is defined based on the lifespans of solar panels and PHS storage systems.

The optimization process begins with the initial selection of solar PV and BS capacities from a randomly generated population. After performing the required calculations, constraints are evaluated, and solutions are ranked based on Pareto dominance. The algorithm uses crowding distance to examine the diversity of the solutions. If the termination criteria are satisfied, the algorithm proceeds to select the next population. Ultimately, the optimal optimal solar PV and BS capacities are obtained through a single optimization pocess, with the results presented on the Pareto optimal front. Theroritically, all solutions provided by the optimization algorithm can be considered as optimal solutions for the study. Therefore, the best optimal solution is selected from the Pareto optimal solutions, considering practical factors.

The flowchart for the proposed optimization algorithm, incorporating energy management strategies for a single optimization process, is shown in Fig. 3.3.

Using the randomly generated population, the capacities of solar PV and BS are selected for optimization. These capacities are used to calculate the capital expenditure, operational and maintenance costs, and replacement costs, considering unitary cost predictions for each system. The time duration for a single optimization is determined based on the construction duration of the solar PV and BS systems. This allows the construction costs of these systems to be accounted for within the specific time duration, without needing to be distributed over longer periods. In order to include PHS into the system, the construction cost is distributed over the construction time periods, rather than just the short-term duration. Once the PHS is added, predicted operational and maintenance costs for PHS are included in the calculations for each year. During the short time period considered in the optimization process, solar curtailment costs and additional oil-fired thermal generation costs are also calculated. To ensure the system remains balanced, an energy management control strategy is developed. This strategy aims to balance energy generation form existing power plants, energy demand, and the charging and discharging of the energy storage systems. It also incorporates the limitations of the BS, PHS, and other factors.

The flowchart provided in Fig. 3.3 also outlines the power dispatch strategy implemented by the energy management control system for the proposed configuration. This strategy calculates the costs associated with solar curtailment and additional oil-fired thermal power generation over the considered short time duration, providing these costs as inputs for the optimization algorithm.

The energy management system ensures system-wide energy balance at a given

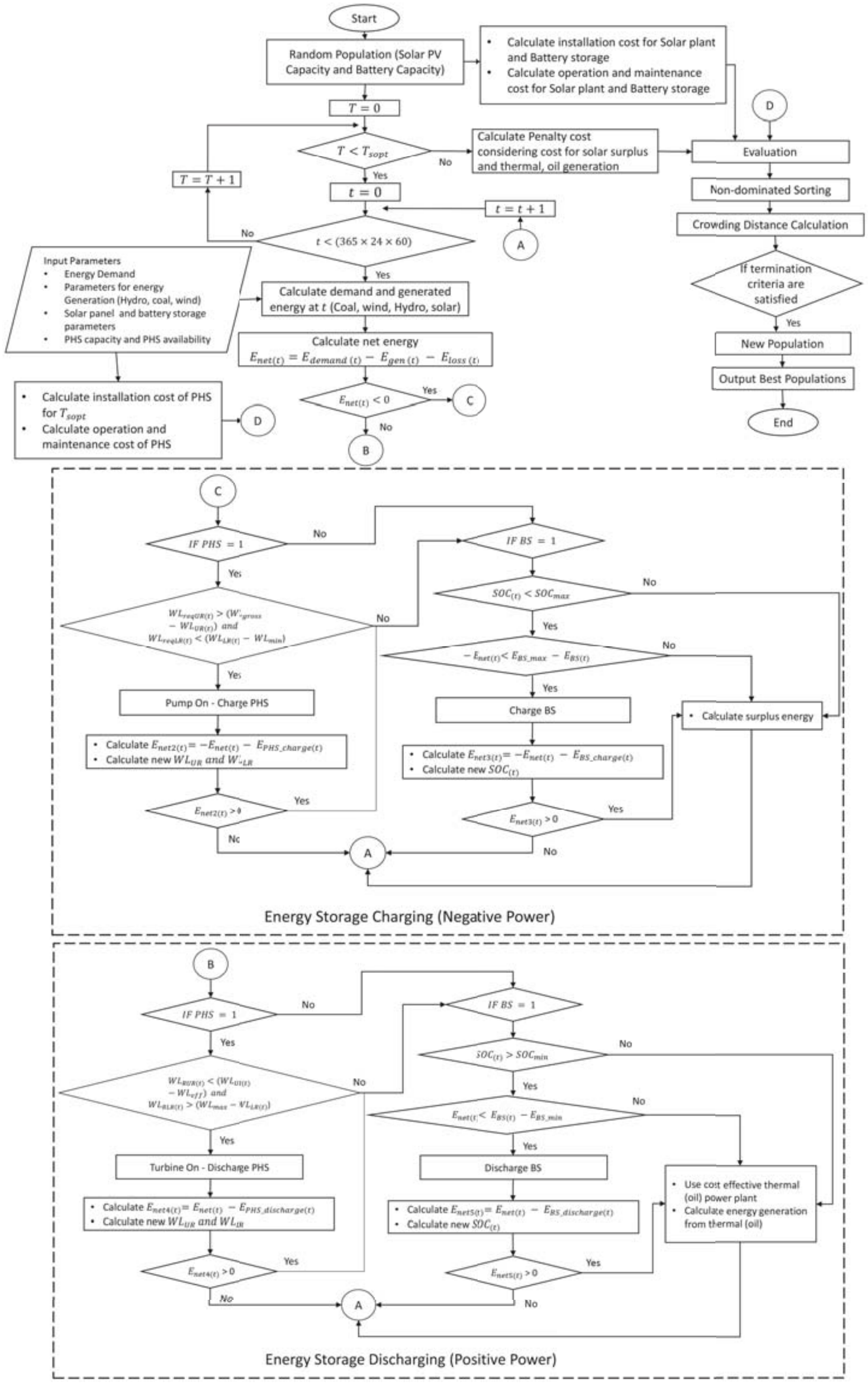

Fig. 3.3: The proposed optimization algorithm, incorporating energy management strategies for a single optimization process

time t, based on the selected solar PV and BS capacities from the randomly generated population. The time period for a single optimization is denoted as T_{sopt} in the flowchart. At the specified time t, the input parameters for the energy management system include energy demand, energy generation from each generation source, solar PV panel specifications, battery storage model parameters, pumped hydro Storge capacity and associated characteristics, besides wind speed, solar irradiation, and other weather-related data.

Energy demand, energy generation and energy loss at a specific time t are calculated using the input parameters. Subsequently, the net energy is determined using these calculated values, as shown in Eq. (3.28).

$$E_{net(t)} = E_{demand(t)} - E_{gen(t)} - E_{loss(t)} \tag{3.28}$$

Where,

$E_{net(t)}$ - The net energy at specfic time t considering energy generation, demand and losses at specific time in W

$E_{demand(t)}$ - The energy demand at specfic time t in W

$E_{gen(t)}$ - The generated energy from all sources at specfic time t in W

$E_{loss(t)}$ - The energy loss due to transmission and distribution at the specified time t in W

The charging or discharging state of the HESS is then identifed based on the positivity or negativity of the net energy value.

A negative value of $E_{net(t)}$ indicates that energy generation exceeds consumption at time t, allowing the surplus to be stored in the HESS. This stage is referred to as a negative power state for the HESS, as it undergoes charging. Conversely, a positive value of $E_{net(t)}$ indicates that energy generation is insufficient to meet the demand, necessitating the discharge of energy from the HESS to support the system. This stage is referred to as a positive power state for the HESS, as it discharges energy.

During the charging process of the energy storage system, excess energy may be directed to either the PHS or BS, depending on their capacity limits and availability. When PHS is available, the system checks the water levels in both the UR and LR. For energy to be stored via pumping, the LR must hold enough water, and the UR must have adequate space to store the pumped volume. Equations (3.29) and (3.30) are applied to assess the availability of UR storage capacity and the LR water availability. Specially, $WL_{reqUR(t)}$ denotes the required increase in UR water level, which must not exceed the gap between the gross water level (WL_{gross}) and the current water level in the UR ($WL_{UR(t)}$). Likewise, $WL_{reqLR(t)}$ indicates the required decrease in the LR water level, which must not fall below the minimum permissible level (WL_{min}) minus the current water level in the LR ($WL_{LR(t)}$). Once the pump is activated and the PHS system is charged, the updated water levels in the UR and LR, represented by $WL_{UR(t)}$ and $WL_{LR(t)}$ respectively, are calculated using Equations (3.31) and (3.32). The energy stored in the PHS at time t, denoted as ($E_{PHS\_charge(t)}$), is determined using Eq. (3.13). Any remaining surplus energy, ($E_{net2(t)}$), is then determined using Eq. (3.33). This residual energy, if available, can be kept in the battery storage system. If no additional excess energy remains, the process advances to the subsequent time period.

$$WL_{reqUR(t)} > (WL_{gross} - WL_{UR(t)}) \tag{3.29}$$

$$WL_{reqLR(t)} < (WL_{LR(t)} - WL_{min}) \tag{3.30}$$

$$WL_{UR(t)} = WL_{UR(t-1)} + WL_{reqUR(t)} \tag{3.31}$$

$$WL_{LR(t)} = WL_{LR(t-1)} - WL_{reqLR(t)} \tag{3.32}$$

$$E_{net2(t)} = -E_{net(t)} - E_{PHS\_charge(t)} \tag{3.33}$$

If the PHS system is unavailable due to insufficient water levels or storage limitations or if extra energy remains after PHS utilization, the battery storage system is used for energy storage. Prior to charging the battery storage, the SOC must be evaluated. If the SOC is below its upper limit, the battery storage system is eligible for charging. Eq. (3.34) is utilized to assess the capacity availability and identify whether it is adequate to accommodate the surplus energy. In this context, E_{BS_max} and $E_{BS(t)}$ give the maximum capacity of storage and the current energy level of the battery storage system, respectively. Following the charging process, the updated SOC is computed applying Eq. (3.9), while the energy saved in the BS system ($E_{BS\_charge(t)}$) is calculated using Equations (3.5) and (3.35). Any remaining surplus energy after BS charging ($E_{net3(t)}$) is determined using Eq. (3.36). If no excess energy remains, the algorithm advances to the next time step. Any portion of excess energy that cannot be stored in the proposed HESS is considered solar curtailment throughout the corresponding time period.

$$-E_{net(t)} < E_{BS\_max} - E_{BS(t)} \tag{3.34}$$

$$E_{BS\_ch(t)} = E_{BS(t)} - E_{BS(t-1)} \tag{3.35}$$

$$E_{net3(t)} = -E_{net(t)} - E_{BS\_charge(t)} \tag{3.36}$$

In the course of energy discharge process, energy can be discharged from either the PHS or battery storage system, as determined by the available energy and the operational constraints of each system. If PHS is available, the UR water level is first assessed to confirm sufficient water is present for discharge, at the same time the LR must have adequate capacity to accommodate the discharged water. Equations (3.37) and (3.38) are utilized to examine the available discharge UR volume and the LR storage capacity, respectively. The reduced water level in the UR after discharge, denoted as $\mathrm{WL}_{RUR(t)}$, should be less than the difference between the current water level ($WL_{UR(t)}$) and the effective water level (WL_{eff}) in the UR. Similarly, the raised LR water level after receiving the discharged water, $WL_{RLR(t)}$, should be less than the difference between the maximum allowable level (WL_{max}) and the current LR level ($WL_{LR(t)}$). The turbine is activated, when both conditions are satisfied, and the PHS release energy to fulfill system demand. The renewed water levels in the UR and LR, ($WL_{UR(t)}$ and $WL_{LR(t)}$), are calculated using Equations (3.39) and (3.40), respectively. The energy discharge from the PHS ($E_{PHS\_discharge(t)}$) is computed using Eq. (3.14), while any remaining energy demand after PHS discharge ($E_{net4(t)}$) is determined using Eq. (3.41). If additional energy is required beyond what the PHS can supply, the BS system is utilized to fulfill the deficit. If no further energy is needed, the process proceeds to the next time step.

$$WL_{RUR(t)} < (WL_{UR(t)} - WL_{eff}) \tag{3.37}$$

$$WL_{RLR(t)} > (WL_{max} - WL_{LR(t)}) \tag{3.38}$$

$$WL_{UR(t)} = WL_{UR(t-1)} - WL_{RUR(t)} \tag{3.39}$$

$$WL_{LR(t)} = WL_{LR(t-1)} + WL_{RLR(t)} \tag{3.40}$$

$$E_{net4(t)} = E_{net(t)} - E_{PHS\_discharge(t)} \tag{3.41}$$

If PHS is not implement or not available or its water levels are not sufficient to meet the required energy demand, the battery storage system can be used to supply the surplus energy for the system. Prior to beginning the discharge procedure, the SOC of the battery storage system is verified. If the SOC is above the smallest allowable threshold, the BS system is able to discharge the necessary energy to the system. Eq. (3.42) is utilized to evaluate the capacity availability of the battery storage system and determine whether it can provide the energy requirement. In this context, E_{BS_min} represents the minimum energy storage capacity, while $E_{BS(t)}$ denotes the available energy in the battery storage system. After energy has been discharged, the updated SOC is calculated using Eq. (3.9). The energy discharged by the battery storage system ($E_{BS\_discharge(t)}$) is determined by Eq. (3.43), and any remaining energy required to balance the system ($E_{net5(t)}$) is determined using Eq. (3.44). If further energy is not needed, the process advances to the next time period. The most profitably efficient oil-fired thermal power plant is activated, additional energy is required to fulfill the remaining demand and balance the system. Then, energy generated from oil-fired thermal generation is calculated for identify the costs relavant to the required addtional thermal oil generation.

$$E_{net(t)} < E_{BS(t)} - E_{BS\_min} \tag{3.42}$$

$$E_{BS\_dch(t)} = E_{BS(t-1)} - E_{BS(t)} \tag{3.43}$$

$$E_{net5(t)} = E_{net(t)} - E_{BS\_discharge(t)} \tag{3.44}$$

Once all costs related to the solar PV and HESS systems are calculated, the findings enter an assessment stage. This stage comprises non-dominated sorting and crowding distance measures. After assessing whether the specified optimization constrains are met, a new set of individuals is created. The optimization algorithm continues refining the results over successive generations, resulting in the selection of the most optimal population.

3.2.5 Computational tools for solving the optimization problem

To solve the multi-objective optimization problem, a computational problem solver is required. In this study, the open-source framework for multi-objective optimization in Python (Pymoo) is used to solve the optimization problem using the NSGA-II.

NSGA - II is selected as the evolutionary algorithm from GA, which are particularly highly effective in addressing complex real-world problems involving multiple variables. It offers greater speed and practicality compared to traditional optimization methods like dynamic and linear programming. The NSGA is a specialized version of GA designed for multi-objective optimization problems, where multiple objectives need to be optimized simultaneously while maintaining computational efficiency. NSGA-II is an enhanced updated implementation of the original NSGA, adding characteristics such as non-dominated sorting, crowding distance, and elitism. The aforementioned improvements enable NSGA-II to ensure diversity among solutions along the Pareto front during optimization, producing reliable outcomes. Additionally, crowding distance helps maintain a diverse population without converging to a single solution, and the algorithm operates without requiring manual tuning of parameters or objective weighting. NSGA-II is computationally efficient, versatile, and highly adaptable, making it ideal for applications like optimizing HESS with multiple objectives and variables in renewable energy systems.

Google Colaboratory (Colab), a cloud-based Jupyter Notebook service, is used to write and execute the Python code for the optimization process. The Python code is designed based on the power system parameters considered in the study. Therefore, the power system configurations and parameters may vary for different applications, the code must be modified to reflect the specific power system.

3.2.6 Identification of the roadmap for integrating the proposed system to existing power system

All the solutions on the Pareto optimal front, obtained through the optimization algorithm, can be identified as theoretically optimal solutions. Among the solutions, the best optimal solution is chosen based on practical considerations and the specific requirements of the country or region. The two objectives relevant to this study are the total expenditure resulting from the installation, operation, and maintenance of the proposed system, and the additional costs due to solar curtailment and oil-fired thermal generation. These objectives are represented on two axes, and the middle point of the optimal solutions is selected as the best optimal solution as shown in Fig. 5.1. This approach helps to balance the total and additional costs at a moderate level, ensuring an efficient and cost-effective solution. By using this method, the optimal solar PV and battery storage capacities are identifed for each short time duration during the planning horizon. This method generates a roadmap for effectively integrating the solar PV and BS systems into the power system.

Due to the complexity of construction and the challenges in identifying suitable locations for implementing PHS, the optimal capacities and integration timeline cannot be directly determined by the optimization algorithm. Instead, feasibility studies must first be conducted in the target country or region to identify potential locations and determine the appropriate PHS capacities. Multiple case studies with varying timeframes and capacities are analyzed to determine the appropriate PHS capacity and the optimal timeline for its integration into the system.

Economic aspects are evaluated through a detailed economic analysis, while environmental parameters are assessed through an environmental analysis. Based on these analyses, the most cost-effective and environmentally sustainable solution is identified. Finally, a sensitivity analysis is conducted to determine the minimum cost variation in response to fluctuations in interest rates.

CHAPTER 4

VALIDATION WITH REAL WORLD DATA

To quantitatively validate the proposed optimization algorithm and energy management system for implementing solar PV and HESS systems, a power system from a specific country or region can be utilized. In this study, the Sri Lankan power system is used as a case study to validate the proposed solar PV and HESS systems, based on data released in 2023. Key factors such as energy generation sources and capacities, energy demand, solar irradiation, wind speed and other environmental paramerers are adjusted to the selected country or region. All the parameters must be organized according to the specific power system, and solutions are applicable to the respective country.

To effectively analyze the results of the proposed system, the lifetime of the system needs to be a sufficiently long period. Given that solar PV and PHS are main components of the system, their lifetimes are key considerations when selecting the planning horizon. Both solar PV panels and PHS systems have operational lifetimes exceeding 25 years without the need for major replacements or modifications. Consequently, a 25-year planning horizon is chosen for this proposed system.

4.1 Identification of the time duration for a single optimization

The proposed system is designed for a 25-year planning horizon. To achive optimal performance, the capacities for solar PV and BS are determined for shorter time intervals within this horizon. Therefore, optimization is conducted for the identified short duration, which primaraly depends on the construction timelines for the solar PV, BS, and other national requirements. If any additional major requirements, beyond the construction period of the solar PV and BS systems, they need to be considered into the selection of the time frame for a single optimization. The construction period is dependent on several factors, including project size, location, regulatory approvals, and complexity.

For this study, utility-scale or MW-scale solar PV systems are considered. The design and approval process of these systems typically requires approximately six months or more, depending on factors such as environmental impact assessments, permits, and land acquisition. Following design and approval process, the construction takes between three months to one year, depending on the size and complexity of the project. Similarly, the utility-scale and MW-scale BS systems, the design and approval process takes between six months to one year, influenced by regulatory requirements and grid interconnection Standards. The construction phase for BS systems generally ranges from three to nine months, depending on the storage size of the BS system.

In addition, delays in permits and regulations may arise due to environmental reviews, grid connection studies, or local permitting during the project development process. The availability of components such as solar panels, inverters, batteries, and other system elements, as well as the availability of skilled labor for installation and testing, can also impact the project timeline, either accelerating or delaying completion. Considering all these factors, a two-year time span is chosen as the duration for single short-term optimization to validate the developed algorithms effectively.

4.2 Demand forecast

Energy demand is influenced by various factors, including economic activities, population size and their lifestyle, weather conditions, and other region-specific dynamics. Furthermore, energy demand increases annually due to population growth, rising energy consumption driven by economic development, technological advancements, and industrial expansion. As a result, energy demand growth varies across countries and fluctuates over time based on consumer requirements. The Sri Lankan power system has an average demand growth of 6% and an average peak demand growth of 4.8% for every five years, as specified in the generation plan of the country [11]. Using historical data from 2023, an average load profile was generated, and the predicted load profiles for every five years, based on the historical data and average demand growth, are shown in Fig. 4.1.

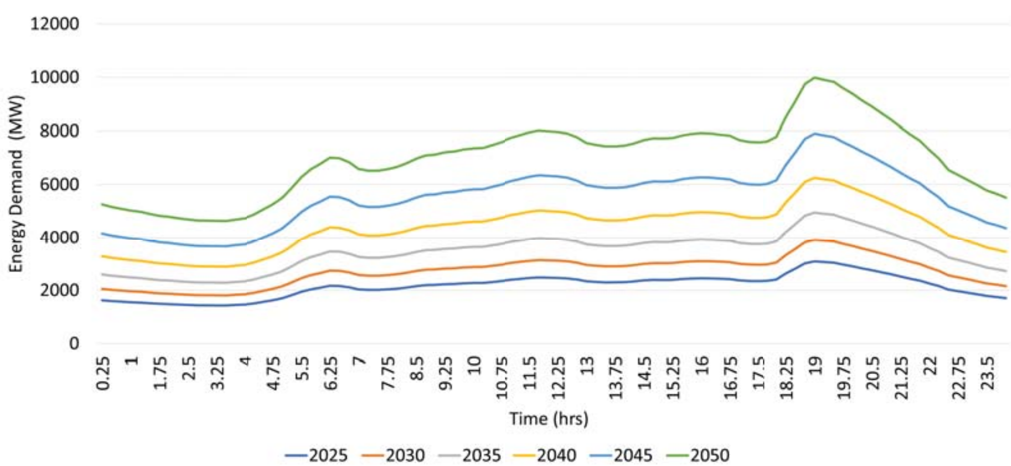

Fig. 4.1: The predicted load profiles for every five years according to the data given in CEB long-term generation plan 2023-2047

Energy demand fluctuates throughout the year due to weather conditions and other seasonal factors. To improve the accuracy of this study, energy demand is predicted at 15-minute intervals using historical data and the average demand growth rate for the simulation process. Demand forecasting in this study utilizes data released by the

Public Utilities Commission of Sri Lanka (PUCSL) for the period from 1^{st} January 2023, to 31^{st} December 2023, recorded at 15-minute intervals [63]. To enhance the accuracy of the system, data spanning more than one year can be utilized for analysis and forecasting.

4.3 Existing power plants and generation forecast

Coal and oil fired thermal, hydro, solar and wind power plants are the major power-generating power plants in Sri Lankan power system. Currently, the installed renewable energy capacity consists 1383 MW of major hydro, 414 MW of minor hydro, 100 MW of utility scale solar, 516 MW of rooftop solar, and 251.5 MW of wind power plants [64].

New major hydro power plants (with capacities exceeding 10 MW) are not planned for the next 25 years due to the limited availability of land in the country according to the long-term energy generation plan in the Sri Lanka [11]. Consequently, new major hydropower plants are not included in the proposed system for the planning horizon. Further, mini hydro power plants are not considered due to their samll scale, and detailed plans for their development over the next 25 years have not been published. However, wind power plants are planned for implementation within this timeframe. For this study, the planned wind power plants are assumed to be installed according to their designated years with planned capacities, because wind power is a renewable energy source. The planned wind power plant capacities for each year, from 2023 to 2042, are shown in Table 4.1. Additionally, solar power plant capacities are included in the generation plan, allowing for a comparison of the solar PV capacities obtained from the proposed system. This alignment ensures that the proposed solar PV capacities match the actual energy requirements of the country.

Regarding the existing non-renewable power plants in Sri Lankan power system, a 900 MW coal-fired thermal power plant operates in three stages, and oil-fired thermal power plants with a total capacity of 659.1 MW are in operation to fulfill the national energy requirements. The existing oil-fired thermal power plants in the power system are detailed in Table 4.2, which provides information on the number of units, their individual capacities, and the total capacity of each power station [11]. Some of the thermal power plants are nearing the end of their operational life and are in the retirement stage. To replace these plants, new thermal power plants have been proposed in the generation plan. However, the scheduled thermal power stations in genration plan are not considered for this system. Instead, it is assumed that the existing oil-fired thermal power plants will continue to operate throughout the planned 25-year period. Additionally, the plan aims to reduce the reliance on oil-fired thermal plants to reach the required energy demand. Due to uncertainty associated with renewable energy, such as intermittency, unpredictability caused by weather conditions, renew-

TABLE 4.1: WIND POWER PLANTS CAPACITIES WITH PLANNING YEAR ACCORDING TO THE SRI LANKAN LONG-TERM ENERGY GENERATION PLAN

Year	Wind (MW)
2023	25
2024	60
2025	200
2026	150
2027	100
2028	100
2029	200
2030	200
2031	100
2032	0
2033	100
2034	100
2035	100
2036	100
2037	100
2038	100
2039	100
2040	100
2041	100
2042	100

able energy sources cannot fully cover the energy demand at this stage. Therefore, conventinal power plant with reliable performance are needed to keep the base load of the power system. Consequently, the coal-fired thermal power plant will continue to operate at full capacity to manage the base load due to its low cost and reliability. Existing oil-fired thermal power plants will be maintained to balance the system by providing additional oil-fired thermal energy when the proposed solar PV and HESS are unable to meet the required demand [11].

The existing Sri Lankan power system does not include nuclear power plants, Liquefied Natural Gas (LNG) power plants or other similar types of energy generations. However, if any significant capacities of these types are introduced in the future, they should be considered for the power system. Apart from renewable energy power plants, other types of power plants in the country generation plan are not considered in this study.

Details of the existing power plants in Sri Lanka, including their capacities, types of the source, percentage of annual plant capacity factor, and the expected percentage of output from each source (including the power plants that are going to minimize output), are summarized in Table 4.3, based on the data released in 2022 [64]. For

TABLE 4.2: EXISTING OIL-FIRED THERMAL POWER PLANTS IN SRI LANKAN POWER SYSTEM

Plant Name	No of Units	Name Plate Capacity (MW)	Total Capacity (MW)
Kalanitissa Power Station			
Gas turbine (Small GTs)	4	20	80
Gas turbine (GT 7)	1	115	115
Combined Cycle	1	165	165
Sapugaskanda Power Station			
Diesal	4	20	80
Diesal (Ext.)	8	10	80
Other Thermal Power Plants			
Uthuru Janani	3	8.9	26.7
Barge Mounted Plant	4	15.6	62.4
Containnerized Emergency Power Plant	50	1	50

this study, it is assumed that all existing power plants will be operational for the entire planned system lifetime.

TABLE 4.3: EXISTING POWER PLANTS IN SRI LANKAN POWER SYSTEM

Generator	Power (MW)	Carrier	Annual Plant Capacity factor (%)	Output (%)
Thermal (Coal)	900	Non-renewable	48.4	100
Major Hydro	1383	Renewable	36.3	100
Mini Hydro	414	Renewable	36.3	100
Wind	251.5	Renewable	35.6	100
Thermal (Oil)	659.1	Non-renewable	52	Minimum
Solar (Utility Scale)	100	Renewable	14.4	100
Solar (Roof top)	516	Renewable	14.4	100

All existing power plants cannot be fully utilized for energy generation at all times throughout the planning horizon due to practical considerations. The energy generation from hydro, solar, and wind sources depends on weather patterns throughout the year, with the availability of water, solar radiation, and wind varying seasonally. Due to these factors, the energy output from each power plant varies throughout the year.

When analyzing energy generation in Sri Lanka, the usage of energy-generating power plant depends on the different three seasons throughout the year, driven by the weather patterns in the country. Hydropower plants play a significant role in the Sri Lankan power system, and their use varies depending on the season. The three main seasons in Sri Lanka can be categorized as dry season from January to April, the high wind season from May to August, and the wet season from September to

October.As shown in the generation data for 2023, energy generation patterns from different sources fluctuate across these three seasons. The variation in energy output from different energy sources during these periods is illustrated in Fig. 4.2 ((a) Dry Season – January to April (b) High Wind Season – May to August (c) Wet Season – September to October). Based on these figures, it is possible to identify the usage patterns of different power plants throughout the year, reflecting the impact of seasonal changes.

Furthermore, the generation of wind energy and hydro power has different pattern across the three seasons throughout the year due to varying weather conditions. Wind energy generation depends on the wind speed, and wind speed variations across the three different seasons in 2023 is shown in Fig. 4.3. This figure clearly indicates a high wind season with strong wind speeds, resulting in a significant percentage of wind energy being generated during this period. Similarly, hydropower generation also depends on weather conditions, specially with the rainfall, the availability of the water in reservoirs, and water release from the catchment area. The percentage of hydropower availability in different seasons in 2023 is shown in Fig. 4.4. It also demonstrates a higher percentage of hydro energy generation during the wet season due to the increased water availability compared to the other two seasons.

When considering the energy generation forecast, the predicted generation profile for every five years is shown in Fig. 4.5, including a net loss of power system, based on the data from long-term generation plan (2023-2042) in Sri Lanka [11]. The expected net generation is 18,186 GWh in 2023 and 58,560 GWh in 2047. The average growth rate of energy generation is projected to be 5.9 % for every five years. To supply the predicted energy demand for each year, the required energy generation is estimated considering transmission and distribution losses in the power system. According to published data, transmission and distribution losses were 13.9 % in 2009, and this figure decreased to 9.46 % in 2021. For the next 25 years, the lowest and most recent value of 9.46 % is assumed as the transmission and distribution losses.

The selection of power plants for electricity generation depends on several parameters. Weather conditions are primarily considered for renewable energy generation. Therefore, the same weather pattern is assumed throughout the year for the planning years. Energy generation details, including power plant types and generated energy from each type of sources, were obtained from the historical energy generation data released by PUCSL. This data covers 15-minute intervals from 1 st January 2023, to 31 st December 2023. As an example, the generated power plant details for a specific day (24th May 2023) are provided in ANNEX A, including the generated energy by each type of power plants.

To improve the accuracy of the energy generation forecast, historical data released for the year 2023 is used to predict the generation pattern for the planning years. For meeting the base load demand of the system, a coal-fired thermal power plant is in-

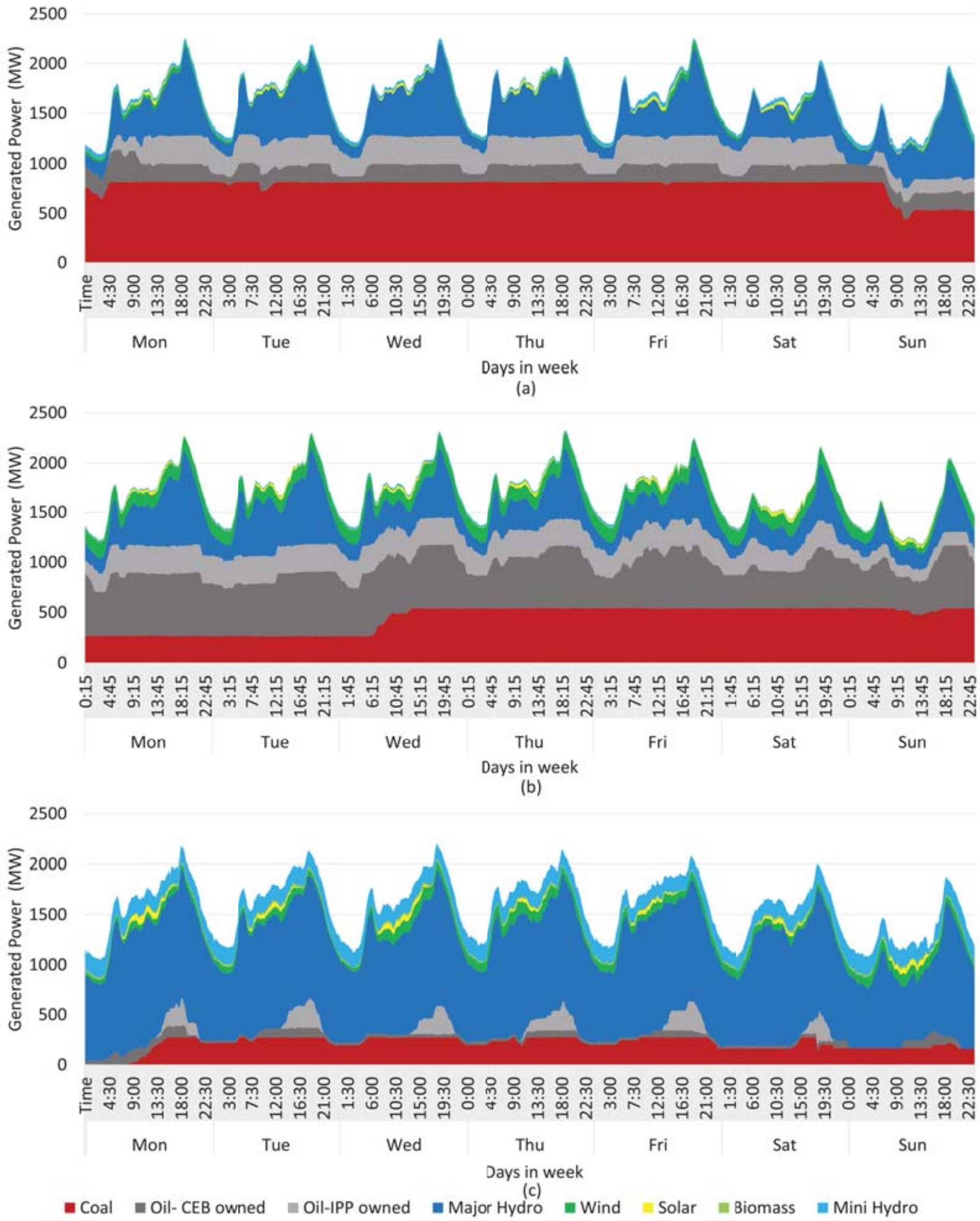

Fig. 4.2: Variation in energy generation patterns from different energy sources across three seasons throughout the year (a) Dry Season – January to April (b) High Wind Season – May to August (c) Wet Season – September to October

cluded at its maximum capacity throughout the planning horizon. It is assumed that the coal-fired thermal plant will operate continuously throughout the year and for the entire lifetime of the proposed system

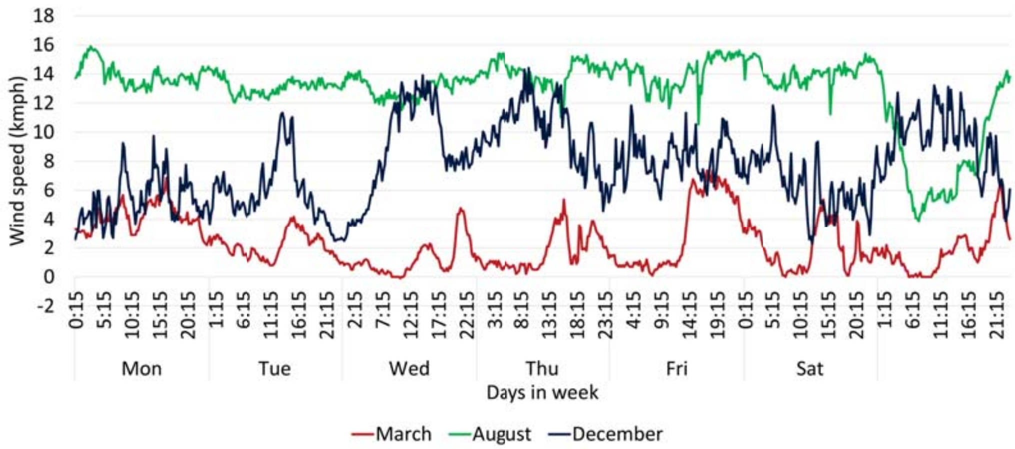

Fig. 4.3: Wind speed in three different seasons

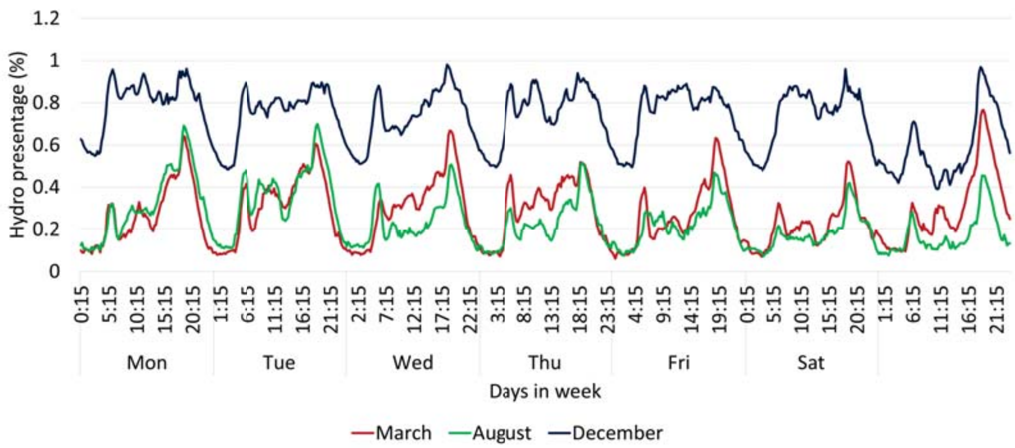

Fig. 4.4: Hydro power availability percentage in different seasons

4.4 Sizing solar PV system

All the required equations for sizing the solar PV system are given in Section 3.1.1. Based on these equations, the energy generated by a solar PV system depends on the type of solar panel selected for designing the power plant, the solar irradiance levels, and the temperature conditions specific to the chosen installation site. The selection of optimal locations for the implementation of solar PV power plants is based on geological factors, solar irradiance, and other relevant aspects. Panel efficiency is a key parameter when choosing solar panels for designing solar PV power plants, as it directly impacts the energy output and overall performance of the system.

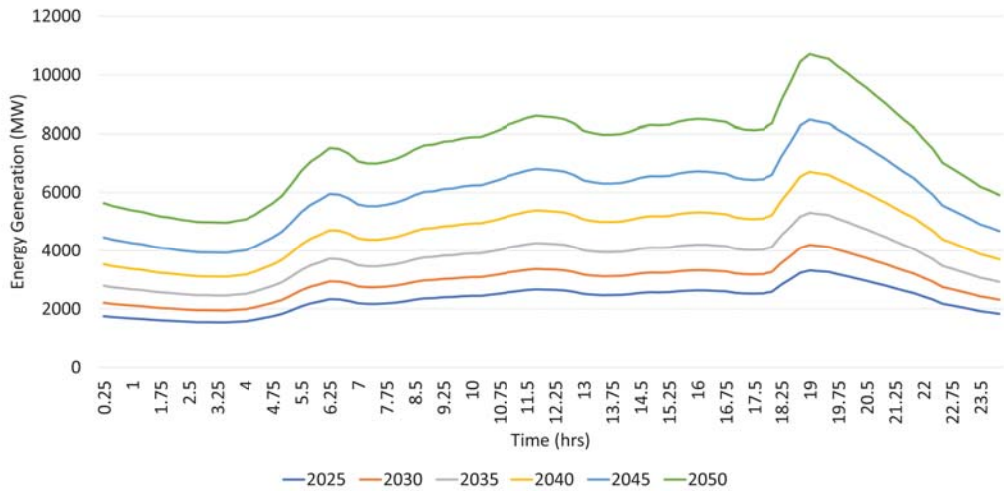

Fig. 4.5: The predicted generation profiles for every five years according to the data given in CEB long-term generation plan 2023-2047

4.4.1 Locations identification for solar PV power plants

When selecting sites for solar PV power plants, several factors must be considered, including areas with acceptable levels of solar irradiation, low population density of humans and wildlife, and minimal environmental impact.

The availability of solar irradiation is analyzed using Global SolarAtlas [65], which provides a summary of solar power potential, including direct and annual solar irradiation levels. Land availability is examined using Google Earth, which offers 3D satellite imagery [66]. When selecting acceptable land for solar PV power plants, factors such as the distribution of the human population, availability of forests, and wildlife habitats are carefully considered. The goal is to mitigate the impact on social lifestyles and the environment, ensuring the proposed system causes minimal disruption to ecosystems and local communities while maintaining environmental sustainability.

When selecting locations for solar power plants, preference is given to sites near existing grid substations to minimize the costs associated with constructing new substations and to reduce stress on the power system. Additionally, locations near oil-fired thermal power plants with high solar irradiation are prioritized, as solar power generation can replace from oil-fired thermal plant generation. These substations are considered sufficient to transmit the generated power, ensuring that energy balance is maintained. To select the suitable substations, existing substation details are taken from the *"Long-Term Transmission Line Development Plan 2018-2027"* in Sri Lanka. The locations of available substations are mapped in (ANNEX B) [66], based on the published data on 2021.

After evaluating all the discussed factors, six locations were identifed for the installation of solar PV power stations: Valachchanai (Batticaloa District), Galmetiyawa

(Trincomalee District), Kilinochchi (Kilinochchi District), Samanthurei (Ampara District), Okkampitiya (Monaragala District), and Padalangala (Rathnapura District). These locations were selected basedon their high solar penetration potential, land availability, and the proximity of grid substations for integration with the national power system. A Sri Lankan map, including the selected locations for implementing new power stations, is provided in ANNEX C. Details of the identified locations solar PV plant installation are summarized in Table 4.4, including the site location, corresponding grid substation location, the nearest oil-fired thermal power plant capacity (if available), annual average direct normal irradiation, average sun hours per day, and direct normal irradiation per day.

TABLE 4.4: DETAILS OF THE IDENTIFIED LOCATIONS FOR SOLAR PV POWER PLANTS

Solar Power plant	Solar Power plant Location	Grid Subst-ation	Grid Subst-ation Location	Nearest Thermal Power stations Capacity (MW)	Annual Avg. Direct normal irradia-tion (kWh/m2 per Year)	Avg sun hours per day	Direct normal irradia-tion (kWh/m2 per Day)
1	valach-chanai	valach-chanai	7.9292, 81.5087	40	1518.0	5	4.1561
2	Galmet-iyawa	Kappal-thurai	8.5527, 81.1298	0	1398.2	5	3.8281
3	Kilino-chchi	Kilino-chchi	9.3788, 80.4094	0	1443.1	5	3.9510
4	Saman-thurei	Ampa-ra	7.2918, 81.6930	0	1567.8	5	4.2924
5	Okkam-pitiya	Mona-ragala	6.8354, 81.3152	10	1492.8	5	4.0871
6	Padala-ngala	Embili-pitiya	6.2870, 80.8611	100	1469.6	5	4.0235

4.4.2 Solar irradiation

Solar irradiance and temperature vary throughout the day and across different seasons, depending on weather conditions. These variations follow similar patterns within the same seasons. In this study, the Sri Lankan power system is used to validate the results, considering these seasonal and daily fluctuations in solar irradiance and temperature. Sri Lanka is located near to the equator, becasuse of that relatively consistent solar irradiance patterns prevail throughout the year. Furthermore, due to the relatively short distances between the selected locations within the country, the solar irradiance patterns can be assumed to be similar across these sites. After analzing the solar irradiance patterns across different periods of the year, the daily solar irradiation trends can be identifed throughout the day. Base on this data, the average daily solar irradiation curve in Sri Lanka is shown in Fig. 4.6. The solar irradiation data is sourced from the selected areas designated for solar power plants in Sri Lanka [65]. For the purpose of calculations, the average solar irradiance is considered between 10.00 AM and 03.00 PM, corresponding to the peak sun hours. These five hours are regraded as the effective solar generation period for this study, representing the active hours for the solar PV system.

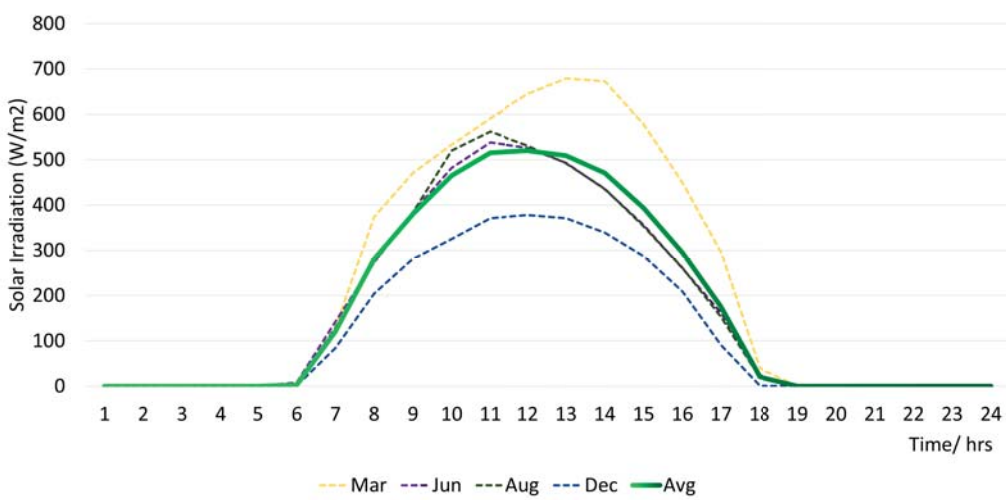

Fig. 4.6: Average daily solar irradiation

Fig. 4.7 illustrates the calculated average daily solar irradiation for the selected areas over three seasons throughout the year, measured over the course of one week, using solar irradiation and temperature data. This analysis helps to identify variations in solar irradiation patterns across the identifed three seasons. Based on this evaluation, the peak sun hours are consistently confirmed to be 5 hours, occurring between 10.00 AM and 03.00 PM. Consequently, this time period can be identified as the most efective period for solar energy generation.

Additionally, Sri Lanka, located in the equatorial belt, experiences consistent solar energy availability throughout the year. Due to the relatively small distance between the selected areas for solar plants, the solar irradiation patterns are assumed to be similar across all locations. Therefore, the solar irradiance is assumed to have an equal effect on all locations with solar PV power plants. Historical data were obtained using NASA's Prediction of Worldwide Energy Resources (POWER) Data Access Viewer (DAV) version 2.3.6, from 1^{st} January 2023 to 31^{st} December 2023 at 15-minute intervals to improve the accuracy of the proposed system [67]. The same solar irradiation

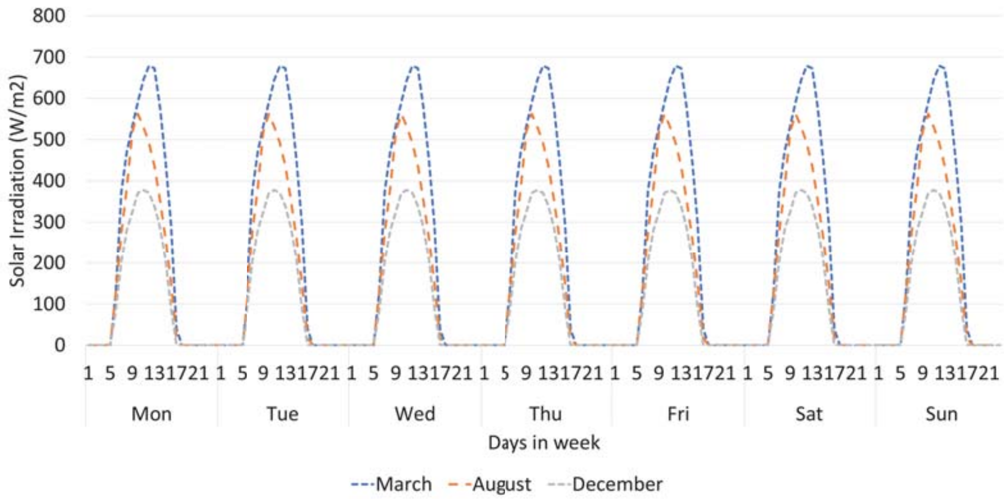

Fig. 4.7: Average daily solar irradiation

pattern is assumed for the entire lifetime of the system.

4.4.3 Selection of solar PV panel

The amount of solar energy generated depends significantly on the performance of the solar PV panels. With ongoing advancements in technology, high energy efficiency and cost-effective solar PV panals are being manufactured Worldwide. Consequently, solar PV power plants are increasingly recognized as a sustainable energy solution.

The *Trinasolar Vertex backsheet monocrystalline module TSM - DE21* is selected as the solar PV panel module for the solar PV plant design in this study, with the 21.6 % of efficiency. The design parameters of the selected solar PV panel module are detailded in Table 4.5 [68], based on the datasheet of the solar PV panel module.

4.4.4 Solar PV cost projection

The global trend for solar PV energy is increasing as renewable energy sources and the usage of solar PV is increased for electricity generation. Most of research efforts are focused on improving the efficiency of solar PV panels and reducing costs to promote solar energy adoption. With the development of technologies, the capital cost, installation cost, and operation and maintenance cost of solar panels have been decreasing annually. As a result, the costs associated with installing solar PV plants are expected to vary over time. The predicted capital, operation and maintenance costs are incorporated into the optimization algorithm to assure the accuracy of the results.

For this study, a utility-scale solar PV system is considered. The unitary capital cost γ_{sys_0} and the unitary operation and maintenance cost for each year β_{sys_0} for each year are tabulated in Table 4.6 [69]. Additionally, the unitary cost of the solar PV

TABLE 4.5: DETAILS OF THE IDENTIFIED LOCATIONS FOR SOLAR PV POWER PLANTS

Parameter		Value	Unit
$P_{R,pv}$	The PV rated power	670	W
R_{ref}	The solar radiation at reference conditions	1000	W/m^2
T_{ref}	The reference cell temperature	25	$°C$
N_T	The temperature coefficient	-0.34	$\%\,°C^{-1}$
T_{air}	The ambient air temperature	28	$°C$
$NOCT$	Nominal operating cell Temperature	43	$°C$
T_{PV}	Solar panel life time	25	yrs
η	The solar PV module efficiency	21.6	$\%$
Panel Dimensions			
	Length	2384	mm
	Width	1303	mm

generation α_{sys_0} is taken to be 57.6 USD/MWh. This value is useful for calculating the cost associated with solar energy curtailment.

4.5 Sizing of HESS

When increasing renewable energy integration, controllable resources become essential to manage the power system due to the unpredictability and limited controllability of renewable energy generation. Energy storage, particularly at the utility scale, can serve as an effective controllable resource. As the penetration of grid-connected renewable energy sources increases, an optimal grid-scale energy storage solution becomes important for future energy systems. To increase the reliability and efficiency of the power system, HESS that combine multiple energy storage technologies are considered. An optimal HESS is required to fulfill all requirements of a certain application, such as handling bulk energy and energy management. For this study, PHS and BS are selected for implementing the HESS. PHS provides energy balancing, stability, and storage capacity, while BS provides high power, energy density, and efficiency for the HESS.

4.5.1 Selection of battery model and battery cost projection

The sizing strategy for the BS system is explained in Section 3.1.2. Li-ion battery technology is selected for the BS system due its high power and energy density and technological maturity. The *EFS480-120IIB high-rate lithium battery pack* is selected for the simulation model. These batteries are rated for 3,000 cycles at 50% Depth of Discharge (DOD) and an 80% End of Life (EOL) threshold [70]. Key parameters for the BS system include a battery efficiency (η_{bs}) of 85% and a self-discharging rate (σ)

TABLE 4.6: COST PROJECTION OF UTILITY-SCALE SOLAR PV

Year	The unitary capital cost (γ_{sys_0}) (\$/kW)	The unitary operation and maintenance cost (β_{sys_0}) (\$/kW-yr)
2024	1244.6	21.0
2025	1204.2	20.5
2026	1163.8	20.0
2027	1123.4	19.5
2028	1083.0	19.0
2029	1042.6	18.5
2030	1002.2	18.0
2031	961.9	17.5
2032	921.5	17.0
2033	881.1	16.5
2034	840.7	16.0
2035	800.3	15.5
2036	787.6	15.4
2037	775.0	15.2
2038	762.3	15.1
2039	749.7	15.0
2040	737.0	14.8
2041	724.4	14.7
2042	711.7	14.6
2043	699.0	14.4
2044	686.4	14.3
2045	673.7	14.2
2046	661.1	14.0
2047	648.4	13.9
2048	635.7	13.8

of 5%. The minimum and maximum SOC (SOC_{min} and SOC_{max}) for the BS system are determined to be 10% and 90%, respectively.

With the rapid development of renewable energy technologies, BS systems have also trended and BS manufacturing industry is increasingly focusing on improve the technology. Manufacturers are prioritizing the enhancement of efficiency, extension of battery lifetime, and reduction of costs. Consequently, capital costs and operation and maintenance (O&M) costs are projected to evolve over time for each year. To enhance the accuracy of the proposed system, the predicted costs are considered into the analysis. The unitary capital cost (γ_{sys_1}) and the unitary operation and maintenance cost (β_{sys_1}) for the BS system are taken for each year from Table 4.7 [69]. The locations for the BS system are selected near the solar PV power plant locations and therefore, they are not described separately in this section. The identified locations are detailed in Section 4.4.1.

TABLE 4.7: COST PROJECTION OF UTILITY-SCALE BS SYSTEM

Year	The unitary capital cost (γ_{sys_1}) ($/kW)	The unitary operation and maintenance cost (β_{sys_1}) ($/kW-yr)
2024	1638.8	41.0
2025	1436.2	35.9
2026	1389.7	34.7
2027	1343.3	33.6
2028	1296.8	32.4
2029	1250.3	31.3
2030	1203.8	30.1
2031	1185.3	29.6
2032	1166.7	29.2
2033	1148.1	28.7
2034	1129.6	28.2
2035	1111.0	27.8
2036	1092.5	27.3
2037	1073.9	26.8
2038	1055.3	26.4
2039	1036.8	25.9
2040	1018.2	25.5
2041	999.6	25.0
2042	981.1	24.5
2043	962.5	24.1
2044	944.0	23.6
2045	925.4	23.2
2046	906.9	22.7
2047	888.3	22.2
2048	869.7	21.7

4.5.2 Location and capacity identification of PHS

Unlike solar PV and BS systems, PHS cannot be installed on a small scale, and identifying suitable locations is more challenging. Due to complexity of location identification and construction, a feasibility study is required to determine appropriate location and capacities for the PHS system. Published results from previous feasibility studies are used for this study. Two projects were conducted by Ceylon Electricity Board (CEB) and Japan International cooperation Agency (JICA) in 2015 and 2018 to identify the most feasible location for implementing PHS. Based on those studies, the capacities and locations were identified as potential sites for the PHS system. The studies provide valuable insights into suitable locations, plant capacities, and cost estimates. It provides a clear understanding of the feasibility of integrating PHS systems into the energy infrastructure

Two key studies provide important findings for the development of PHS systems in Sri Lanka. The first study identifies eleven recommended sites for constructing a 600 MW PHS system, which were evaluated and ranked based on environmental, topographical, geological, and technical criteria. Among these, Halgran Oya in the Nuwara Eliya district, Maha Oya in the Kegalle district and Loggal Oya in the Badulla district were recognized as the best locations for future development. The unitary investment cost (γ_{PHS}) of these system is 1306.9 USD/kW. The second study suggests a 1400 MW setup that uses the existing Victoria reservoir (in Kandy District, Central Province) as the lower pond and an existing irrigation pond at Wewathenna (located to the east of the Victoria reservoir) as the upper pond. The unitary investment cost (γ_{PHS}) of that project is 649 USD/kW for construction of a 1400 MW power plant with four 350 MW generators. If developed in two stages, the cost for stage I (two 350 MW generators) is 842 USD/kW, and for stage II (two 350 MW generators) it is 455 USD/kW [71]. The most suitable three sites from the first study and the selected site from second study for the PHS sysem installation are shown on the map provided in ANNEX D.

Here, the unitary operation and maintenance cost β_{PHS} for the PHS system is 19 USD/kW-yr. A construction period is given as five years, with an economic plant life of 25 years, based on the findings from the studies. Among all the identified PHS systems, a 1400 MW PHS is selected due to its relatively low cost and high capacity. The total capacity of 1400 MW PHS is considered for sizing the HESS, divided into two stages, with each stage having a capacity of 700 MW capacity.This approach is identified as an efficient method for integrating PHS into the system. All other relevant parameters for the upper and lower reservoirs are detailed in Table 4.8.

TABLE 4.8: PARAMETERS RELEVANT TO THE UPPER AND LOWER RESERVOIRS FOR SELECTED PHS

Details	Upper Reservoir	Lower Reservoir
Name of River	Wewathenna	Mahaweli Ganga River System
Catchment Area	$0.3km^2$	$6.7km^2$
Gross storage capacity	$5.5 \times 10^6 m^3$	$10.0 \times 10^6 m^3$
Effective storage capacity	$5.1 \times 10^6 m^3$	$5.1 \times 10^6 m^3$
Reservor area	$0.17km^2$	$0.3km^2$
Water Discharge	$240m^3/s$	$188m^3/s$
Gross head	$727m$	-
Effective head	$686m$	-
Max. pumping head	-	$754m$
Min. pumping head	-	$687m$

In pumping mode, the minimum power required to operate the pump motor for PHS can be calculated using Eq. 4.1. Considering the efficiency of the pump-turbine at 80 %, an effective head of 686 m, and a water discharge of 188 m$^3/s$, the required minimum power to operate the pumped hydro system in pumping mode can be determined.

$$P = \frac{\rho g h Q}{\eta} \tag{4.1}$$

4.5.3 Simulation and Case Study

The proposed multi-objective optimization algorithm is simulated based on the Sri Lankan Power system, which consists of thermal (oil and coal), hydro, solar, wind and HESS components. A novel energy management system is incorporated to effectively balance the energy generated from solar PV and HESS. To obtain an accurate and optimal solution from the developed optimization algorithm and an integrated energy management system needs to be analyzed using small sample values. For this purpose, all parameters are considered over a 15-minute time interval for a one-year period. To implement this, a program has been developed using Python programming language within an open-source framework to solve the optimization algorithm. Python is chosen due to its high-level capabilities as a general-purpose programming language. Furthermore, Pymoo, an open source framework for multi-objective operation in pyhton, is utilized as a platform to solve multi-objective optimization algorithms. The NSGA-II is selected as an evolutionary algorithm base on genetic algorithm technologies, to solve the optimization problem. In this study, NSGA-II parameters are configured according to established standards. The population size is set to 40, with 100 generations. Crossover and mutation probabilities are assigned values of 0.9 and 0.2, respectively. The crowding distance is automatically calculated by NSGA-II to preserve solution diversity, ensuring a well-distributed spread along the Pareto front.

The parameters required to solve the algorithm are described in this chapter. Furthermore, additional parameters essential for the simulation process are highlighted below. The lifetime of the proposed system (T_{sys}) is considered to be 25 years. The interest rate (r) is taken as 8.5 % for the developed system, with variations ranging from 4.5 % (lowest) to 12.5 % (highest), based on the interest rates given provided by Central Bank of Sri Lanka in 2023 [72].

The solar PV capacity and the BS system capacity can be taken as a decision variables in the optimization process. The time span for a single optimization is determined by the construction period of the solar PV and battery storage systems. For utility-scale or medium-voltage (MV) scale solar PV plants, the design and approval process typically takes six months to one year or more, depending on environmental impact assessments, permitting procedures, and land acquisition requirements. Additionally, the construction phase may take three months to one year, depending on the size of project and complexity. Similarly, for battery storage systems, the design and approval process usually takes six months to one year, depending on regulatory requirements and grid interconnection procedures. Construction can take approximately three to nine months, depending on the capacity of system. Considering the time required for the design, approval, and construction of both the solar PV and battery storage systems, the time span for a single optimization cycle is assumed to be two years.

A single optimization is performed for a two-year time span, with the system lifetime considered to be 25 years. As a result, the optimal solar capacity and battery storage are determined for each two-year period throughout the lifetime of the system. Based on the conducted feasibility studies, a 1400 MW PHS capacity is planned to be integrated into the system in two stages. A case study is carried out to identify the best time periods for integrating the PHS into the system. A total of fourteen cases are defined according to the proposed years for PHS integration. The construction time period for the selected PHS is five years, as determined by the feasibility study.It is assumed that construction will be completed within this five-year timeframe without any delays. Consequently,the first step of PHS integration will occur after five years. The most effective time periods for adding the PHS to the system are considered, and cases are defined accordingly. Table 4.9 presents the identified cases in this study and the planned years for PHS addition, with "Year No" beginning in 2024..

TABLE 4.9: ANALYZED CASES WITH DIFFERENT PLANNED YEARS FOR ADDING PHS

Case No	Planned year for adding PHS Stage I (Year No)	Planned year for adding PHS Stage II (Year No)
Case 1	5	5
Case 2	5	7
Case 3	5	9
Case 4	5	11
Case 5	5	13
Case 6	7	7
Case 7	7	9
Case 8	7	11
Case 9	7	13
Case 10	9	9
Case 11	9	11
Case 12	9	13
Case 13	11	11
Case 14	11	13

For each case outlined in Table 4.9, a roadmap for solar PV capacity and BS capacity is developed after performing a single short-term optimization. Following this, environmental, economic, and sensitivity analyses are carried out to evaluate and determine the optimal solution among the different cases.

CHAPTER 5

RESULTS AND DISCUSSION

The optimal capacities for the solar PV and HESSs over the planning horizon are determined as outcomes, and these results are utilized to achieve the primary objectives of this research: maximizing solar PV energy generation and minimizing reliance on oil-fired thermal energy generation. The optimal capacities of solar PV and BS for each short time duration are identified using an optimization algorithm integrated with the energy management system. However, the optimal capacity of the PHS cannot be obtained directly from the optimization algorithm due to the complexity of its construction and its unsuitability for small-scale installation. To determine the most suitable time period for integrating PHS into the proposed system, fourteen cases are considered, as presented in Section 4.5.3. Additionally, environmental and economic analyses, along with sensitivity analysis, are conducted to identify the most effective solutions from the evaluated scenarios.

The analysed results are presented in detail, including the final capacities of the solar PV and HESS systems and recommended timelines for their integration into the power system. Furthermore, the proposed solar PV capacities are compared with the national solar energy targets outlined in the long-term generation plan to assess alignment with national energy requirements. This chapter provides a comprehensive discussion of the results and their implications.

5.1 Identification of the best optimal solar and battery capacities from optimization algorithm

An optimization algorithm integrated with the energy management system is used to identify the optimal capacities for PV and BS over short time durations. NSGA II is employed to solve the optimization problem, considering the identified objective functions and constraints. Utilizing the principles of Evolutionary Multi-Objective Optimization (EMO), the process generates multiple Pareto-optimal solutions simultaneously. These solutions are visualized on the Pareto optimal front, where all points are identifed as a theoretically optimal solutions. After considering the national requirements of the considered country and other practical factors relavent to that country or region, the most suitable solution is selected. Often, the midpoint of the Pareto optimal front is chosen as the best solution, as it balances the two key objectives of this study. This approach ensures the minimization of all costs associated with the system. For the entire system lifetime, solar PV and BS capacities are iteratively optimized over short time intervals.

For this study, an optimization is conducted for a two-year period, considering the design and installation timeline for solar PV and BS, as discussed in Section 4.1. The optimization algorithm generates forty Pareto-optimal solutions after one hundred iterations, based on a population size of forty and a total of one hundred generations. The most suitable solution is then selected by considering the minimum cost associated with the proposed system.

To demonstrate the process of identifying the optimal solution for a short time period, the first two-year interval (2024-2025) of *Case* 6 is used as outlined in the case studies presented in Table 4.9. The identified Pareto-optimal solutions for Case 6 during the 2024–2025 period are illustrated in Fig. 5.1 as blue dotted points. This set of Pareto-optimal solutions is used to explain the steps followed in selecting the most appropriate solution.

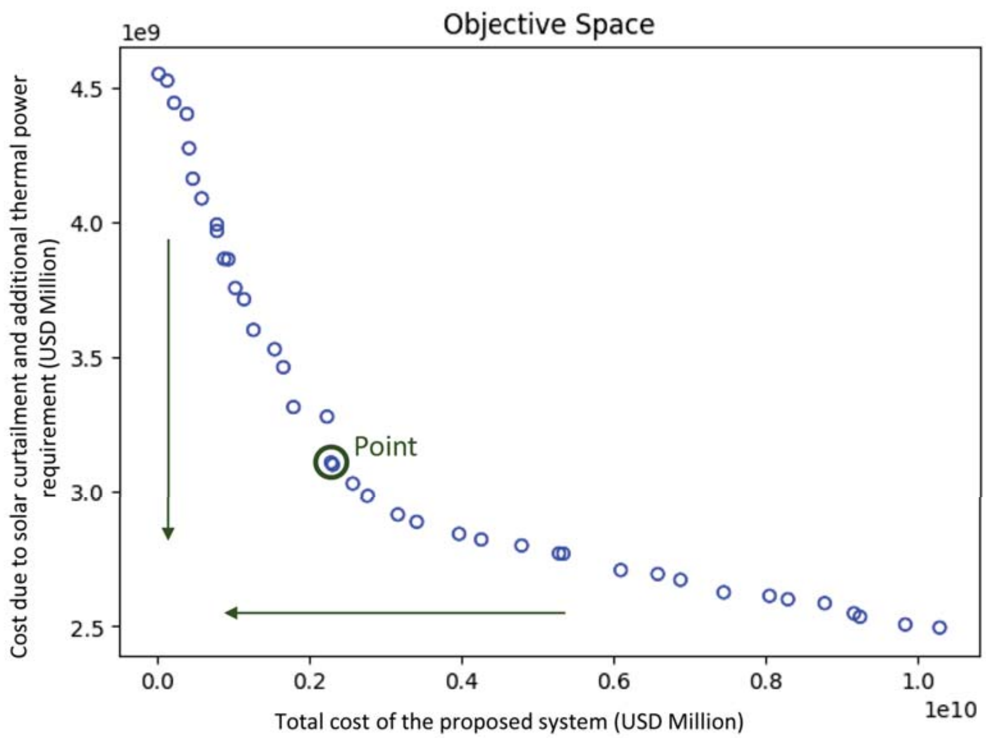

Fig. 5.1: Pareto-optimal solutions obtained in *Case* 6 over the initial two-years (during 2024 and 2025)

A second stage of optimization is carried out after obtaining the Pareto optimal solutions. Equation 5.1 is then used to identify the best optimal solution among the Pareto optimal set. When identifying the best solution, the total cost of the proposed system should be less than or equal to the combined cost of solar curtailment and additional thermal power requirements. In selecting the best optimal solution, this criterion is taken into account, and the corresponding solar PV and battery capacities

TABLE 5.1: IDENTIFIED PARETO-OPTIMAL SOLUTIONS

Solutions	f_{TOTEX} (USD MM)	$f_{Surcharge}$ (USD MM)	$C_{solarPV}$(MW)	C_{BS} (MW)
1	22.51	4551.89	5.36	0.37
2	132.59	4527.00	14.37	4.99
3	224.71	4444.30	45.36	5.04
4	391.56	4403.06	60.62	11.78
5	419.88	4275.51	110.7	5.2
6	468.89	4162.29	158.75	0.08
7	585.67	4089.01	190.46	1.38
8	784.83	3991.89	233.28	5.42
9	785.97	3967.80	244.64	3.64
10	878.89	3866.58	292.49	0.98
11	934.71	3865.10	292.49	4.07
12	1025.89	3758.34	344.97	0.57
13	1140.29	3716.51	364.97	3.64
14	1264.02	3602.36	425.52	0.62
15	1541.56	3530.53	461.8	10.06
16	1655.62	3463.75	499.97	10.16
17	1788.87	3315.58	599.2	1.37
18	2229.06	3279.99	611.33	23.74
19	**2282.39**	**3109.20**	**773.01**	**0.37**
20	2304.95	3101.06	781.83	0.18
21	2566.32	3031.00	863.48	1.34
22	2764.14	2984.93	931.06	1.28
23	3167.37	2915.01	1075.36	0.08
24	3415.08	2887.98	1155.24	0.78
25	3971.76	2843.08	1215.03	21.82
26	4263.02	2822.27	1252.53	31.82
27	4793.21	2799.97	1421.65	33.61
28	5284.11	2770.69	1462.84	54.05
29	5341.14	2769.87	1482.21	54.05
30	6095.36	2708.69	1212.86	139.59
31	6581.54	2693.97	1155.24	175.85
32	6879.34	2672.57	1185.51	187.39
33	7448.30	2625.95	1376.85	187.7
34	8049.93	2613.11	1581.2	187.7
35	8290.86	2600.37	1589.67	199.64
36	8774.03	2585.74	1666.97	213.78
37	9158.55	2548.10	1567.01	251.31
38	9237.97	2535.22	1472.47	271.09
39	9832.94	2506.72	1472.24	304.02
40	10284.00	2495.14	1617.21	305.36

are determined for the selected time period.

$$Cost_{total} \leq Cost_{CSC} + Cost_{CTB} \tag{5.1}$$

Where,

$Cost_{total}$ - The total cost of the proposed system USD

$Cost_{CSC}$ - The cost due to solar curtailment USD

$Cost_{CTB}$ - The cost due to additional thermal power requiremnt USD

To identify the most optimal solution, the set of optimal solutions obtained from the optimization algorithm is arranged in ascending order based on the total installation, operation, and maintenance cost of the proposed system, as presented in Table 5.1. The minimum values for both objectives are observed near the middle of the listed solutions. Among these, 19^{th} solution is selected due to its reduced cost associated with solar curtailment and additional thermal energy requirements. Therefore, the 19^{th} solution is considered as the best optimal solution for the considered period. BThis is because the priority is to reduce the costs associated with solar curtailment and additional thermal energy, rather than focusing solely on the cost of the proposed system. This solution minimizes both the total captical, replacement, operational, and maintenance costs of the proposed system, as well as the costs associated with curtailment of the solar power and additional oil-fired thermal power requirements. For the identified solution, the total installation,replacement, operational and maintenance costs of the proposed system is 2282.39 million USD, and 3109.20 million USD is the cost due to solar curtailment and additional oil-fired thermal power requirement. This solution gives a 773.01 MW solar PV capacity and a 0.37 MW Li-ion BS capacity, representing the optimal configuration for *Case* 6 during the 2024-2025 time period. These two capacity values can be taken as the optimal solution for considered two-year time period.

By applying the same steps in above to each two-year time period throughout the lifespan of the proposed system, the optimal solar PV and Li-ion BS capacities are identified for each considered two-year time period within the planning horizon. The same approach can also be applied across the considered cases outlined in Table 4.9. In the end, the most suitable optimal capacities for solar PV and BS are determined.

5.2 Identification of the roadmap for defined cases

Once the capacities for each short duration within the planning horizon are identified, the roadmap for that case can be determined. Using the same procedure, the roadmap is identified for each of the identified cases in Table 4.9. This section summarizes all the solutions obtained from the case studies.

The capacities of solar PV for each two-year period across the fourteen considered cases are presented in Table 5.2 and Table 5.3. Similarly, the capacities of BS for each two-year period across the fourteen considered cases are provided in Table 5.4 and Table 5.5. The optimal solution identified for *Case* 6 during the 2024-2025 is highlighted in Table 5.2, with a 773.01 MW solar PV capacity and a 0.4 MW battery storage capacity, as shown in Table 5.4.

TABLE 5.2: SOLAR POWER CAPACITY DISTRIBUTION THROUGHOUT THE PLANNING HORIZON FOR CASE 1 TO CASE 7

Year	Case 1	Case 2	Case 3	Case 4	Case 5	Case 6	Case 7
2024 - 2025	931.1	931.1	931.1	931.1	931.1	**773.0**	773.0
2026 - 2027	801.2	801.2	801.2	801.2	801.2	801.2	801.2
2028 - 2029	407.6	275.9	275.9	327.3	327.3	145.7	145.7
2030 - 2031	487.2	514.2	416.1	350.6	350.6	607.5	533.1
2032- 2033	399.4	400.6	576.8	411.6	411.6	544.4	627.0
2034- 2035	627.0	690.4	704.9	840.5	634.2	771.2	568.6
2036- 2037	731.6	832.3	816.1	808.3	807.2	517.8	808.8
2038- 2039	706.7	679.7	539.7	601.5	683.0	836.7	729.1
2040- 2041	702.1	776.6	849.9	798.6	888.6	755.9	849.3
2042- 2043	1016.3	751.3	780.1	1008.3	1032.6	956.6	905.7
2044- 2045	1141.2	1287.5	1313.6	1093.9	1019.1	1194.4	1240.5
2046- 2047	1436.5	1382.6	1269.9	1451.9	1516.5	1116.7	1150.6

TABLE 5.3: SOLAR POWER CAPACITY DISTRIBUTION THROUGHOUT THE PLANNING HORIZON FOR CASE 8 TO CASE 14

Year	Case 8	Case 9	Case 10	Case 11	Case 12	Case 13	Case 14
2024 - 2025	773.0	773.0	773.0	773.0	773.0	773.0	773.0
2026 - 2027	801.2	801.2	801.2	801.2	801.2	801.2	801.2
2028 - 2029	145.7	145.7	145.7	145.7	145.7	145.7	145.7
2030 - 2031	533.1	533.1	485.4	485.4	401.3	485.4	401.3
2032- 2033	415.8	415.8	584.0	420.5	474.4	384.9	393.9
2034- 2035	716.7	660.5	809.0	766.7	583.2	942.9	740.3
2036- 2037	932.7	916.4	590.3	806.9	1018.0	715.7	836.2
2038- 2039	604.6	683.6	683.6	598.5	594.2	671.2	837.9
2040- 2041	857.1	798.6	794.0	886.9	826.1	849.4	935.4
2042- 2043	926.7	933.9	943.3	1002.5	1031.4	966.2	930.6
2044- 2045	1014.2	1323.0	1172.0	1241.7	1179.2	1073.2	1164.2
2046- 2047	1407.3	1471.6	1332.9	1590.3	1438.0	1218.2	1489.1

The optimal solar PV capacity and BS capacity vary across different time durations due to the integration of PHS into the system. With PHS integration, a greater amount of energy can be stored in the energy storage system. Furthermore, the required BS

TABLE 5.4: BS CAPACITY DISTRIBUTION THROUGHOUT THE PLANNING HORIZON FOR CASE 1 TO CASE 7

Year	Case 1	Case 2	Case 3	Case 4	Case 5	Case 6	Case 7
2024 - 2025	1.3	1.3	1.3	1.3	1.3	**0.4**	0.4
2026 - 2027	95.2	95.2	95.2	95.2	95.2	95.2	95.2
2028 - 2029	192.3	202.9	202.9	197.4	197.4	238.4	238.4
2030 - 2031	110.9	95.1	127.5	130.3	130.3	48.4	77.2
2032- 2033	123.3	134.0	81.7	167.7	167.7	134.3	110.0
2034- 2035	123.8	115.6	135.0	47.8	52.0	133.1	157.3
2036- 2037	127.1	115.4	112.3	129.1	172.2	185.1	105.9
2038- 2039	196.6	215.9	238.3	203.4	195.0	192.1	196.6
2040- 2041	255.9	190.7	238.1	181.4	190.3	188.4	237.8
2042- 2043	207.2	284.8	327.1	239.8	190.0	199.1	228.2
2044- 2045	289.9	211.1	114.6	318.8	405.1	246.2	277.7
2046- 2047	348.5	273.5	451.6	354.9	269.3	608.9	447.7

TABLE 5.5: BS CAPACITY DISTRIBUTION THROUGHOUT THE PLANNING HORIZON FOR CASE 8 TO CASE 14

Year	Case 8	Case 9	Case 10	Case 11	Case 12	Case 13	Case 14
2024 - 2025	0.4	0.4	0.4	0.4	0.4	0.4	0.4
2026 - 2027	95.2	95.2	95.2	95.2	95.2	95.2	95.2
2028 - 2029	238.4	238.4	238.4	238.4	238.4	238.4	238.4
2030 - 2031	77.2	77.2	77.2	77.2	102.1	92.2	102.1
2032- 2033	126.8	126.8	126.8	126.8	125.5	158.9	177.8
2034- 2035	115.3	115.3	115.3	115.3	117.5	10.5	43.4
2036- 2037	126.2	126.2	126.2	126.2	44.1	213.2	120.5
2038- 2039	273.2	273.2	273.2	273.2	294.3	199.9	158.8
2040- 2041	96.6	96.6	96.6	96.6	373.0	296.9	338.8
2042- 2043	252.1	252.1	252.1	252.1	212.0	134.9	162.7
2044- 2045	347.7	347.7	347.7	347.7	132.5	256.6	435.7
2046- 2047	519.8	519.8	519.8	519.8	343.2	539.7	216.5

capacity to store surplus energy decreases with the integration of PHS. As demand increases, both the solar PV capacity and energy storage capacity expand accordingly. Moreover, the required solar PV plant capacity increases over time due to growing demand, driven by population growth and increased energy consumption. Consequently, across all cases considered, the solar PV capacity increases over time.

The identified capacities for each two-year period in each case are used to draw roadmaps for solar PV and BS capacities. The developed roadmaps for solar PV and Li-ion BS capacities across all case studies are presented in Fig.5.2 and Fig. 5.3, respectively. These figures graphically represented the distribution of solar PV and battery storage capacities throughout the planning horizon, highlighting variations across different cases. Furthermore, the optimal solution identified for *Case* 6 during 2024 and 2025 is circled in the figures, with a solar PV capacity of 773.01 MW and a BS capacity of 0.37 MW. All solar PV and BS capacities are determined using the optimization algorithm integraded with energy management system and then follow the procedure described in Section 5.1. When comparing the values for solar PV and BS capacities, differences in capacity across the different cases can be observed.

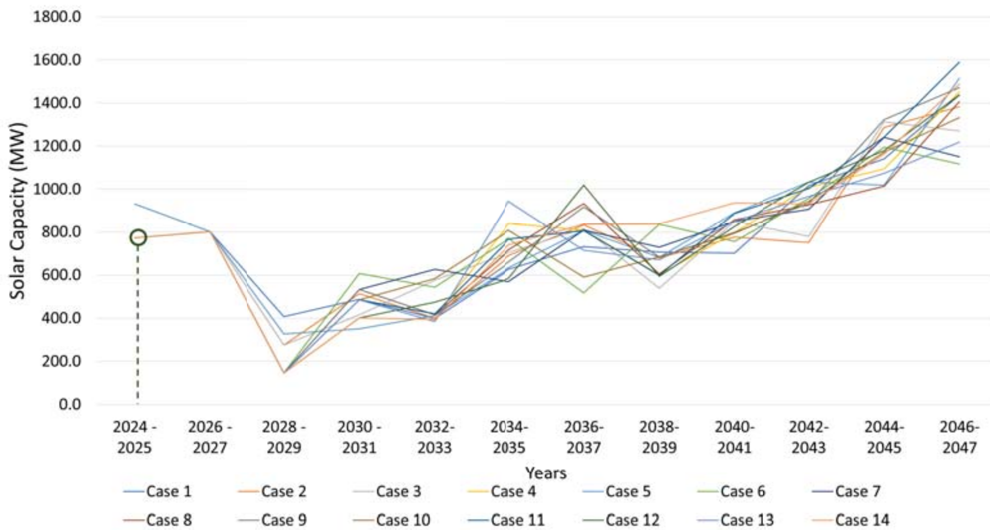

Fig. 5.2: Distribution of solar power capacity over the planning horizon

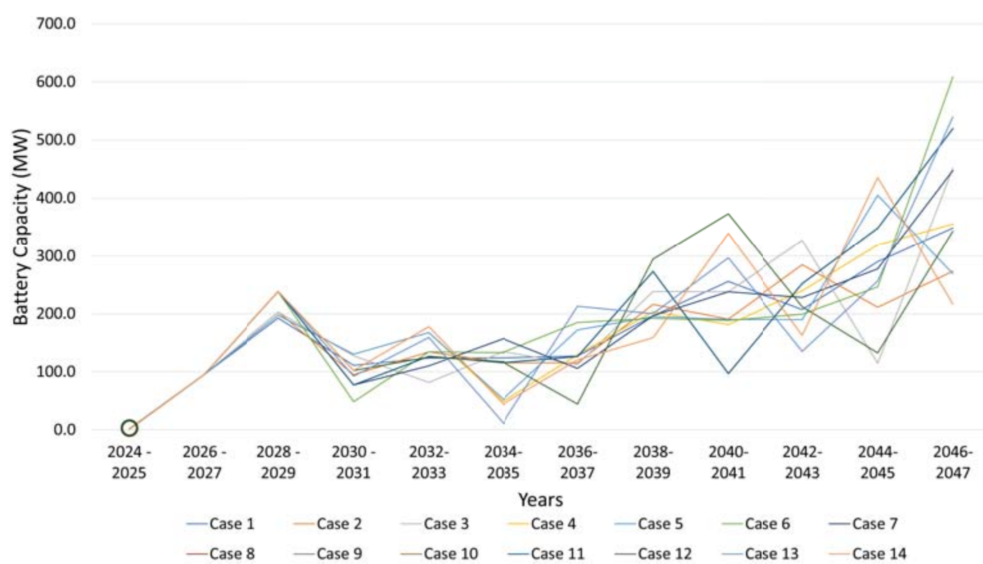

Fig. 5.3: Distribution of battery capacity over the planning horizon

The solar PV capacity and required BS capacity vary across cases, depending on the available capacity in the energy storage system and the applied PHS capacity in each case. The capacities of solar PV and HESS along with the year of their integration into the system, affect the total system cost and the environmental impact of the proposed system. Therefore, after conducting economic and environmental analyses, the most suitable cases can be identified that minimize both cost and environmental impact.

5.3 Economic Analysis

An economic analysis is carried out to evaluate the costs and benefits of the proposed system, providing insights into its economic feasibility. In this study, fourteen cases are identified with different capacities for each year. After developing a roadmap for each case, the economic analysis is carried out to identify the most economical option based on economic viability. This analysis accounts for the total cost of the proposed system, featuring construction, operation, and maintenance costs, as well as costs associated with solar energy curtailment due to insufficient energy storage, additional oil-fired thermal energy required due to limited storage, and carbon emissions from energy generation. The total cost of the proposed system, incorporating both solar PV and HESS, is calculated over the planning horizon. For analytical purposes, the cases are listed in ascending order based on their total cost values. Furthermore, to identify the most economic cluster from the analyzed cases, the total cost for each case is tabulated in Table 5.6 in ascending order, from minimum to maximum value. Three clusters are identified based on the total cost of the proposed system.

With the lowest total cost values, *Case* 1, *Case* 2, *Case* 3, *Case* 4, and *Case* 6 are categorized into the TCOST-A cluster as the minimum total cost. *Case* 7, *Case* 5, *Case* 12, *Case* 8, and *Case* 10 are assigned to the TCOST-B cluster with middle range of total cost, while *Case* 13, *Case* 9, *Case* 14, and *Case* 11 are categorized as the TCOST-C cluster with highest total cost. Among the three clusters, TCOST-A represents the cases with the lowest total cost and is identified as the most economical cluster for this study cases.

5.4 Environmental Analysis

Both economic performance and environmental performance must be considered when selecting the optimal solution from the developed cases. An environmental analysis is conducted to access the existing and future conditions of the proposed system and their potential impacts on human and natural systems, including animals. The implementation and operation of the proposed system may lead to environmental consequences. This analysis primarily focuses on GHG emissions resulting from the operation of the

TABLE 5.6: TOTAL COST FOR THE LIFETIME OF THE SYSTEM ACROSS EACH CASES

Cases	Total Cost (USD Million)	Clusters	
Case 2	20540.62	TCOST - A	Lowest total cost cluster
Case 1	20808.80		
Case 3	20910.81		
Case 4	21090.52		
Case 6	21099.14		
Case 7	21164.00	TCOST - B	Middle total cost cluster
Case 5	21186.51		
Case 12	21284.03		
Case 8	21406.62		
Case 10	21460.25		
Case 13	21625.83	TCOST - C	Highest total cost cluster
Case 9	21954.58		
Case 14	22042.86		
Case 11	22074.32		

proposed system. Given that GHG emissions directly affect weather patterns and contribute to global warming, they are a critical factor to consider.

To analyze the environmental impact of the proposed system, GHG emissions over the system lifetime are calculated for each case. Carbon dioxide (CO_2), nitrogen dioxide (NO_2) and sulfur dioxide (SO_2) are considered as GHGs, and their emissions are calculated separately for each case within the planning horizon. After calculating the GHG emissions, the cases are arranged from least to greatest emissions. The sorted GHG emissions for each case are presented in Table 5.7. From the analysis of these results, the cases are divided into three clusters: the lowest GHG emission cluster, GHG-A, includes *Case* 1, *Case* 6, *Case* 7, *Case* 3, and *Case* 2; the middle emission cluster, GHG-B, includes *Case* 4, *Case* 9, *Case* 8, *Case* 11, and *Case 10*; and the highest emission cluster, GHG-C, includes *Case* 5, *Case* 13, *Case* 14, and *Case* 12. These clusters are also shown in Table 5.7. Among these defined clusters, GHG-A is identified as the best cluster, with the minimum environmental impact from the proposed system.

5.5 Identification of environmental and economic solutions

Once the system roadmap is established, detailing the exact capacities for each year, an economic evaluation is conducted to determine the total cost of the proposed system. Simultaneously, an environmental analysis is performed to assess GHG emissions for each case. To determine the most economically and environmentally sustainable solutions, the total emissions due to CO_2 from oil-fired thermal power generation and the

TABLE 5.7: GREENHOUSE GAS EMISSION OF THE SYSTEM ACROSS EACH CASES

Cases	CO2 (Million tons)	NO2 (Thosand tons)	SO2 (Thosand tons)	Clusters	
Case 1	136.66	838.84	2221.79	GHG - A	Lowest GHG
Case 6	137.78	845.67	2239.89		
Case 7	137.95	846.71	2242.65		
Case 3	138.11	847.69	2245.24		
Case 2	138.50	850.13	2251.70		
Case 4	138.72	851.46	2255.23	GHG - B	Middle GHG
Case 9	139.50	856.28	2268.00		
Case 8	140.02	859.44	2276.36		
Case 11	140.08	859.81	2277.33		
Case 10	140.18	860.40	2278.90		
Case 5	140.77	864.05	2288.58	GHG - C	Highest GHG
Case 13	140.97	865.27	2291.80		
Case 14	141.07	865.89	2293.44		
Case 12	142.40	874.06	2315.08		

total costs for the capital, operation and maintenance of solar PV and HESS for each case are computed. The cases are then ranked from lowest to highest total CO_2 emissions to identify the case with the lowest environmental impact. Similarly, the cases are ranked from lowest to highest total costs for the construction, operation and maintenance of solar PV and HESS to identify the most economical scenarios. Based on the rankings of both economical and environmental outcomes, the cases are presented in Table 5.8.

Based on CO_2 emissions, *case 1*, *case 2*, *case 3*, *case 6* and *case 7* are identified as the five scenarios with the minimum environment impact. In terms of economic performance, evaluated through the total cost of solar PV and HESS installation, operation, and maintenance, *case 1*, *case 2*, *case 3*, *case 4* and *case 6* are identifed as the most cost-effective. when considering these cases, *Case 1*, *case 2*, *case 3*, and *case 6* are stand out as the effectively balanced solutions, offering both low CO_2 emissions and reduced system costs.Consequently, the remaining ten scenarios are excluded from further consideration due to their relatively higher environmentally or/and economically impacts. The solar PV and BS capacities for each two-years period of the planning horizon are presented in Fig. 5.4, illustrating the capacity variations across the four selected environmentally and economically optimal cases.

Additionally, the solar PV system, Li-ion BS system and PHS system capacities for each two-year time period within the planning timeframe are detailed for the selected four economic and environmental cases. The identified capacities for each of these economic and environmental solutions are tabulated and presented in Table 5.9 and

TABLE 5.8: RESULTS FROM ECONOMICAL AND ENVIRONMENTAL ANALYSIS FOR EACH IDENTIFIED CASES

Economic Analysis		Environment Analysis	
Cases	Total Cost (USD Million)	Cases	CO2 (Million tons)
Case 2	**20540.62**	**Case 1**	**136.66**
Case 1	**20808.8**	**Case 6**	**137.78**
Case 3	**20910.81**	**Case 7**	**137.95**
Case 4	**21090.52**	**Case 3**	**138.11**
Case 6	**21099.14**	**Case 2**	**138.50**
Case 7	21164.00	Case 4	138.72
Case 5	21186.51	Case 9	139.50
Case 12	21284.03	Case 8	140.02
Case 8	21406.62	Case 11	140.08
Case 10	21460.25	Case 10	140.18
Case 13	21625.83	Case 5	140.77
Case 9	21954.58	Case 13	140.97
Case 14	22042.86	Case 14	141.07
Case 11	22074.32	Case 12	142.40

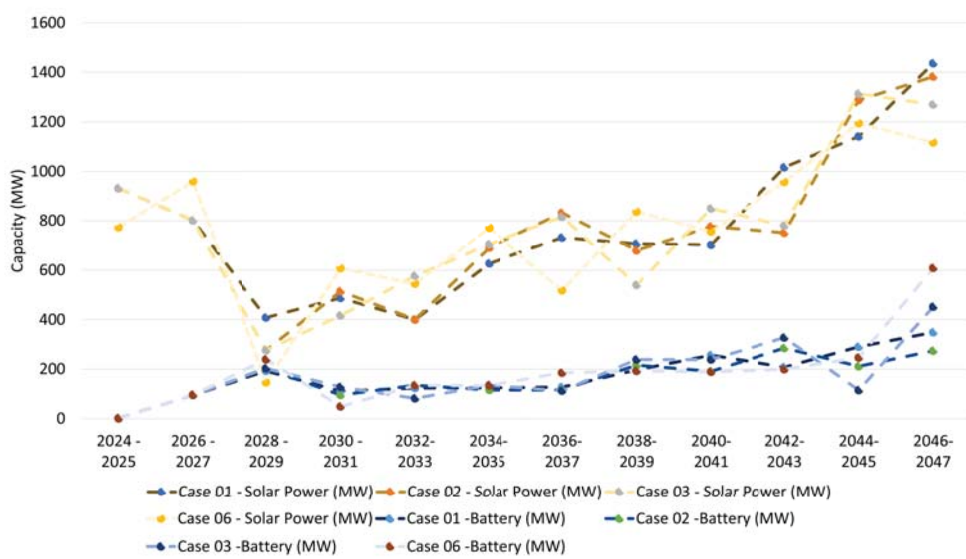

Fig. 5.4: Solar PV and BS capacity distribution throughout the planning horizon for identifed environmental and economical solutions

5.10.

TABLE 5.9: RESULTS FROM ECONOMIC AND ENVIRONMENTAL ANALYSIS FOR CASE 1 AND CASE 2

Case	Case 1 (MW)			Case 2 (MW)		
Years	Solar PV	BS	PHS	Solar PV	BS	PHS
2024 - 2025	931.1	1.3	0	931.1	1.3	0
2026 - 2027	801.2	95.2	0	801.2	95.2	0
2028 - 2029	407.6	192.3	1400	275.9	202.9	700
2030 - 2031	487.2	110.9	0	514.2	95.1	700
2032- 2033	399.4	123.4	0	400.6	134.0	0
2034- 2035	627.0	123.8	0	690.4	115.6	0
2036- 2037	731.6	127.1	0	832.3	115.4	0
2038- 2039	706.7	196.6	0	679.8	215.9	0
2040- 2041	702.1	255.9	0	776.6	190.7	0
2042- 2043	1016.3	207.2	0	751.3	284.8	0
2044- 2045	1141.2	289.9	0	1287.5	211.1	0
2046- 2047	1436.5	348.5	0	1382.6	273.5	0

TABLE 5.10: RESULTS FROM ECONOMIC AND ENVIRONMENTAL ANALYSIS FOR CASE 3 AND CASE 6

Case	Case 3 (MW)			Case 6 (MW)		
Years	Solar PV	BS	PHS	Solar PV	BS	PHS
2024 - 2025	931.1	1.3	0	773.0	0.4	0
2026 - 2027	801.2	95.2	0	959.2	96.1	0
2028 - 2029	275.9	202.9	700	145.7	238.4	0
2030 - 2031	416.1	127.5	0	607.5	48.4	1400
2032- 2033	576.8	81.7	700	544.4	134.3	0
2034- 2035	704.9	135.0	0	771.2	133.1	0
2036- 2037	816.1	112.3	0	517.8	185.1	0
2038- 2039	539.7	238.3	0	836.7	192.1	0
2040- 2041	849.9	238.1	0	756.0	188.4	0
2042- 2043	780.1	327.1	0	956.7	199.1	0
2044- 2045	1313.6	114.6	0	1194.5	246.2	0
2046- 2047	1269.9	451.6	0	1116.7	608.9	0

5.6 Sensitivity Analysis

Sensitivity analysis is used to identify the most suaitable case among the identified ecomonic and environmental solutions. This method evaluates how uncertainties in input parameters influence the output of the system. For this study, an interest rate of 8.5 % is adopted as the baseline for the year 2024, in accordance with official data from the Central Bank of Sri Lanka. According to their records, the interest rate are expected to fluctuate between 4.5 % (lowest) and 15.5 % (highest) [72]. To provide a reliable analysis, the most economically and environmentally sustainable scenarios are evaluated under both the minimum and maximum interest rates cases. Other variables are kept constant during this analysis to accurately assess the impact of interest rate variations. This approach identifies the best cases for implementation, ensuring minimal cost fluctuations and maximizing overall system benefits, even under changing economic conditions.

When planning a new system, minimizing cost variations due to interest rate fluctuations is essential. Reducing the impact of interest rate changes helps maintain financial stability and mitigate investment risks. Through sensitivity analysis, the case with the least cost fluctuations can be identified and it provides a more stable and predictable investment outcome. By focusing on the scenario with minimal fluctuations, the system can be better protected from economic uncertainties, ensuring a more reliable and sustainable financial performance over time.

The solar PV and BS capacities are recalculated for both the lowest (4.5 %) and highest (15.5 %) interest rate scenarios, following the methodology outlined in Section 5.1 and Section 5.2. These updated capacities are calculated exclusively for the four identified economically and environmentally sustainable cases. The new capacities, along with the changes (increase or decrease) for each two-year period in the planning horizon, are calculated and presented in ANNEX E. The variations in solar PV capacity (*Case* 1) under the lowest and highest interest rates, compared to an 8.5% interest rate, are plotted in Fig. 5.5. This clearly illustrates the differences in solar PV capacity across short-term duration due to interest rate fluctuations. Likewise, Fig. 5.6 shows the variation in BS capacity for *Case* 1, based on an 8.5 % interest rate, across each short-term duration.

To identify the variations in solar PV and BS capacities for other economically and environmentally sustainable solutions (*case* 2, *case* 3, and *case* 6), the changes in capacity at the lowest and highest interest rates, relative to an 8.5% interest rate, are illustrated in the corresponding figures. The variations in solar PV capacity for *case 2*, *case 3*, and *case6* are shown in Fig. 5.7, 5.8, and 5.9, respectively. Similarly, the variations in BS capacity for these cases are presented in Fig. 5.10, 5.11, and 5.12, respectively.

For the identified economically and environmentally sustainable cases, solar PV and BS capacities change significantly due to fluctuations in interest rates, as shown in the figures. These capacity changes result in notable fluctuations in the construction and maintenance costs of the proposed system, as well as the costs related with solar curtailment and additional oil-fired thermal energy generation. Interest rate fluctuations present a substantial challenge in the financial planning of energy systems, particularly in developing countries like Sri Lanka, where such fluctuations have been noticeable in recent years. These variations are influenced by various economic factors, including the ongoing economic crisis, the impacts of the COVID-19 pandemic,

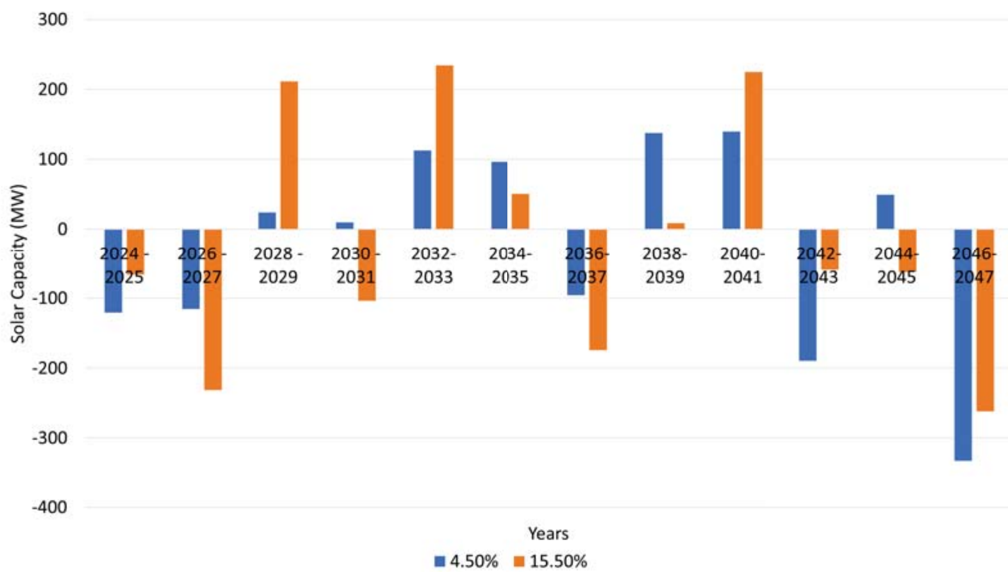

Fig. 5.5: Solar PV capacity variation based on an 8.5% interest rate relevant to *case* 1

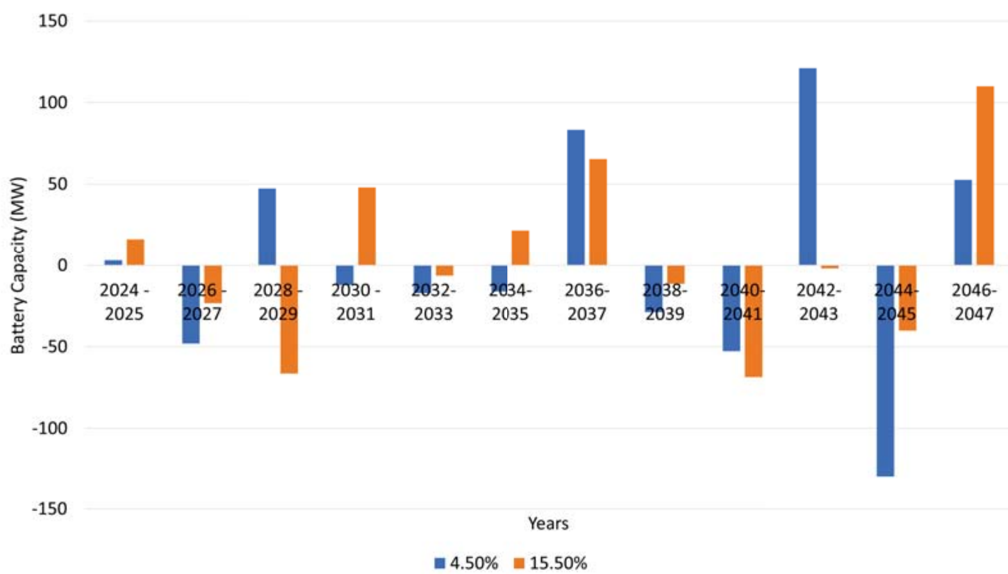

Fig. 5.6: BS capacity variation based on an 8.5% interest rate relevant to *case* 1

political instability, foreign exchange rate volatility, and a lack of investor confidence have further contributed to the instability. According to the Central Bank of Sri Lanka, the interest rate is projected to fluctuate between 4.5 % and 15.5 % range in 2024, which can significantly affect the cost calculations for the proposed system.

The interest rate is one of the key input parameters for the optimization algorithm, specially it can be identified as external factor for the proposed system. Based on the given data, interest rates ranging from 4.5% and 15.5% represent the minimum and

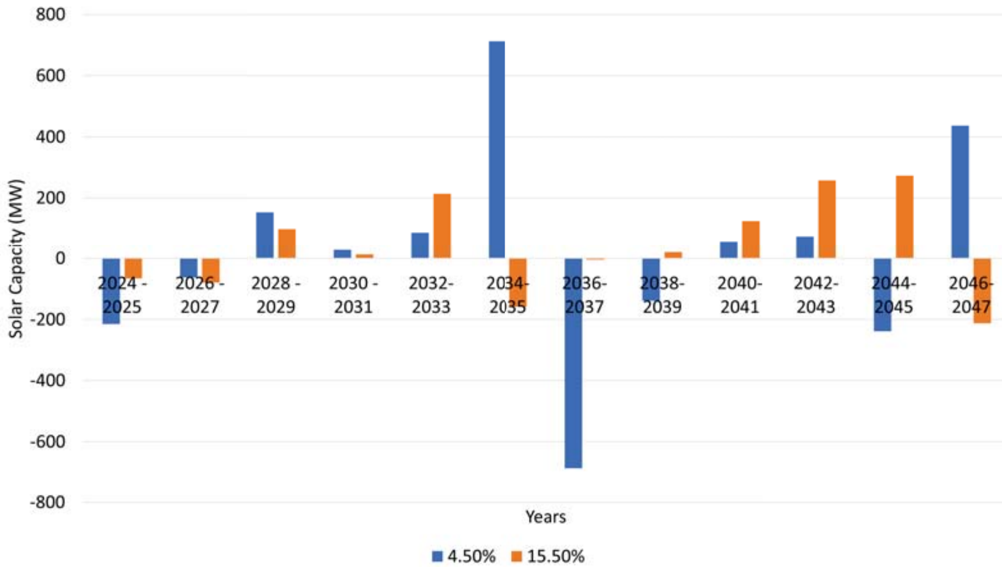

Fig. 5.7: Solar PV capacity variation based on an 8.5% interest rate relevant to *case* 2

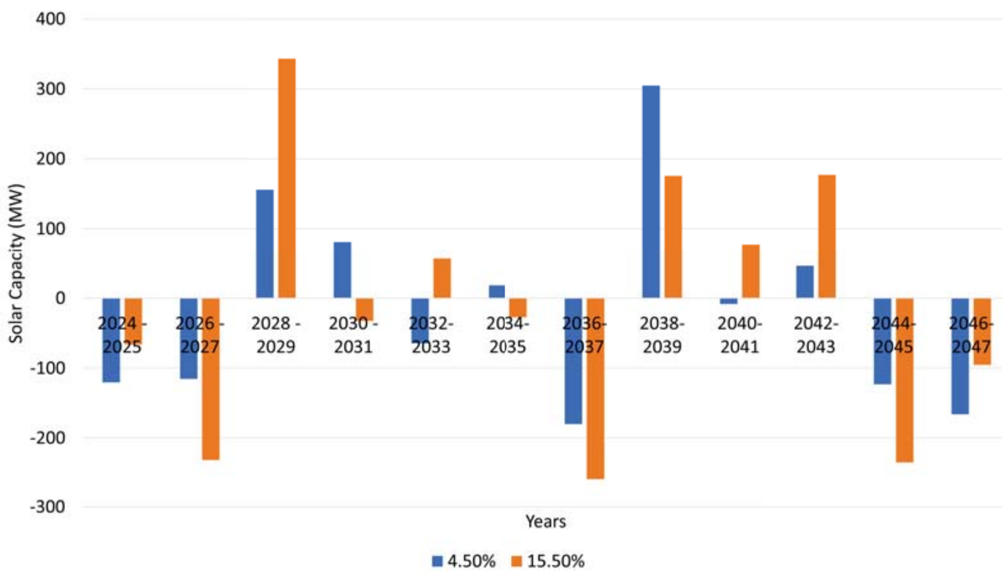

Fig. 5.8: Solar PV capacity variation based on an 8.5% interest rate relevant to *case* 3

maximum optimization results for the proposed system. With these defined upper and lower limits, all other interest rate values fall within this range. Therefore, the costs associated with these newly calculated capacities can be considered as the upper and lower bounds for the financial evaluation of the proposed system.

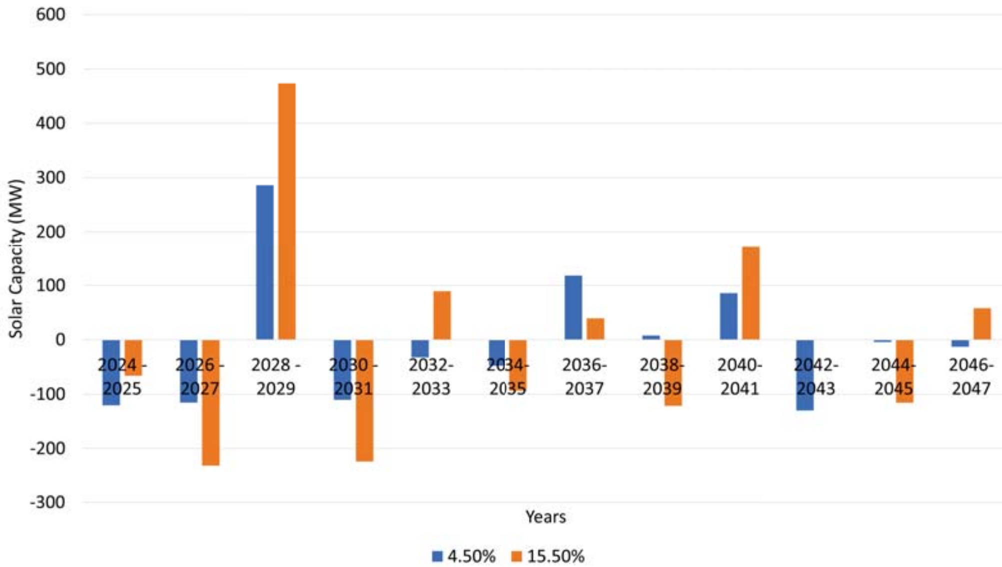

Fig. 5.9: Solar PV capacity variation based on an 8.5% interest rate relevant to *case* 6

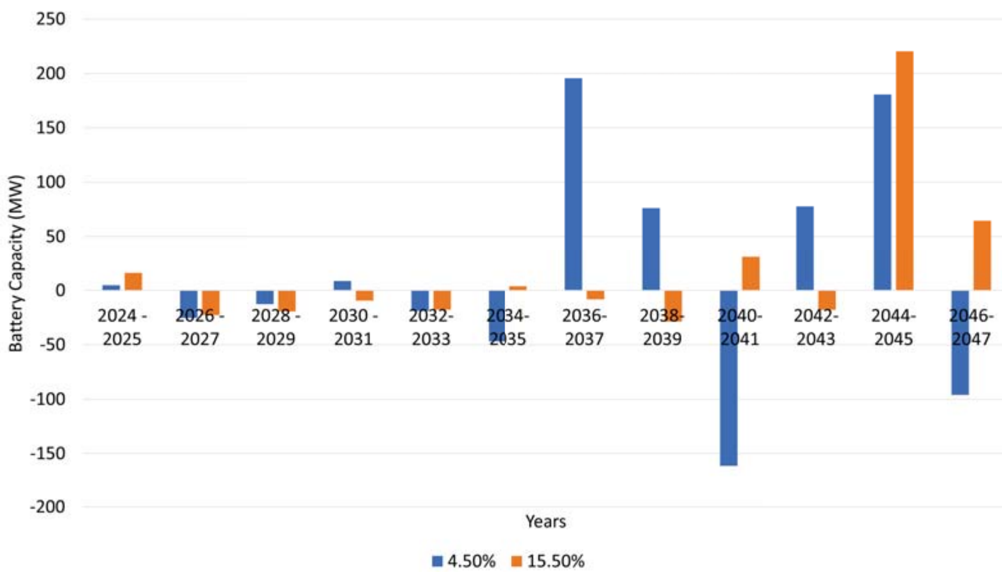

Fig. 5.10: BS capacity variation based on an 8.5% interest rate relevant to *case* 2

5.6.1 Identification of optimal roadmap for proposed system

An increase in the interest rate to 15.5 % results in a higher proposed system total cost, while a decrease to 4.5 % result in to a reduction in the total cost. This relationship occurs because the total cost of the proposed system is directly proportional to the interest rate, with all predicted cost values being sensitive to fluctuations in the interest rate. The capacities of solar PV and Li-ion BS system are reevaluated using the proposed optimization algorithm incorporated alongside an energy management control

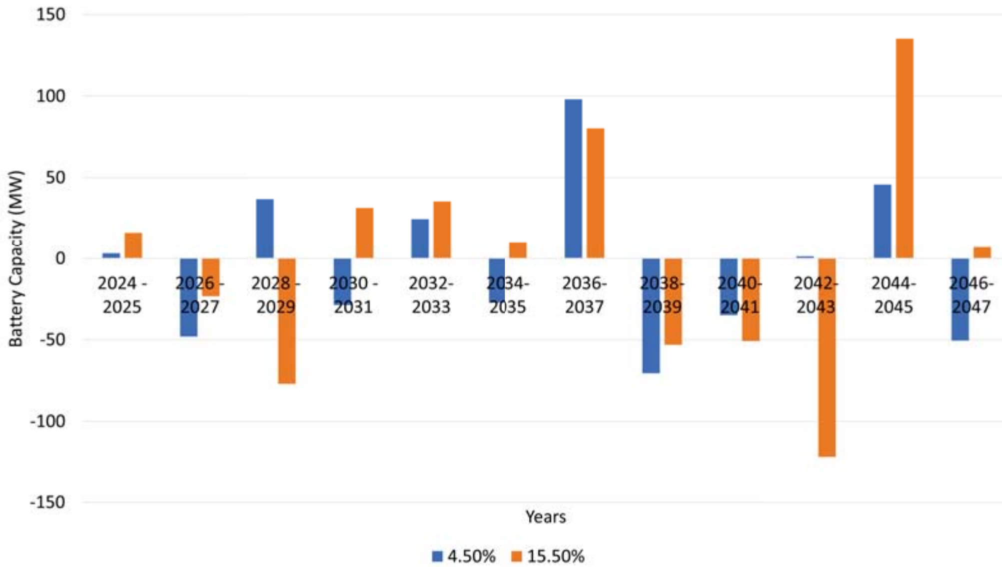

Fig. 5.11: BS capacity variation based on an 8.5% interest rate relevant to *case* 3

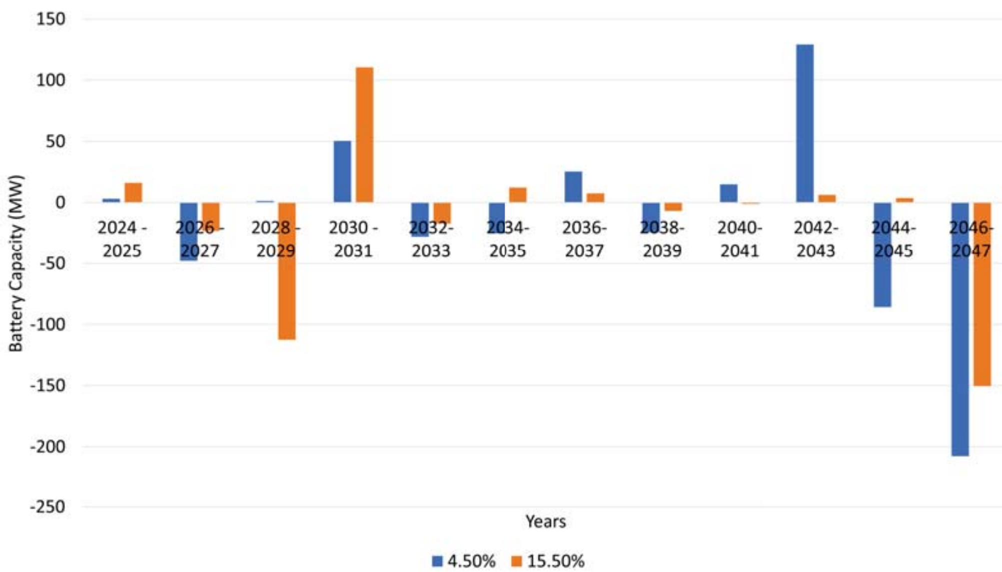

Fig. 5.12: Solar PV capacity variation based on an 8.5% interest rate relevant to *case* 6

strategy for scenarios involving both the highest and lowest interest rates and all other variables keep constant, as outlined in Section 5.6. According to the recalculated solar PV and battery storage capacities for the lowest, actual, and highest interest rates, the corresponding cost values of the proposed system are presented in Table 5.11.

To assess the financial impact of interest rate fluctuations on the proposed system, the total cost of the percentage change at both the lowest and highest interest rates, corresponding to the baseline 8.5 % interest rate, is calculated.The resulting percentage

TABLE 5.11: PROPOSED SYSTEM COST IN EACH CASE FOR DIFFERENT INTEREST RATES SCENARIOS

Case No	Total cost (Million USD)		
	8.50%	4.50%	15.50 %
Case 1	154333.2	130185.5	258161.7
Case 2	153128.7	131601.3	239940.2
Case 3	152736.3	130422.6	255481.6
Case 6	153826.4	143631.0	258069.9

changes in total cost for the most economical and environmentally sustainable cases, based on the 8.5 % interest rate, are displayed in Fig. 5.13.

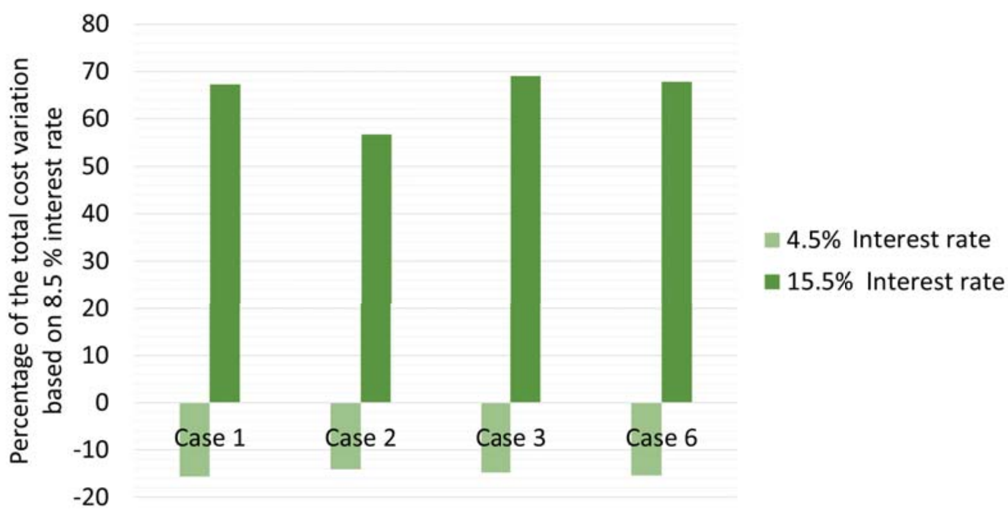

Fig. 5.13: Percentage change of total cost at lowest and highest interest rates relative to an 8.5 % interest rate

When considering about the identified cases, *case* 2 experiences the smallest increase in total cost, with a 56.69 % rise at the highest interest rate of 15.5 %, in relation to the other scenarios. Furthermore, at the lowest interest rate of 4.5 %, the total cost for Case 2 decreases by 14.05 %, representing the most significant reduction relative to the other cases. Because of that, *case* 2 shows the smallest range of total cost variation, spanning from a 56.69 % increase to a 14.05 % decrease. This range indicates that when the interest rate fluctuates between its minimum and maximum values, the total cost will remain within these bounds. Choosing the case with the least cost variation enhances financial predictability and minimizes the risk of budgeting errors. For further analysis, the percentage change in total capacity for both the solar PV and Li-ion battery storage systems is presented in Fig. 5.14 and Fig. 5.15, respectively, based on an 8.5 % interest rate. It clearly shows the variations in solar PV and BS system capacities with different interest rates.

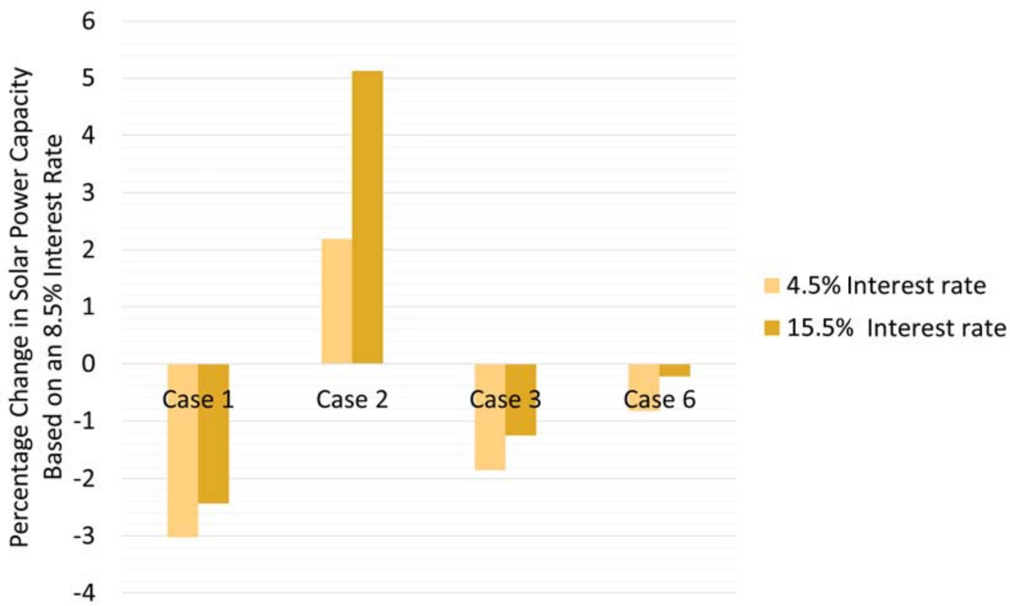

Fig. 5.14: Percentage change in overall solar power capacity according to the proposed system

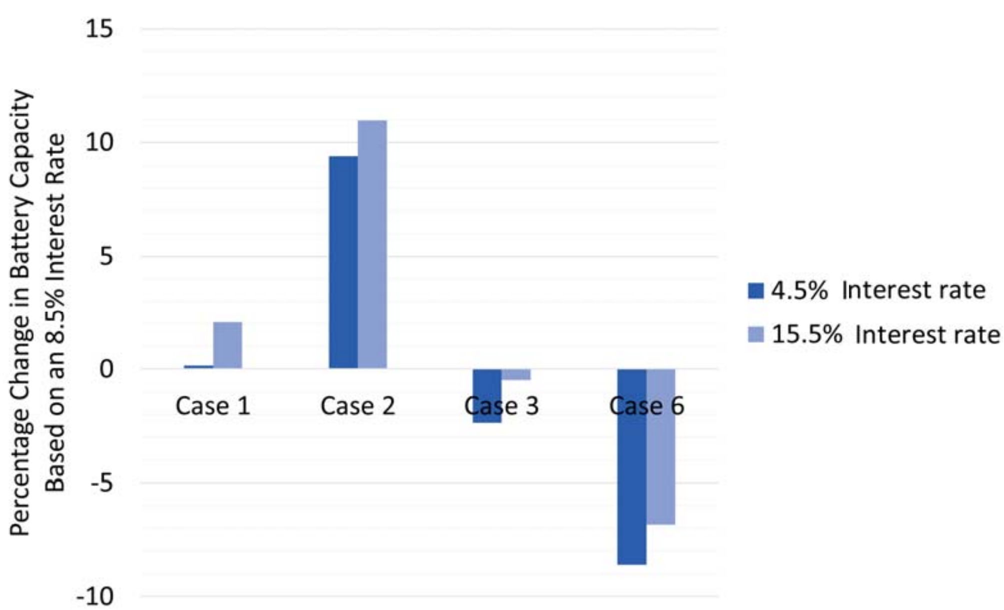

Fig. 5.15: Percentage change in overall battery capacity according to the proposed system

While identifying the capacities of the PV power and Li-ion BS systems for the proposed system, these capacities are calculated by based on the minimum total cost, which incorporates costs related to additional oil-fired thermal power generation and the cost due to solar energy curtailment, using the optimization algorithm. The maximum percentage change in capacities of solar power for both the lowest and highest interest rates is given by *case* 2 based on the 8.5 % interest rate. The percentage change in capacity of solar PV is increased by 2.19 % at a 4.5 % lowest interest rate and by 5.13 % at a 15.5 % highest interest rate, as shown in Fig. 5.14. Additionally, same case indicates the maximum percentage of Li-ion battery storage capacity change, with an increase of 9.42 % at a 4.5 % lowest interest rate and 10.97 % at a 15.5 % highest interest rate, as determined from the analysis results.

Case 2 is determined as having the lowest cost variation in response to interest rate fluctuations, while also providing the highest capacity of solar PV among economic and environmental sustainable cases, based on the factors discussed. The final results of the proposed system roadmap including the optimal capacities of solar PV and Li-ion battery storage for each two-year time period and the most appropriate time to integrate the pumped hydro storage system are summarized in Table 5.12 for the grid-connected solar PV system with HESS. Furthermore, Fig. 5.16 graphically represents the capacities of the solar PV system, BS system, and PHS system.

TABLE 5.12: IDENTIFIED OPTIMAL CAPACITIES OF SOLAR PV AND BS FOR EACH TWO-YEAR PERIOD, ALONG WITH THE RECOMMENDED TIME FOR INTEGRATING PHS TO THE PROPOSED SYSTEM

Years	Solar PV Capacity (MW)	BS Capacity (MW)	PHS Capacity (MW)
2024 - 2025	773.01	0.37	0
2026 - 2027	959.24	96.14	0
2028 - 2029	275.87	202.87	700
2030 - 2031	514.16	95.06	700
2032- 2033	400.56	134.04	0
2034- 2035	690.43	115.57	0
2036- 2037	832.30	115.43	0
2038- 2039	679.75	215.90	0
2040- 2041	776.59	190.67	0
2042- 2043	751.31	284.82	0
2044- 2045	1287.50	211.13	0
2046- 2047	1382.58	273.53	0

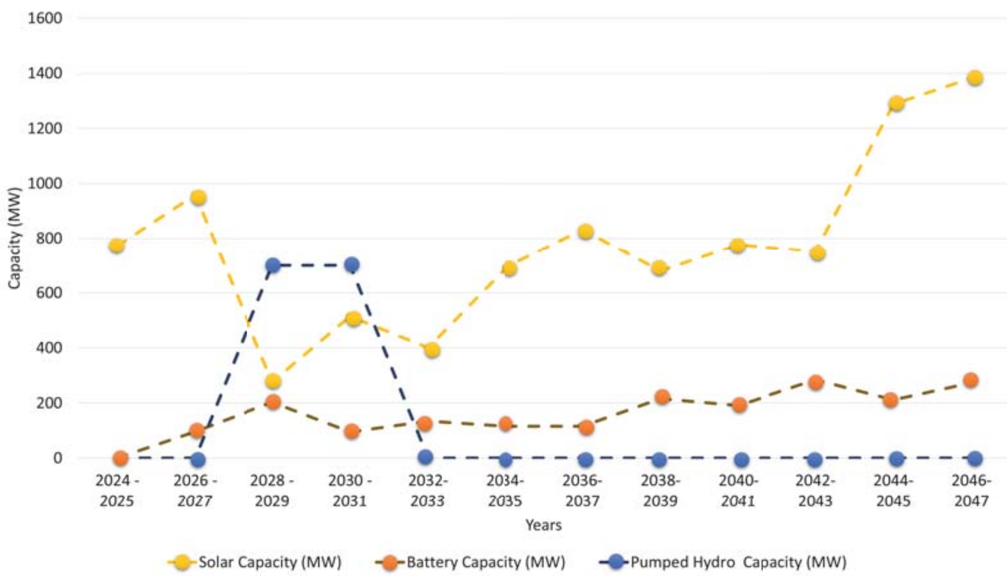

Fig. 5.16: Identified Optimal Roadmap for the Proposed System

5.7 Identification of oil-fired thermal energy generation minimization

The identified solar PV and HESS capacities for each year in the planning horizon are detailed in Section 5.6.1. By comparing the required oil-fired thermal power generation with and without the proposed system, the overall benefits of the system are evaluated. The energy generation percentages with and without the proposed system are provided in Table 5.13. In this table, the second column provides the supplied energy percentages in each year from existing power plants, including coal-fired thermal, hydro, wind, and the existing solar plants in the studied power system. Without the proposed system, the required additional capacity is provided by oil-fired thermal energy generation, and this is shown in the fifth column of the table. The third and fourth columns indicate the contribution of the proposed system to energy generation and the required oil-fired thermal energy generation with the proposed system, respectively.

When comparing the system with and without the proposed system, there is a significant reduction in the percentage of oil-fired thermal energy generation. Specifically, the proposed system leads to nearly a 50 % reduction in oil-fired thermal generation for one year. When considering year-by-year changes, the reliance on oil-fired thermal power generation increases each year due to the fixed capacity of the existing power plants over the planning horizon, while energy demand continues to grow over time.

TABLE 5.13: ENERGY GENERATION PERCENTAGES WITH AND WITHOUT THE PROPOSED SYSTEM

Year	From existing power plant (%)	From proposed system (%)	From oil-fired thermal with proposed system (%)	From oil-fired thermal without proposed system (%)
2024	74.19	10.41	15.40	25.81
2025	71.20	9.86	18.95	28.80
2026	70.39	17.78	11.83	29.61
2027	68.76	16.84	14.40	31.24
2028	66.44	20.85	12.71	33.56
2029	64.18	19.74	16.08	35.82
2030	63.16	24.62	12.22	36.84
2031	62.07	23.31	14.62	37.93
2032	59.85	25.40	14.75	40.15
2033	56.67	24.06	19.27	43.33
2034	54.63	27.59	17.79	45.37
2035	52.64	26.12	21.24	47.36
2036	50.71	29.87	19.42	49.29
2037	48.83	28.29	22.88	51.17
2038	47.01	30.83	22.16	52.99
2039	45.25	29.19	25.56	54.75
2040	43.54	31.67	24.79	56.46
2041	41.89	29.99	28.12	58.11
2042	40.29	32.08	27.64	59.71
2043	38.15	30.38	31.47	61.85
2044	36.13	33.96	29.92	63.87
2045	34.21	32.15	33.63	65.79
2046	32.40	35.52	32.09	67.60
2047	30.68	33.63	35.69	69.32

5.8 Proposed solar PV capacities compared with the national requirement

The proposed solar power capacities for planning horizon (2024 to 2047), relavent to the developed optimization algorithm, and the solar power capacities for national generation planning horizon (2024 to 2042), according to the Sri Lankan generation expansion plan released from CEB, are analysed in Table 5.14 [11]. Further, proposed solar power capacities from proposed optimization algorithm with energy managment strategy and capacities of the solar power plants (2024-2042) from Sri Lankan generation expansion plan is given in Figure 5.17. According to generation expansion plan in Sri Lanka, it aims to reaching 70 % renewable energy by 2030, maintaining 70 %

this level thereafter, and refraining from introducing any new coal-fired power plants throughout the planning horizon. The proposed algorithm is structured to enhance solar power generation, exclude the addition of coal-fired plants, and minimize the use of fossil fuel-based electricity generation over the long term. This comparison facilitates an evaluation of how well the proposed system aligns with national energy objectives and assesses its effectiveness in supporting the achievement of the renewable energy targets in the country.

TABLE 5.14: COMPARISON OF PROPOSED CAPACITIES OF SOLAR PV (2024-2047) FROM THE PROPOSED OPTIMIZATION ALGORITHM WITH CAPACITIES OF SOLAR POWER PLANT (2024-2042) IN THE SRI LANKAN GENERATION EXPANSION PLAN

Years	Solar Capacity (MW)	
	According to Sri Lanka Long term Plan	According to proposed Plan
2024 - 2025	663	931.06
2026 - 2027	660	801.19
2028 - 2029	720	275.87
2030 - 2031	560	514.16
2032- 2033	610	400.56
2034- 2035	660	690.43
2036- 2037	660	832.3
2038- 2039	660	679.75
2040- 2041	640	776.59
2042- 2043	320	751.31
2044- 2045	N/A	1287.5
2046- 2047	N/A	1382.58

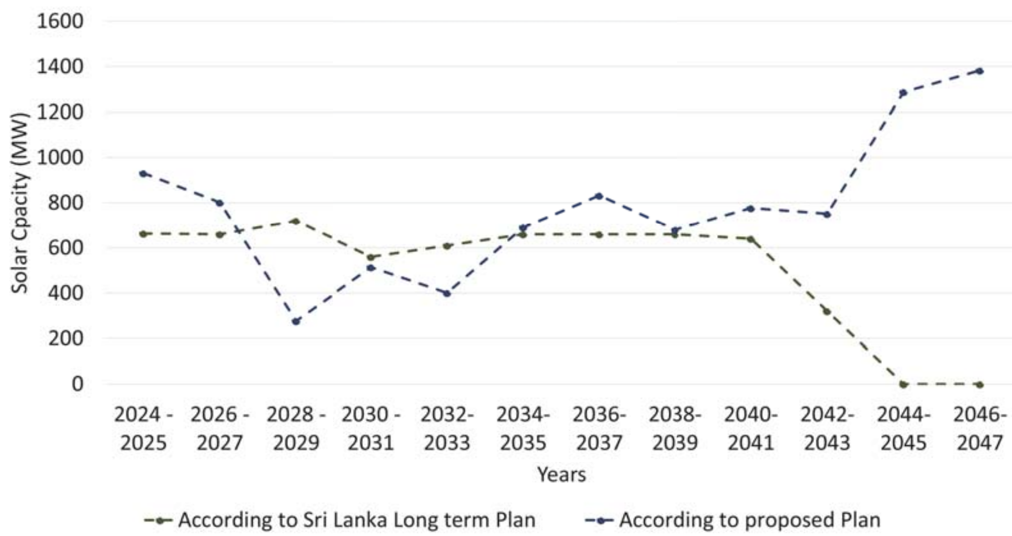

Fig. 5.17: Proposed capacities of solar PV (2024-2047) from the optimization algorithm and projected capacities of solar power plant (2024-2042) from Sri Lankan generation expansion plan

CHAPTER 6

CONCLUSION

Future energy demand is expected to rise due to population growth and increased electricity consumption. To meet these growing energy requirements, future energy generation must be scaled accordingly. In addition, there is a serious environmental challenge to reduce GHG emissions and mitigate climate change caused by human activities. Therefore, the global focus is shifting towards sustainable energy generation. This study aims to maximize solar energy generation, a key renewable energy source, while reducing oil-fired thermal generation, which contributes significantly to GHG emissions, to enhance the sustainability of the power system.

This chapter summarizes the key findings, discusses the challenges and implications of the proposed system, examines its adaptability and outlines potential future improvements.

6.1 Summary of key findings

To overcome the limitations of solar energy, such as unpredictability and intermittency, a HESS is introduced as a controllable solution. Li-ion BS and PHS are selected as energy storage technologies to achieve optimal benefits from the HESS due to their proven maturity and reliability in renewable energy management. An optimization algorithm is employed to determine the capacities of solar PV and lithium-ion BS for short-term intervals throughout the planning horizon. PHS capacity is identified through a feasibility study conducted to the specific country or region. The proposed multi-objective optimization algorithm aims to minimize the installation and operational costs of solar PV and HESS systems, including costs associated with solar curtailment and supplementary oil-fired thermal power generation. Further, an energy management conttrol strategy is developed to balance the energy demand, generation from power plants, and energy storage, thereby ensuring stability and reliability of the system. Considering the potential time periods to integrating PHS into the system, various cases are identified to analyze the results. The optimization problem is addressed using the NSGA-II in conjunction with the open-source Python framework Pymoo. Python code is written and executed within the Google Colab environment. The optimal capacities for solar PV and Li-ion BS are determined for each short-term interval throughout the planning horizon for each identified case. A set of optimal solutions is generated from the optimization algorithm after multiple iterations. The most suitable optimal solution is selected from the Pareto optimal front, considering practical constraints. Economical, environmental, and sensitivity analyses are performed to detemine the higherly applicable and sustainable solution from a range of potential scenarios.

The developed optimization algorithm and energy management strategy can be applied to any power system by incorporating the relevant parameters into the proposed framework. To validate the algorithm integrated with the energy management strategy, the Sri Lankan power system is used as a case study. For the analysis, all necessary data for the planning horizon, such as energy demand, solar irradiation, and wind speed, are forecasted based on historical data from the previous year; for this study, 2023 is used. The data set can be expanded to include multiple years, which would improve the accuracy of the results. In selecting PHS for the study, previously conducted feasibility studies are referenced to determine appropriate PHS capacities and locations. A PHS system with a total capacity of 1400 MW is selected, which can be implemented in two stages of 700 MW each. Based on the selected PHS configuration, fourteen potential cases for integrating PHS into the system are determined. The optimal capacities of solar PV and Li-ion BS are identified for each short-term time span throughout the planning horizon using the optimization algorithm incorporated with energy management strategy. According to the economical and environmental analyses, *Case* 1, *Case* 2, *Case* 3 and *Case* 6 are determined as the greatest economically viable and environmentally sustainable solutions from the evaluated scenarios.

Considering the interest rate fluctuations in the country, a sensitivity analysis is conducted to detemine the scenario with least cost variation, thereby supporting effective long-term planning for the proposed system. *Case* 2 can be identifed as the narrowest range of total cost variation, fluctuating between -14.05 % and 56.69 %, with the lowest interest rate at 4.5 % and the highest at 15.5 %, when comparing economically and environmentally sustainable solutions. Furrthermore, *Case* 2 gives a maximum solar PV capacity increase of 2.19 % and a BS capacity increase of 9.25 %, under the lowest interest rate. Conversely, at the highest interest rate, the solar PV and BS capacities increase by 5.13% and 10.97%, respectively. Among the evaluated cases, *Case* 2 emerges as the most effective solution, offering minimal cost variability and the highest solar capacity responsiveness relavent to the change of interest rate. The optimal capacities of solar PV and BS for each short-term time period are identified using the optimization algorithm, and the final optimal capacities are summarized in Table 5.12. In accordance with these results, PHS can be developed in two stages: an initial 700 MW PHS first stage in the 2028–2029 period, and 700 MW PHS second stage in the 2030–2031 period.

Additionally, the determined capacities of solar PV for the 2024 to 2047 planning horizon are relative to the solar PV power plant capacities outlined in the national energy plan for the 2024 to 2040 given planning period, in order to evaluate their alignment with the RE targets in the country or region. The solar PV capacities from the proposed system and those specified in long-term generation plan in Sri Lanka are presented in Table 5.14 to compare the proposed solar PV and solar energy requirement in the country. The results indicate that the proposed system aligns well with the national energy plan.

When developing the proposed system for a specific country, results are derived under certain assumptions, particularly as many values need to be predicted based on historical data and future requirement. Most of these predictions are currently based on historical data from a single year. To improve the accuracy of the system, a larger set of data covering multiple years can be used. Furthermore, the results may vary due to practical challenges encountered during system implementation.

6.2 issues and implications

It is necessary to make certain assumptions and simplifications to manage the complexity of the system, when implementing the proposed system using this model. These assumptions serve to highlight key factors relavent to both the computational and practical feasibility of the proposed model. Nevertheless, they also influence the applicability as well as reliability of the proposed model. Power systems do not operate according to the idealized assumptions employed in this study, under real-world conditions, and system parameters may vary due to faults or other practical considerations throughout the planning horizon.

Weather patterns (including solar irradiation and wind speed), enrgy demand trends, and energy generation patterns from power plants are forecasted based on historical weather, demand, and generation data from the preceding year. For this study, data from the most recent year, 2023, is used for these predictions. Consequently, the accuracy of these predictions is heavily based on the quality of the selected dataset. Enhancing the accuracy of the dataset can result in more reliable outcomes. The developed compulational program is capable of performing accurate analyses on large datasets, thereby improving the reliability of the system, even though it involves extensive computation time when handling larger datasets. Nevertheless, it demands considerable computational resources when processing extensive data. In contrast, outdated data, missing, or inaccurate, such as erroneous historical records, can generate misleading predictions and potentially flawed conclusions. Incorporating data spanning multiple years could improve the robustness of weather and demand forecasts. Furthermore, the study does not account for dynamic influences such as climate change or extreme weather events, which may significantly affect future predictions.

In addtion, the construction and installation phases may extend beyond the planned timeline due to practical challenges and uncontrollable factors. Additionally, during the planning horizon, changes in national policies could directly influence the final outcomes.

PHS is employed as a storage technology, requiring a feasibility study to identify the suitable capacity and location, whereby necessitates a comprehensive feasibility study to determine suitable capacity and location, in this study. Both capacity and location are highly dependent on the geological characteristics of the region o country.

Similarly, for solar PV power plants, identifying optimal locations with adequate solar irradiation is essential to maximize the effectiveness of the proposed system. In this study, solar irradiation patterns were assumed to remain consistent throughout the year, based on geographic proximity of the Sri Lanka to the equator. However, for other countries, solar irradiation profiles must be determined and incorporated according to their specific geographical and climatic conditions.

6.3 Proposed model adaptability for general power systems

The developed model is designed to be adaptable to other power systems by applying the same multi-objective optimization approach, tailored to the specific characteristics of the target country or region. It can be configured to accommodate a wide range of technological, economical, and geographical conditions. The proposed model incorporates two objective functions, as described in Section 3.2, in addition to their respective constraints. These components including objective functions, constraints, sizing methodologies, and decision variables, can be customized for any type of power system by giving appropriate parameter values that represent the unique attributes of the power system. For the purpose of validation, the proposed model was employed to a specific country, taking its available resources, energy demand profile, and infrastructure capabilities.

An essential step of the implementing the proposed model is the selection of power plants from the existing power system to be included in the study. This process involves analyzing the load profile and generation capacities of current facilities. Emphasis should be placed on incorporating renewable energy sources and power plants that are critical for maintaining the base load, in order to maximize output. It is also necessary to identify power plants capability for operating at minimum output levels to support flexible system operation. The use of oil-fired and coal-fired thermal power plants should be minimized whenever alternative generation sources can sufficiently meet demand. After selecting the relevant power plants, selected power plants technical and operational details can be given as a input to the model. The model supports a wide range of plant capacities by allowing input of specific capacity values and corresponding plant factors, enabling adaptation to the available generation assets. In addition, solar PV panel configurations and BS setups can also be customized according national requirements. Likewise, the parameters for PHS can be modified based on feasibility studies relevant to the region being studied.

The model is versatile and can be applied to both small-scale and large-scale power systems, requiring only that system-specific parameters be accurately defined.

6.4 Future improvements

With the current focus on a sustainable future, renewable energy usage has become a primary goal, and its limitations must be addressed to enhance its applicability and effectiveness. Improving the performance of renewable energy is a broad area of research. This study specifically focuses on solar PV and HESS with Li-ion BS and PHS to enhance system effectiveness. To further refine and expand this focus, suggestions are provided in this section.

In the future, the developed multi-objective optimization algorithm can be further extended by considering the limitations explained in Section 6.2. The algorithm may be improved by incorporating a broader range of renewable energy sources, such as wind power, with the ability to optimize their capacities dynamically rather than relying on fixed inputs. Additionally, exploring alternative energy storage technologies could enhance both the efficiency and sustainability of the system. The algorithm can also be developed to account for uncertain and incomplete parameters, thereby increasing its adaptability and making it more suitable for real-world applications.

6.5 Conclusion

In conclusion, a roadmap is introduced for integrating solar PV and HESS into the power system. This provides an economically and environmentally sustainable solution with minimal investment risk due to reduced cost fluctuations throughout economic changes. When applied to the Sri Lankan power system using the developed algorithm, the results align closely with the energy requirements of the country. Finally, the developed algorithms can be utilized to effectively plan the integration of solar PV and HESS, thereby enhancing renewable energy usage.

REFERENCES

[1] European Commission, "Causes of climate change," 2024, accessed: 2024-10-08. [Online]. Available: https://climate.ec.europa.eu/climate-change/causes-climate-change_en

[2] United Nations, "Goal 7: Ensure access to affordable, reliable, sustainable and modern energy for all," 2024, accessed: 2024-10-08. [Online]. Available: https://sdgs.un.org/goals/goal7#targets_and_indicators

[3] United Nations Framework Convention on Climate Change, "Key aspects of the Paris Agreement," 2024, accessed: 2024-10-10. [Online]. Available: https://unfccc.int/most-requested/key-aspects-of-the-paris-agreement

[4] Joint Research Centre, "GHG Emissions of All World Countries – 2023," 2023, accessed: 2024-10-08. [Online]. Available: https://edgar.jrc.ec.europa.eu/report_2023

[5] International Energy Agency, "CO2 Emissions in 2022," 2023, accessed: 2024-10-09. [Online]. Available: https://www.iea.org/reports/co2-emissions-in-2022

[6] International Energy Agency1, "Greenhouse Gas Emissions from Energy Data Explorer," 2024, accessed: 2024-10-09. [Online]. Available: https://www.iea.org/data-and-statistics/data-tools/greenhouse-gas-emissions-from-energy-data-explorer

[7] International Energy Agency, *World Energy Outlook 2019*. Paris: OECD Publishing, 2019, accessed: 2024-10-10. [Online]. Available: https://www.iea.org/reports/world-energy-outlook-2019

[8] S. M. G. Dumlao and K. N. Ishihara, "Dynamic cost-optimal assessment of complementary diurnal electricity storage capacity in high pv penetration grid," *Energies*, vol. 14, no. 15, p. 4496, 2021. [Online]. Available: https://www.mdpi.com/1996-1073/14/15/4496

[9] Ray and Douglas, "Lazard's Levelized Cost of Energy Analysis—Version 13.0," Lazard, 2020, accessed: 2024-10-09. [Online]. Available: https://www.lazard.com/media/451419/lazards-levelized-cost-of-energy-version-130-vf.pdf

[10] M. Aneke and M. Wang, "Energy storage technologies and real life applications – a state of the art review," *Applied Energy*, vol. 179, pp. 350–377, 2016, accessed: 2024-10-10. [Online]. Available: https://doi.org/10.1016/j.apenergy.2016.06.097

[11] Ceylon Electricity Board, "Long Term Generation Expansion Plan (LTGEP) 2023-2042," 2023, accessed: 2024-10-09. [Online]. Available: https://www.ceb.lk/publication-media/planing-documents/121/en

[12] A. Wangsupphaphol, Sutikno, and W. Arsadiando, "A review of recent advances on hybrid energy storage system for solar photovoltaics power generation," *IEEE Access*, vol. 10, pp. 42 346–42 364, 2022, accessed: 2024-10-12. [Online]. Available: https://doi.org/10.1109/ACCESS.2022.3165798

[13] S. Rehman, L. M. Al-Hadhrami, and M. M. Alam, "Pumped hydro energy storage system: A technological review," *Renewable and Sustainable Energy Reviews*, vol. 44, pp. 586–598, 2015, accessed: 2024-10-12. [Online]. Available: https://doi.org/10.1016/j.rser.2014.12.040

[14] G. Venkataramani, P. Parankusam, and V. Ramalingam, "A review on compressed air energy storage – a pathway for smart grid and polygeneration," *Renewable and Sustainable Energy Reviews*, vol. 62, pp. 895–907, 2016, accessed: 2024-10-12. [Online]. Available: https://doi.org/10.1016/j.rser.2016.05.002

[15] A. Evans, V. Strezov, and T. J. Evans, "Assessment of utility energy storage options for increased renewable energy penetration," *Renewable and Sustainable Energy Reviews*, vol. 16, no. 6, pp. 4141–4147, 2012, accessed: 2024-10-12. [Online]. Available: https://doi.org/10.1016/j.rser.2012.03.048

[16] M. Amir, R. G. Deshmukh, H. M. Khalid, Z. Said, A. Raza, S. M. Muyeen, A.-S. Nizami, R. M. Elavarasan, R. Saidur, and K. Sopian, "Energy storage technologies: An integrated survey of developments, global economical/environmental effects, optimal scheduling model, and sustainable adaptation policies," *Journal of Energy Storage*, vol. 72, p. 108694, 2023, accessed: 2024-10-14. [Online]. Available: https://doi.org/10.1016/j.est.2023.108694

[17] V. Vega-Garita, A. Hanif, N. Narayan, L. M. Ramirez-Elizondo, and P. Bauer, "Selecting a suitable battery technology for the photovoltaic battery integrated module," *Journal of Power Sources*, vol. 438, p. 227011, 2019, accessed: 2024-10-14. [Online]. Available: https://doi.org/10.1016/j.jpowsour.2019.227011

[18] W. Sun, Z. Wang, and Z. Chen, "Optimization of battery–supercapacitor hybrid energy storage station in wind/solar generation system," *IEEE Transactions on Sustainable Energy*, vol. 5, no. 1, pp. 408–415, 2014, accessed: 2024-10-14. [Online]. Available: https://doi.org/10.1109/TSTE.2013.2288804

[19] Energi og Klima, “A forecast of the energy transition to 2050,” 2024, accessed: 2024-12-22. [Online]. Available: https://www.energiogklima.no/articles-in-english/a-forecast-of-the-energy-transition-to-2050

[20] A. Z. A. Shaqsi, K. Sopian, and A. Al-Hinai, “Review of energy storage services, applications, limitations, and benefits,” *Energy Reports*, vol. 6, pp. 288–306, 2020. [Online]. Available: https://doi.org/10.1016/j.egyr.2020.07.028

[21] X. Luo, J. Wang, M. Dooner, and J. Clarke, “Overview of current development in electrical energy storage technologies and the application potential in power system operation,” *Applied Energy*, vol. 137, pp. 511–536, 2015. [Online]. Available: https://doi.org/10.1016/j.apenergy.2014.09.081

[22] F. Geth, T. Brijs, J. Kathan, J. Driesen, and R. Belmans, “An overview of large-scale stationary electricity storage plants in europe: Current status and new developments,” *Renewable and Sustainable Energy Reviews*, vol. 52, pp. 1212–1227, 2015. [Online]. Available: https://doi.org/10.1016/j.rser.2015.07.145

[23] M. Aneke and M. Wang, “Energy storage technologies and real life applications – a state of the art review,” *Applied Energy*, vol. 179, pp. 350–377, 2016. [Online]. Available: https://www.sciencedirect.com/science/article/pii/S0306261916308728

[24] M. A. Hannan, S. B. Wali, and P. J. Ker, “Battery energy-storage system: A review of technologies, optimization objectives, constraints, approaches, and outstanding issues,” *Journal of Energy Storage*, vol. 42, p. 103023, 2021. [Online]. Available: https://doi.org/10.1016/j.est.2021.103023

[25] I. E. Atawi, A. Q. Al-Shetwi, A. M. Magableh, and O. H. Albalawi, “Recent advances in hybrid energy storage system integrated renewable power generation: Configuration, control, applications, and future directions,” *Batteries*, vol. 9, no. 1, p. 29, 2023. [Online]. Available: https://doi.org/10.3390/batteries9010029

[26] A. A. Kebede, T. Coosemans, M. Messagie, T. Jemal, H. A. Behabtu, J. V. Mierlo, and M. Berecibar, “Techno-economic analysis of lithium-ion and lead-acid batteries in stationary energy storage application,” *Journal of Energy Storage*, vol. 40, p. 102748, 2021. [Online]. Available: https://doi.org/10.1016/j.est.2021.102748

[27] J. Carroquino, C. Escriche-Martínez, L. Valiño, and R. Dufo-López, “Comparison of economic performance of lead-acid and li-ion batteries in standalone photovoltaic energy systems,” *Applied Sciences*, vol. 11, no. 8, p. 3587, 2021. [Online]. Available: https://doi.org/10.3390/app11083587

[28] W. Wang, Q. Luo, B. Li, X. Wei, L. Li, and Z. Yang, "Recent progress in redox flow battery research and development," *Advanced Functional Materials*, vol. 23, no. 8, pp. 970–986, 2013. [Online]. Available: https://onlinelibrary.wiley.com/doi/10.1002/adfm.201200694

[29] T. M. Gür, "Review of electrical energy storage technologies, materials and systems: challenges and prospects for large-scale grid storage," *Energy & Environmental Science*, vol. 11, pp. 2696–2767, 2018. [Online]. Available: https://doi.org/10.1039/c8ee01419a

[30] Y. Li, W. Gao, Y. Ruan, and Y. Ushifusa, "The performance investigation of increasing share of photovoltaic generation in the public grid with pump hydro storage dispatch system, a case study in japan," *Energy*, vol. 164, pp. 811–821, 2018. [Online]. Available: https://www.sciencedirect.com/science/article/pii/S0360544218317894

[31] T. Sudhakar, K. R. Vasudevan, and V. K. Ramachandaramurthy, "A comprehensive review of hybrid energy storage systems: Converter topologies, control strategies, and future prospects," *IEEE Access*, vol. 8, pp. 110–130, 2020. [Online]. Available: https://ieeexplore.ieee.org/document/9165104/

[32] C.-H. Li, X.-J. Zhu, G.-Y. Cao, S. Sui, and M.-R. Hu, "Dynamic modeling and sizing optimization of stand-alone photovoltaic power systems using hybrid energy storage technology," *Renewable Energy*, vol. 34, no. 3, pp. 815–826, 2009. [Online]. Available: https://doi.org/10.1016/j.renene.2008.04.018

[33] T. B. Nkwanyana, M. W. Siti, Z. Wang, I. Toudjeu, N. T. Mbungu, and W. Mulumba, "An assessment of hybrid-energy storage systems in the renewable environments," *Journal of Energy Storage*, vol. 72, p. 108307, 2023. [Online]. Available: https://doi.org/10.1016/j.est.2023.108307

[34] Z. Yang, Z. Han, and X. Zhang, "A grid connected photovoltaic inverter with battery-supercapacitor hybrid energy storage," *Sensors*, vol. 17, no. 8, p. 1856, 2017. [Online]. Available: https://doi.org/10.3390/s17081856

[35] S. Alshahrani, M. Khalid, and M. Abido, "Frequency regulation coordinated framework: Hybrid battery energy storage system and supercapacitor," in *Proceedings of the 26th International Conference and Exhibition on Electricity Distribution (CIRED 2021)*. The Institution of Engineering and Technology, 2021, pp. 2339–2344. [Online]. Available: https://digital-library.theiet.org/content/conferences/10.1049/icp.2021.1920

[36] N. Tephiruk, P. Jamjang, A. Taweesap, and K. Hongesombut, "Hybrid energy storage system to enhance efficiency of renewable energy usage," in *Proceedings*

of the 19th International Conference on Electrical Engineering/Electronics, Computer, Telecommunications and Information Technology (ECTI-CON 2022). IEEE, 2022, pp. 1–4. [Online]. Available: https://doi.org/10.1109/ECTI-CON54298.2022.9795622

[37] Y. Feng, L. Zhang, Y. Zhang, X. Zhang, and Y. Zhang, "Performance analysis of hybrid energy storage integrated with distributed renewable energy," *Energy Reports*, vol. 8, pp. 1829–1837, 2021. [Online]. Available: https://doi.org/10.1016/j.egyr.2021.12.078

[38] J. Ni, Y. Chen, T. Wang, and W. Jin, "Optimization strategy for wind-solar complementary energy storage capacity leveraging photovoltaic virtual energy storage," in *Proceedings of the 3rd Conference on Fully Actuated System Theory and Applications (FASTA 2024)*. IEEE, 2024, pp. 1317–1322. [Online]. Available: https://doi.org/10.1109/FASTA61401.2024.10595202

[39] J. Canales, M. A. S. Masoum, M. A. S. Masoum, and M. A. S. Masoum, "Cost-reliability analysis of hybrid pumped-battery storage for solar and wind energy integration in an island community," *Sustainable Energy Technologies and Assessments*, vol. 44, p. 101062, 2021. [Online]. Available: https://doi.org/10.1016/j.seta.2021.101062

[40] T. Ma, H. Yang, and L. Lu, "Feasibility study and economic analysis of pumped hydro storage and battery storage for a renewable energy powered island," *Energy Conversion and Management*, vol. 79, pp. 387–397, 2014. [Online]. Available: https://doi.org/10.1016/j.enconman.2013.12.047

[41] M. S. Javed, D. Zhong, T. Ma, A. Song, and S. Ahmed, "Hybrid pumped hydro and battery storage for renewable energy based power supply system," *Applied Energy*, vol. 257, p. 114026, 2020. [Online]. Available: https://doi.org/10.1016/j.apenergy.2019.114026

[42] P. N. D. Premadasa and D. P. Chandima, "An innovative approach of optimizing size and cost of hybrid energy storage system with state of charge regulation for stand-alone direct current microgrids," *Journal of Energy Storage*, vol. 32, p. 101703, 2020. [Online]. Available: https://doi.org/10.1016/j.est.2020.101703

[43] Z. Wu, Y. Chi, X. Tang, X. Yang, R. Lin, Y. Lu, and J. Liu, "Real-time scheduling method based on deep reinforcement learning for a hybrid wind-solar-storage energy generation system," in *IET Conference Proceedings*. Institution of Engineering and Technology (IET), 2021. [Online]. Available: https://doi.org/10.1049/icp.2021.2317

[44] J. Kang, Y. Zhang, Y. Zhang, Y. Zhang, and Y. Zhang, "Optimal planning of hybrid energy storage systems using curtailed renewable energy through deep reinforcement learning," *Energy*, vol. 284, p. 128623, 2023. [Online]. Available: https://doi.org/10.1016/j.energy.2023.128623

[45] A. Hedayatnia, J. Ghafourian, R. Sepehrzad, A. Al-Durrad, and A. Anvari-Moghaddam, "Two-stage data-driven optimal energy management and dynamic real-time operation in networked microgrid based on a deep reinforcement learning approach," *International Journal of Electrical Power & Energy Systems*, vol. 141, p. 110142, 2024. [Online]. Available: https://doi.org/10.1016/j.ijepes.2024.110142

[46] S. Safari, M. M. Ardehali, and M. J. Sirizi, "Particle swarm optimization based fuzzy logic controller for autonomous green power energy system with hydrogen storage," *Energy Conversion and Management*, vol. 65, pp. 41–49, 2013. [Online]. Available: https://doi.org/10.1016/j.enconman.2012.08.012

[47] A. D. Falehi, "Novel harmonic elimination strategy based on multi-objective grey wolf optimizer to ameliorate voltage quality of odd-nary multi-level structure," *Heliyon*, vol. 6, no. 3, p. e03585, 2020. [Online]. Available: https://doi.org/10.1016/j.heliyon.2020.e03585

[48] M.-E. Choi, S.-W. Kim, and S.-W. Seo, "Energy management optimization in a battery/supercapacitor hybrid energy storage system," *IEEE Transactions on Smart Grid*, vol. 3, no. 1, pp. 463–472, 2012.

[49] T. Terlouw, T. AlSkaif, C. Bauer, and W. van Sark, "Multi-objective optimization of energy arbitrage in community energy storage systems using different battery technologies," *Applied Energy*, vol. 239, pp. 356–372, 2019. [Online]. Available: https://doi.org/10.1016/j.apenergy.2019.01.227

[50] F. Xu, J. Liu, S. Lin, Q. Dai, and C. Li, "A multi-objective optimization model of hybrid energy storage system for non-grid-connected wind power: A case study in china," *Energy*, vol. 163, pp. 585–603, 2018. [Online]. Available: https://doi.org/10.1016/j.energy.2018.08.152

[51] R. Sepehrzad, A. S. G. Langeroudi, A. Khodadadi, S. Adinehpour, A. Al-Durra, and A. Anvari-Moghaddam, "An applied deep reinforcement learning approach to control active networked microgrids in smart cities with multi-level participation of battery energy storage system and electric vehicles," *Sustainable Cities and Society*, vol. 107, p. 105352, 2024. [Online]. Available: https://doi.org/10.1016/j.scs.2024.105352

[52] R. Sepehrzad, A. Hedayatnia, M. Amohadi, J. Ghafourian, A. Al-Durra, and A. Anvari-Moghaddam, “Two-stage experimental intelligent dynamic energy management of microgrid in smart cities based on demand response programs and energy storage system participation,” *International Journal of Electrical Power & Energy Systems*, vol. 155, p. 109613, 2024. [Online]. Available: https://doi.org/10.1016/j.ijepes.2023.109613

[53] A. D. Falehi, “Moba based design of fopid–sssc for load frequency control of interconnected multi-area power systems,” *Smart Structures and Systems*, vol. 22, no. 1, pp. 81–97, 2018. [Online]. Available: https://doi.org/10.12989/sss.2018.22.1.081

[54] F. Cebulla, J. Haas, J. Eichman, W. Novak, and P. Mancarella, “Electrical energy storage in highly renewable european energy systems: Capacity requirements, spatial distribution, and storage dispatch,” *Journal of Energy Storage*, vol. 14, pp. 211–223, 2017. [Online]. Available: https://doi.org/10.1016/j.est.2017.10.004

[55] G. Pleßmann and P. Blechinger, “How much might it cost to decarbonize the power sector? it depends on the generation mix and regional factors,” *Energy Strategy Reviews*, vol. 15, pp. 1–10, 2017. [Online]. Available: https://doi.org/10.1016/j.esr.2016.11.003

[56] S. Canbulat, K. Balci, O. Canbulat, and I. S. Bayram, “Techno-economic analysis of on-site energy storage units to mitigate wind energy curtailment: A case study in scotland,” *Energies*, vol. 14, no. 6, p. 1691, 2021. [Online]. Available: https://doi.org/10.3390/en14061691

[57] S. Rayit, S. S. S. R. Depuru, S. S. R. Depuru, and S. S. S. R. Depuru, “Techno-economic optimisation of battery storage for grid-level energy services using curtailed energy from wind,” *Journal of Energy Storage*, vol. 39, p. 102641, 2021. [Online]. Available: https://doi.org/10.1016/j.est.2021.102641

[58] H. Shin and J. Hur, “Optimal energy storage sizing with battery augmentation for renewable-plus-storage power plants,” *IEEE Access*, vol. 8, pp. 187 730–187 743, 2020. [Online]. Available: https://doi.org/10.1109/ACCESS.2020.3031197

[59] A. Maleki and F. Pourfayaz, “Optimal sizing of autonomous hybrid photovoltaic/wind/battery power system with lpsp technology by using evolutionary algorithms,” *Solar Energy*, vol. 115, pp. 471–483, 2015, accessed: 2024-10-17. [Online]. Available: https://doi.org/10.1016/j.solener.2015.03.004

[60] A. Askarzadeh, “A discrete chaotic harmony search-based simulated annealing algorithm for optimum design of pv/wind hybrid system,” *Solar Energy*,

vol. 97, pp. 93–101, 2013, accessed: 2024-10-17. [Online]. Available: https://doi.org/10.1016/j.solener.2013.08.014

[61] R. Belfkira, L. Zhang, and G. Barakat, "Optimal sizing study of hybrid wind/pv/diesel power generation unit," *Solar Energy*, vol. 85, no. 1, pp. 100–110, 2011, accessed: 2024-10-20. [Online]. Available: https://doi.org/10.1016/j.solener.2010.10.018

[62] K. Katsifarakis and P. Bakanos, "Optimizing operation of a large-scale pumped storage hydropower system coordinated with wind farm by means of genetic algorithms," *Global NEST Journal*, vol. 21, no. 4, pp. 495–504, 2019. [Online]. Available: https://doi.org/10.30955/gnj.002978

[63] Public Utilities Commission of Sri Lanka, "Generation information (archived)," 2024, accessed: 2023-12-15. [Online]. Available: https://www.pucsl.gov.lk/generation-information-archived/

[64] Ceylon Electricity Board, "Annual reports 2022," 2023, accessed: 2023-05-22. [Online]. Available: https://www.ceb.lk/publication-media/annual-reports/en

[65] World Bank Group, "Global solar atlas map," 2024, accessed: 2023-05-10. [Online]. Available: https://globalsolaratlas.info/map

[66] Google, "Google earth," 2024, accessed: 2023-05-10. [Online]. Available: https://earth.google.com/web

[67] NASA Langley Research Center, "Nasa power: Prediction of worldwide energy resource," 2024, accessed: 2023-05-08. [Online]. Available: https://power.larc.nasa.gov/

[68] Trina Solar, "Trina solar vertex de21 datasheet," 2021, accessed: 2023-05-07. [Online]. Available: https://static.trinasolar.com/sites/default/files/DT-M-0012_A_Datasheet_Vertex_DE21_EN_2021_A_web.pdf

[69] National Renewable Energy Laboratory, "Electricity technologies 2023," 2023, accessed: 2024-12-22. [Online]. Available: https://atb.nrel.gov/electricity/2023/technologies

[70] Ecube ESS, "High c-rate lithium batteries," 2024, accessed: 2024-12-22. [Online]. Available: https://www.ecubeess.com/innovative-lfp-battery-system/high-c-rate-lithium-batteries/

[71] Ceylon Electricity Board, "Annual reports 2021," 2022, accessed: 2024-12-22. [Online]. Available: https://www.ceb.lk/publication-media/annual-reports/123/en

[72] Trading Economics, "Sri lanka interest rate," 2024, accessed: 2024-12-22. [Online]. Available: https://tradingeconomics.com/sri-lanka/interest-rate

APPENDIX A

ENERGY GENERATION POWER PLANTS WITH GENERATED CAPACITIES IN 24 MAY 2023 ACCORDING TO THE PUCSL PUBLISHED DATA

Energy generation power plants with generated capacities (MW) in 24 May 2023 according to the PUCSL published data

Time	Coal	Oil-CEB owned	Oil-IPP owned	Major Hydro	Wind power	Solar power	Bio mass	Mini Hydro	Total Generation
0:15	733	317	0	184	101	0	11	77	1423
0:30	732	286	0	185	111	0	11	76	1401
0:45	734	265	0	218	108	0	11	78	1414
1:00	735	264	0	200	105	0	11	78	1393
1:15	733	265	0	187	115	0	11	77	1388
1:30	735	231	0	201	117	0	11	74	1369
1:45	733	233	0	191	116	0	11	74	1358
2:00	734	232	0	167	123	0	10	78	1344
2:15	735	219	0	173	125	0	11	76	1339
2:30	734	194	0	176	120	0	11	76	1311
2:45	734	195	0	162	120	0	11	74	1296
3:00	732	207	0	158	112	0	11	74	1294
3:15	731	208	0	145	116	0	11	74	1285
3:30	734	207	0	157	113	0	11	73	1295
3:45	733	208	0	160	112	0	11	75	1299
4:00	732	207	11	168	112	0	11	76	1317
4:15	736	219	42	172	123	0	11	74	1377
4:30	734	229	60	208	113	0	9	70	1423
4:45	736	261	120	198	119	0	9	70	1513
5:00	737	273	142	238	119	0	9	70	1588

Continued on next page

Energy generation power plants with generated capacities (MW) in 24 May 2023 according to the PUCSL published data (Continued)

5:15	737	309	141	333	117	0	10	67	1714
5:30	733	325	141	464	115	0	10	66	1854
5:45	732	331	142	520	115	0	11	66	1917
6:00	732	331	141	493	111	0	11	65	1884
6:15	732	331	142	437	112	0	10	62	1826
6:30	733	332	142	335	113	3	10	63	1731
6:45	733	309	142	258	114	5	9	62	1632
7:00	732	292	142	193	105	7	10	61	1542
7:15	733	273	141	184	105	10	9	60	1515
7:30	733	276	141	183	96	13	9	60	1511
7:45	732	285	140	216	82	16	9	59	1539
8:00	733	291	149	220	85	18	10	59	1565
8:15	733	320	158	246	86	18	10	58	1629
8:30	734	331	161	287	96	14	10	59	1692
8:45	732	331	163	292	96	22	10	58	1704
9:00	733	331	203	285	102	24	10	61	1749
9:15	732	309	224	294	104	22	9	64	1758
9:30	733	291	251	291	108	26	9	64	1773
9:45	731	275	274	279	106	26	9	64	1764
10:00	731	265	280	275	103	30	8	63	1755
10:15	724	239	280	289	99	25	9	64	1729
10:30	713	239	281	294	105	30	10	65	1737
10:45	730	235	279	303	95	27	10	66	1745
11:00	727	236	279	331	96	20	11	66	1766
11:15	731	246	280	321	101	24	10	66	1779
11:30	731	234	277	344	93	31	11	64	1785
11:45	731	234	277	347	98	18	11	66	1782
12:00	729	225	278	341	106	23	11	57	1770
12:15	732	224	277	331	106	33	10	59	1772

Continued on next page

Energy generation power plants with generated capacities (MW) in 24 May 2023 according to the PUCSL published data (Continued)

12:30	731	215	278	305	111	32	10	62	1744
12:45	728	215	263	311	104	32	10	62	1725
13:00	730	213	263	293	106	32	10	62	1709
13:15	729	208	261	288	113	32	10	61	1702
13:30	730	209	261	291	112	31	11	60	1705
13:45	730	221	261	296	111	30	11	58	1718
14:00	730	223	277	302	117	29	11	58	1747
14:15	732	243	278	333	107	28	11	58	1790
14:30	733	278	281	341	112	28	11	58	1842
14:45	731	308	281	363	115	26	11	58	1893
15:00	732	321	282	360	108	25	11	57	1896
15:15	732	323	281	361	111	24	11	59	1902
15:30	732	326	281	395	119	22	11	59	1945
15:45	733	348	281	417	113	20	11	59	1982
16:00	732	351	282	450	114	19	11	59	2018
16:15	732	353	282	475	94	17	11	58	2022
16:30	730	386	282	438	113	13	11	58	2031
16:45	732	388	282	441	112	10	10	58	2033
17:00	731	389	284	438	116	8	10	55	2031
17:15	731	391	282	416	116	5	11	57	2009
17:30	732	421	283	384	115	3	11	55	2004
17:45	731	442	284	365	116	1	11	55	2005
18:00	730	432	283	363	119	0	11	57	1995
18:15	731	429	284	379	117	0	9	61	2010
18:30	729	448	283	472	118	0	7	58	2115
18:45	731	464	283	571	123	0	8	60	2240
19:00	731	462	284	626	123	0	7	59	2292
19:15	733	466	283	628	115	0	8	56	2289
19:30	731	459	284	616	115	0	9	55	2269

Continued on next page

Energy generation power plants with generated capacities (MW) in 24 May 2023 according to the PUCSL published data (Continued)

19:45	733	446	284	584	114	0	7	55	2223
20:00	732	432	285	564	112	0	7	53	2185
20:15	732	392	285	549	116	0	7	53	2134
20:30	731	326	285	578	123	0	9	58	2110
20:45	730	311	285	545	124	0	9	58	2062
21:00	732	310	285	513	125	0	9	56	2030
21:15	732	312	285	464	123	0	9	54	1979
21:30	732	310	284	437	119	0	11	54	1947
21:45	731	311	284	371	124	0	11	53	1885
22:00	732	312	262	348	123	0	11	51	1839
22:15	730	312	222	340	126	0	10	50	1790
22:30	732	308	163	356	120	0	10	50	1739
22:45	732	319	149	330	119	0	10	50	1709
23:00	732	299	137	311	123	0	11	51	1664
23:15	730	290	113	310	117	0	11	51	1622
23:30	729	290	39	340	121	0	11	53	1583
23:45	730	293	23	299	123	0	10	51	1529
0:00	731	265	0	329	127	0	10	54	1516
Energy (MWh)	17608	7087.3	4410.4	8030.2	3044.6	2546.8	486.2	4146.1	47359.6

APPENDIX B

SRI LANKAN TRANSMISSION LINE NETWORK WITH SUBSTATIONS IN 2023

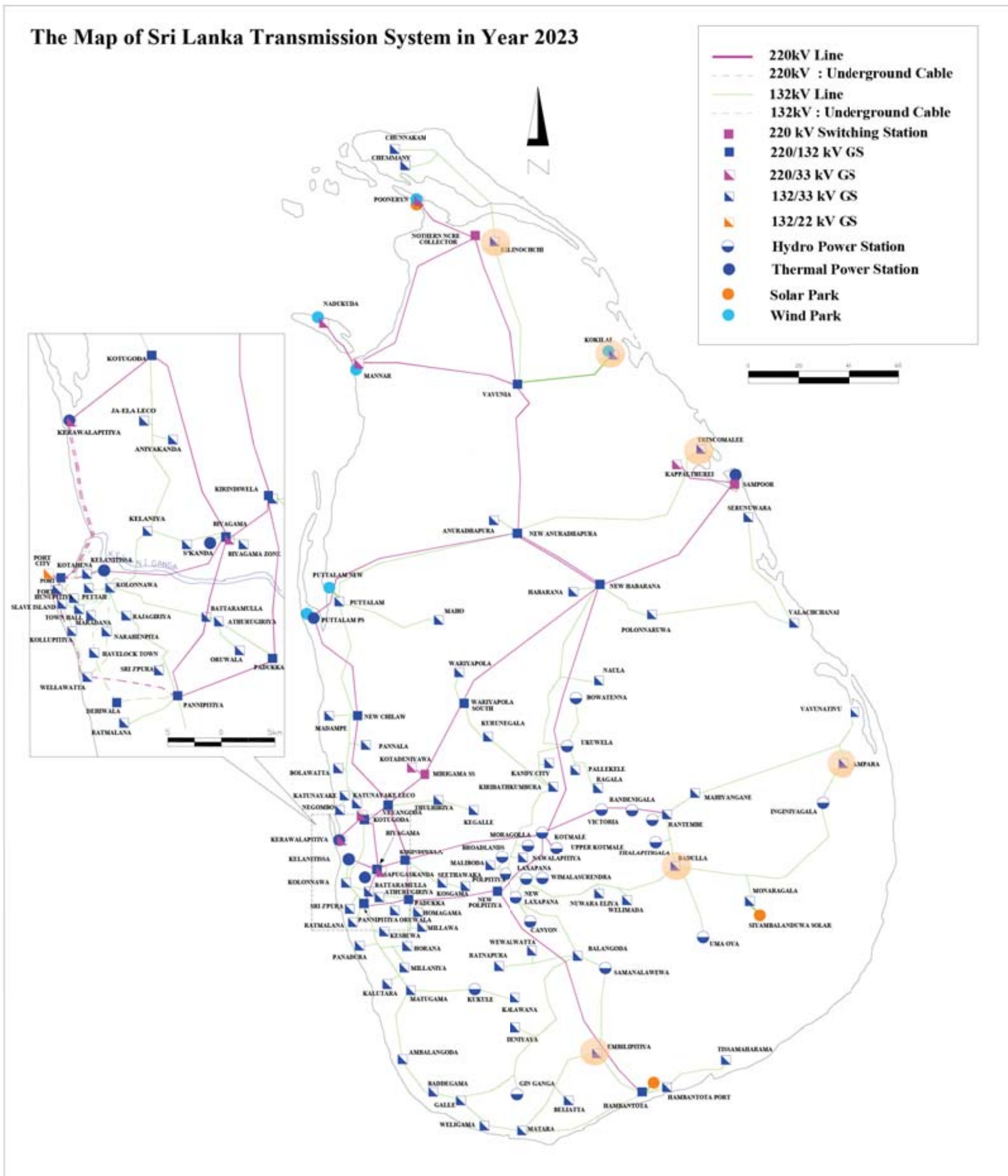

APPENDIX C

MAP WITH SELECTED AREA FOR SOLAR PV POWER PLANTS IN SRI LANKA

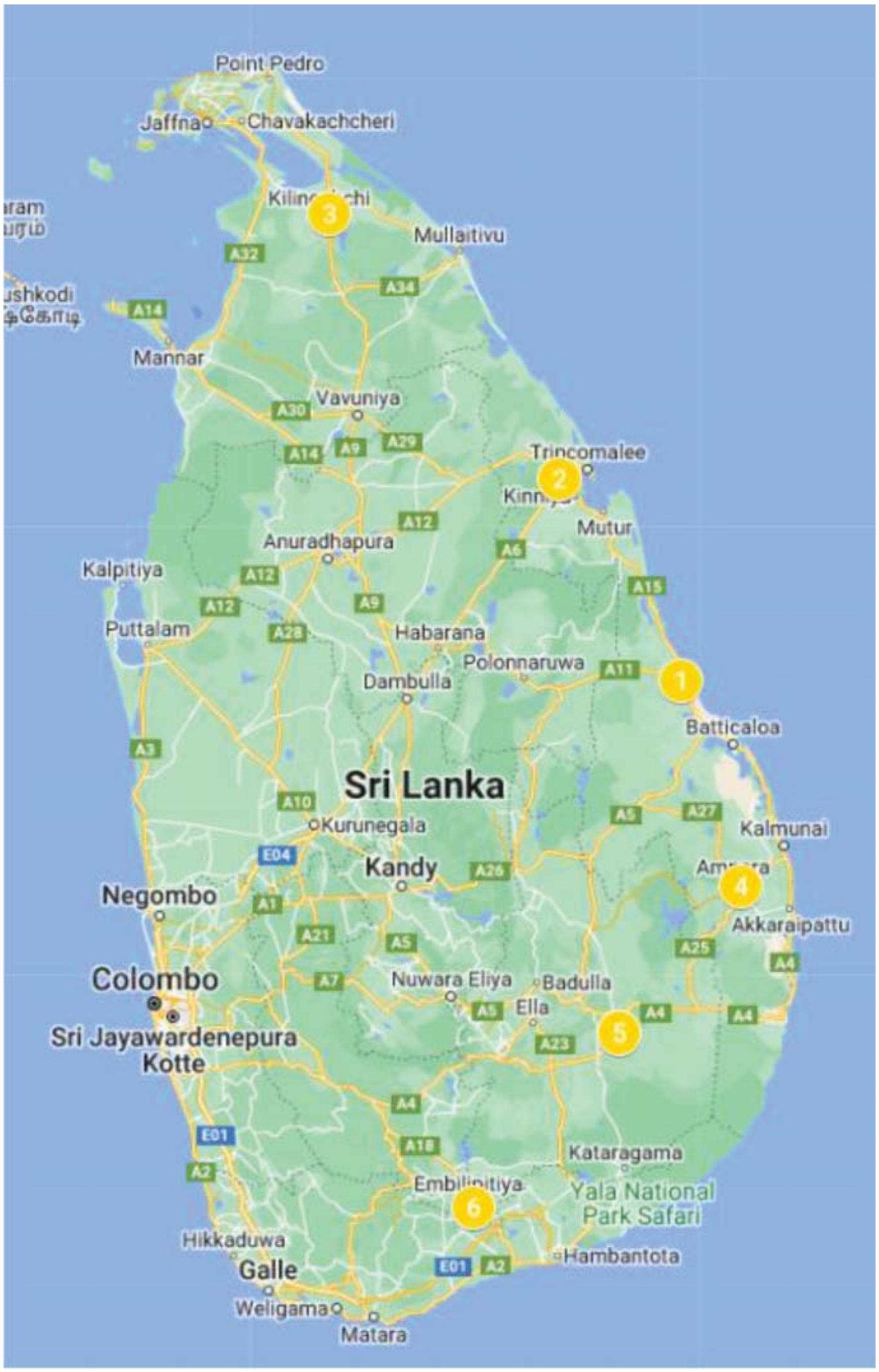

APPENDIX D

MAP WITH IDENTIFIED LOCATIONS FOR PHS SYSTEM IN SRI LANKA

APPENDIX E

SOLAR PV AND BS CAPACITY VARIATION BASED ON AN 8.5% INTEREST RATE RELEVANT TO IDENTIFIED CASES

Solar PV capacity (MW) variation based on an 8.5% interest rate relevant to *case* 1

Years	8.50%	4.50%		15.50%	
	Normal	New	Difference	New	Difference
2024 - 2025	931.06	810.53	(120.53)	864.98	(66.08)
2026 - 2027	801.19	685.69	(115.50)	569.73	(231.47)
2028 - 2029	407.60	431.64	24.04	619.13	211.52
2030 - 2031	487.17	497.00	9.83	383.54	(103.63)
2032- 2033	399.38	512.12	112.74	633.72	234.34
2034- 2035	626.99	723.36	96.37	677.61	50.62
2036- 2037	731.64	636.07	(95.57)	557.37	(174.27)
2038- 2039	706.70	844.47	137.77	715.31	8.61
2040- 2041	702.06	841.72	139.66	927.03	224.97
2042- 2043	1016.26	826.60	(189.66)	957.13	(59.13)
2044- 2045	1141.16	1190.43	49.27	1078.67	(62.49)
2046- 2047	1436.49	1103.74	(332.75)	1174.69	(261.80)

BS capacity (MW) variation based on an 8.5% interest rate relevant to *case* 1

Years	8.50%	4.50%		15.50%	
	Normal	New	Difference	New	Difference
2024 - 2025	1.28	4.36	3.08	17.37	16.09
2026 - 2027	95.23	47.20	(48.02)	71.91	(23.31)
2028 - 2029	192.30	239.63	47.33	125.88	(66.42)
2030 - 2031	110.93	98.79	(12.13)	158.91	47.98
2032- 2033	123.35	106.20	(17.15)	117.02	(6.33)
2034- 2035	123.82	107.76	(16.06)	145.26	21.44

Continued on next page

BS capacity (MW) variation based on an 8.5% interest rate relevant to *case* 1 (Continued)

2036- 2037	127.14	210.41	83.27	192.56	65.42
2038- 2039	196.58	167.78	(28.80)	185.21	(11.37)
2040- 2041	255.87	203.21	(52.66)	187.32	(68.55)
2042- 2043	207.15	328.27	121.12	205.29	(1.86)
2044- 2045	289.92	160.33	(129.60)	249.82	(40.10)
2046- 2047	348.52	401.13	52.61	458.53	110.01

Solar PV capacity (MW) variation based on an 8.5% interest rate relevant to *case* 2

Years	8.50%	4.50%		15.50%	
	Normal	New	Difference	New	Difference
2024 - 2025	931.06	716.14	(214.92)	864.98	(66.08)
2026 - 2027	801.19	738.17	(63.02)	721.80	(79.40)
2028 - 2029	275.87	429.07	153.20	374.13	98.26
2030 - 2031	514.16	542.11	27.94	526.81	12.65
2032- 2033	400.56	486.66	86.10	614.33	213.77
2034- 2035	690.43	1403.08	712.65	531.48	(158.95)
2036- 2037	832.30	145.68	(686.62)	828.00	(4.30)
2038- 2039	679.75	540.92	(138.82)	699.95	20.21
2040- 2041	776.59	833.34	56.74	900.70	124.11
2042- 2043	751.31	824.89	73.58	1008.90	257.59
2044- 2045	1287.50	1048.54	(238.96)	1560.49	272.98
2046- 2047	1382.58	1819.13	436.55	1169.92	(212.66)

BS capacity (MW) variation based on an 8.5% interest rate relevant to *case* 2

Years	8.50%	4.50%		15.50%	
	Normal	New	Difference	New	Difference
2024 - 2025	1.28	6.03	4.76	17.37	16.09
2026 - 2027	95.23	69.92	(25.31)	72.57	(22.65)

Continued on next page

BS capacity (MW) variation based on an 8.5% interest rate relevant to *case* 2 (Continued)

2028 - 2029	202.87	190.28	(12.58)	183.48	(19.39)
2030 - 2031	95.06	103.76	8.70	85.75	(9.31)
2032- 2033	134.04	115.17	(18.87)	116.37	(17.67)
2034- 2035	115.57	68.66	(46.92)	119.42	3.84
2036- 2037	115.43	311.02	195.58	107.32	(8.11)
2038- 2039	215.90	291.96	76.06	187.35	(28.55)
2040- 2041	190.67	29.24	(161.43)	221.63	30.96
2042- 2043	284.82	362.54	77.72	267.08	(17.74)
2044- 2045	211.13	391.76	180.64	431.46	220.33
2046- 2047	273.53	177.41	(96.12)	338.03	64.49

Solar PV capacity (MW) variation based on an 8.5% interest rate relevant to *case* 3

Years	8.50%	4.50%		15.50%	
	Normal	New	Difference	New	Difference
2024 - 2025	931.06	810.53	(120.53)	864.98	(66.08)
2026 - 2027	801.19	685.69	(115.50)	569.73	(231.47)
2028 - 2029	275.87	431.64	155.77	619.13	343.25
2030 - 2031	416.06	497.00	80.94	383.54	(32.52)
2032- 2033	576.84	512.12	(64.71)	633.72	56.88
2034- 2035	704.90	723.36	18.46	677.61	(27.29)
2036- 2037	816.11	636.07	(180.05)	557.37	(258.74)
2038- 2039	539.69	844.47	304.78	715.31	175.61
2040- 2041	849.89	841.72	(8.18)	927.03	77.14
2042- 2043	780.07	826.60	46.53	957.13	177.07
2044- 2045	1313.59	1190.43	(123.16)	1078.67	(234.92)
2046- 2047	1269.94	1103.74	(166.19)	1174.69	(95.24)

BS capacity (MW) variation based on an 8.5% interest rate relevant to *case* 3

Years	8.50%	4.50%		15.50%	
	Normal	New	Difference	New	Difference
2024 - 2025	1.28	4.36	3.08	17.37	16.09
2026 - 2027	95.23	47.20	(48.02)	71.91	(23.31)
2028 - 2029	202.87	239.63	36.77	125.88	(76.98)
2030 - 2031	127.51	98.79	(28.71)	158.91	31.41
2032- 2033	81.67	106.20	24.52	117.02	35.34
2034- 2035	135.02	107.76	(27.26)	145.26	10.25
2036- 2037	112.34	210.41	98.07	192.56	80.21
2038- 2039	238.30	167.78	(70.52)	185.21	(53.09)
2040- 2041	238.10	203.21	(34.90)	187.32	(50.78)
2042- 2043	327.10	328.27	1.17	205.29	(121.81)
2044- 2045	114.60	160.33	45.73	249.82	135.22
2046- 2047	451.62	401.13	(50.49)	458.53	6.91

Solar PV capacity (MW) variation based on an 8.5% interest rate relevant to *case* 6

Years	8.50%	4.50%		15.50%	
	Normal	New	Difference	New	Difference
2024 - 2025	773.01	810.53	37.52	864.98	91.97
2026 - 2027	959.24	685.69	(273.55)	569.73	(389.51)
2028 - 2029	145.70	431.64	285.94	619.13	473.43
2030 - 2031	607.51	497.00	(110.51)	383.54	(223.97)
2032- 2033	544.36	512.12	(32.24)	633.72	89.36
2034- 2035	771.20	723.36	(47.84)	677.61	(93.59)
2036- 2037	517.84	636.07	118.23	557.37	39.53
2038- 2039	836.67	844.47	7.80	715.31	(121.37)
2040- 2041	755.95	841.72	85.77	927.03	171.08
2042- 2043	956.65	826.60	(130.05)	957.13	0.48
2044- 2045	1194.45	1190.43	(4.01)	1078.67	(115.78)

Continued on next page

Solar PV capacity (MW) variation based on an 8.5% interest rate relevant to *case* 6 (Continued)

2046- 2047	1116.66	1103.74	(12.91)	1174.69	58.04

BS capacity (MW) variation based on an 8.5% interest rate relevant to *case* 6

Years	8.50%	4.50%		15.50%	
	Normal	New	Difference	New	Difference
2024 - 2025	0.37	4.36	3.99	17.37	17.00
2026 - 2027	96.14	47.20	(48.94)	71.91	(24.23)
2028 - 2029	238.43	239.63	1.21	125.88	(112.55)
2030 - 2031	48.42	98.79	50.38	158.91	110.49
2032- 2033	134.25	106.20	(28.05)	117.02	(17.24)
2034- 2035	133.05	107.76	(25.29)	145.26	12.21
2036- 2037	185.12	210.41	25.29	192.56	7.44
2038- 2039	192.07	167.78	(24.28)	185.21	(6.85)
2040- 2041	188.36	203.21	14.85	187.32	(1.03)
2042- 2043	199.10	328.27	129.17	205.29	6.19
2044- 2045	246.19	160.33	(85.86)	249.82	3.63
2046- 2047	608.89	401.13	(207.76)	458.53	(150.36)